Employing disease-associated genetic variants to study the influence of *TLR5* and *NLRP6* on gut immunity in humans

Dissertation

der Mathematisch-Naturwissenschaftlichen Fakultät

der Eberhard Karls Universität Tübingen

zur Erlangung des Grades eines

Doktors der Naturwissenschaften

(Dr. rer. nat.)

vorgelegt von

Dipl. Biol. Tharmila Jeyam (geb. Sanmuganantham)

aus Hamburg

Tübingen

2021

Tag der mündlichen Qualifikation:	22.03.2021
Stellvertretender Dekan:	Prof. Dr. József Fortágh
1. Berichterstatter:	Prof. PhD Alexander N.R. Weber
2. Berichterstatter:	Prof. Dr. Hans-Georg Rammensee

Acknowledgements

First, I would like to thank my supervisor Prof. PhD Alexander N.R. Weber, who gave me the opportunity to conduct my doctoral thesis in his laboratory. I am very grateful, he considered me for this position despite my time-off as a care-taker of my mother. His mentoring, encouragement, valuable scientific advice and discussions during my experimental work and thesis writing, allowed me to develop my scientific skills and perform my PhD thesis to my best.

I would like to thank Prof. Dr. Hans-Georg Rammensee, Head of science department at University of Tübingen, who gave me the opportunity to do my PhD at the Department of Immunology in an excellent scientific working environment and granted me financial support by SFB685. I would also like to thank, Prof. Dr. Jürgen Frank, who organized the integrated research training group (IRTG) `Immunotherapy` and further arranged financial support for my extended work. The IRTG has given me an advanced knowledge in the field of Immunology and the research of the members was truly inspiring. I appreciate also the help of Dr. med. Markus Löffler, who supported me in the clinical studies by consulting participants on this study as a doctor and arranging for the collection of additional samples from study participants.

I appreciate the support of all team members from the laboratory of Prof. PhD Alexander N.R. Weber, who facilitated the accomplishment of my thesis by valuable scientific advice, supporting experimental work, and inspiring discussions. In particular, I would like to thank Sabine Dickhöfer, who performed some experimental work for my project and Yesim Tuczku, who helped me to process stool samples and perform preliminary experiments. These contributions have been highlighted in this thesis. I would also like to thank Dr. Olaf-Oliver Wolz, Dr. Truong-Minh Dang and Sabine Dickhöfer for their experienced advice and scientific discussions. I would like to thank Dr. Xiao Liu for her scientific discussions and personal support. I would like to thank Dr. Yamel Cardona Gloria for scientific advice and discussions, review of parts of my thesis and personal support. I am very grateful for the personal support and encouragement, scientific discussions, and inspiring and productive working atmosphere provided by each of the team members, who made this PhD a great experience for me.

Last, but not least, I would like to thank my parents Sanmuganantham and Selvamany, my husband Jeyakumar, my brother Theepan and my friend Andrika, who have all had great patience and provided me with strong encouragement during the entire course of my PhD. Finally, I would like to thank my uncle, Ramakrishnan Kandiah, who initially inspired me for science and pointed out great opportunities in this field, and who has been a great mentor for me.

Abstract

The Nod-like receptor 6 (NLRP6) is a central innate immune receptor, which has drawn attention in mice models, particularly for its relevance in maintaining gut homeostasis. However, mechanistic insights on the molecular level and data regarding the role of NLRP6 in humans are limited. NLRP6 has been described to recruit the adaptor protein ASC and thereby activate NF-κB. Published data from our group indicates that a polymorphism coding for Leucine instead of Methionine at position 163 (M163L) within NLRP6 is associated with significantly higher risk for colorectal cancer (CRC) in humans. Another described exchange from Phenylalanine to Tyrosine (F361Y) is associated with SNP M163L. However, a functional impact of these SNPs on the molecular level and their contribution towards the development of CRC have not been investigated to date. I therefore studied these genetic variants in molecular model systems to gain an insight into possible functional changes and thereby glean general insights into how NLRP6 may participate in gut innate immunity. My i*n vitro* studies showed that NLRP6 SNPs M163L and F361Y together enhance the interaction of NLRP6 with ASC, and F361Y induces higher NF-κB activation. This fits with the observation that CRC is induced in SNP carriers. Whole blood stimulation with respective TLR ligands and assessment of cytokine expression did not show a role of these SNPs in modulating different TLR signaling. Previously, Klimosch et al. reported functional SNPs of the flagellin receptor, TLR5, to be associated with CRC survival. Thus, we included these in the stool sample analysis on the effect of functional *TLR5* and *NLRP6* SNPs on gut immune parameters. By stimulation of, HEK cells stably expressing TLR5 with stool content (which contains shed intestinal flagellin) from different SNP carriers, we observed that TLR5 activation correlated with *TLR5* SNP carriage: Stool samples from carriers of hyperactive *TLR5* alleles revealed significantly reduced TLR5 activation, while increased TLR5 activation was observed for stool from loss-of-function carriers. For calprotectin levels, in stool samples from homozygous carriers for a hypofunctional *TLR5* allele significantly reduced levels were observed. There was also a significant correlation with secretory IgA, a key regulator of intestinal homeostasis. Collectively, my results indicate reduced correlation between immune parameters, inflammatory stool characteristics and SNP carriage, and thus a direct relevance for *TLR5* and *NLRP6* variants for gut homeostasis and CRC. Metagenomic sequencing of the same samples is thus a plausible next step and currently conducted by our collaboration partners. Complementary analysis on immune and microbial parameters in stool samples of CRC patients and comparison with our results could thus further advance our knowledge in changes upon CRC disease development and find possible targets for individual genotype specific treatments or prevention strategies.

Zusammenfassung

Nod-like-Rezeptor 6 (NLRP6) ist ein zentraler Immunrezeptor des angeborenen Immunsystems, welcher in Mausmodellen, insbesondere durch seine Bedeutung in der Aufrechterhaltung des Darmgleichgewichts, Aufmerksamkeit erhielt. Hingegen sind Einblicke in molekulare Mechanismen und Daten bezüglich der Rolle von NLRP6 in Menschen, begrenzt. NLRP6 ist beschrieben worden, das Adaptorprotein ASC zu rekrutieren und dabei NF-κB zu aktivieren. Publizierte Daten unserer Gruppe weisen darauf hin, dass ein Polymorphismus kodierend für Leucin anstatt Methionin an der Position 163 (M163L) innerhalb NLRP6 mit signifikant höherem Risiko für Darmkrebs in Menschen assoziiert ist. Ein weiterer, beschriebener Austausch von Phenylalanin zu Tyrosin, (F361Y), erweist sich als assoziiert mit SNP M163L. Jedoch, sind die funktionelle Bedeutung dieser SNPs auf molekularer Ebene und ihr Beitrag zur Entstehung von Darmkrebs bisher nicht ermittelt worden. Ich untersuchte deshalb diese genetischen Varianten in molekularen Modellsystemen, um einen Einblick in mögliche funktionelle Veränderungen zu gewinnen, und dabei generelle Erkenntnisse zu sammeln, wie NLRP6 im angeborenen Immunsystem des Darms mitwirken kann. Meine *in vitro* Studien zeigten, dass NLRP6 SNPs, M163L und F361Y, zusammen die Interaktion von NLRP6 mit ASC verstärken, und F361Y eine höhere NF-κB Aktivität induziert. Dieses stimmt mit der Beobachtung überein, dass Darmkrebs in diesen SNP Trägern induziert ist. Vollblutstimulation mit entsprechenden TLR Liganden und anschließender Bestimmung der Zytokinexpresssion wiesen keine Rolle für diese SNPs in der Modulierung verschiedener TLR Signalwege auf. Zuvor berichteten, Dr. Klimosch et al., dass funktionelle SNPs des Flagellin Rezeptors, TLR5, mit dem Überleben bei Darmkrebs, assoziiert sind. Daher nahmen wir diese in die Stuhlprobenanalyse zur Wirkung von funktionellen *TLR5* und *NLRP6* SNPs auf Immunparameter im Darm, auf. Durch die Stimulation von HEK Zellen, welche TLR5 stabil exprimieren, mit Stuhlproben (welche ausgeschüttete intestinale Flagella enthalten) von verschiedenen SNP Trägern, beobachteten wir, dass die TLR5 Aktivität mit dem Tragen von *TLR5* SNP korreliert. Stuhlproben von Trägern der hyperaktiven *TLR5* Allele zeigten signifikant reduzierte TLR5 Aktivität, während eine erhöhte TLR5 Aktivität für Stuhlproben von Trägern mit Funktionsverlust beobachtet wurde. Für Calprotectin Mengen, wurden in Stuhl(proben) homozygoter Träger eines hypofunktionalen *TLR5* Allels, signifikant reduzierte Mengen beobachtet. Es gab außerdem eine signifikante Korrelation mit sekretorischem IgA, welche ein Schlüsselregulator des intestinalen Gleichgewichts ist. Zusammengefasst, weisen meine Ergebnisse auf eine reduzierte Korrelation zwischen Immunparametern, inflammatorischen Stuhl Charakteristika und Tragen von SNPs hin und demzufolge

auch für eine direkte Relevanz der *TLR5* und *NLRP6* Varianten auf Darmgleichgewicht und Darmkrebs. Metagenomische Sequenzierung der gleichen Proben ist daher ein plausibler nächster Schritt und wird zurzeit von unseren Kollaborationspartnern durchgeführt. Komplementäre Analysen der immunologischen und mikrobiellen Parameter in Stuhlproben von Darmkrebspatienten und ein Vergleich mit unseren Ergebnissen könnte daher des Weiteren unsere Erkenntnisse in Veränderungen nach Entstehung der Darmkrebserkrankung erweitern und mögliche Ziele für individuelle Genotyp-spezifische Behandlungen oder Präventionsstrategien aufzeigen.

Table of contents

List of figures

List of tables

Abbreviations

ALR	AIM2-like receptor
AP-1	activator protein-1
APC	antigen presenting cell
APRIL	a proliferation-inducing ligand
ASC	apoptosis-associated speck-like protein containing a CARD
ATP	adenosine tri-phosphate
BAFF	B cell activating factor
BRET	bioluminescence resonance energy transfer
CARD	caspase-recruitment domain
CCD	charge-coupled device
CD	cluster of differentiation
cGAS	cyclic GMP-AMP synthase
CLR	C-type lectin receptor
CRC	Colorectal cancer
CTL	cytotoxic T-lymphocyte
CYS	cysteine
DAMP	danger associated molecular pattern
DC	Dendritic cell
DHX	DEAH-box helicase 15
DLA	Dual Reporter Luciferase Assay
DOX	Doxycycline
dsRNA	double stranded RNA
DTT	Dithiothreitol
EV	empty vector
eGFP	enhanced green fluorescent protein
F	Phenylalanine
FAE	follicle-associated epithelium
FCS	fetal calf serum
FRT	Flp Recombination Target
GALT	gut associated lymphoid tissue
GFP	green fluorescent protein
GOI	gene of interest
HA	hemagglutinin
HEK	human embryonic kidney

HR	hazard ratio
HRP	horseradish peroxidase
IB	immunoblot
IEL	intraepithelial lymphocytes
IFN	Interferon
Ig	immunoglobulin
IL	Interleukin
IL-1R	Interleukin-1 receptor
ILC	innate lymphoid cells
ILFs	isolated lymphoid follicles
IP	immunoprectipitation
IRAK	IL-1R-associated kinase
IRF	Interferon regulatory factor
JNK	c-Jun N-terminal kinase
KO	knockout
L	leucine
LPS	lipopolysaccharide
LRR	leucine rich repeat
LTA	lipoteichoic acid
M	methionine
M	cell microfold cell
MAL	MyD88-adaptor-like protein
MAMP	microbe-associated molecular pattern
MAPK	Mitogen-activated protein kinase
MAVS	mitochondrial antiviral singaling protein
MHC	major histocompatibility complex
Myd88	Myeloid differentiation primary response protein 88
NBD	nucleotide binding domain
NF-κB	nuclear factor kappa-light-chain-enhancer of activated B cells
NLR	Nod-like receptor
NLRP	NACHT, LRR and PYD domains-containing protein
NOD	nucleotide-binding-and-oligomerization-domain
OD	optical density
ORF	Open reading frame
OS	overall survival
PCR	polymerase chain reaction

PRR	pattern recognition receptor
ProA	Protein A
RA	retinoic acid
RLR	Rig-1-like receptor
RLU	relative light units
RT	reverse transcription
SD	standard deviation
SDS	sodium dodecyl sulfate
SEAP	secreted alkaline phosphatase
sIgA	secretory Immunglobulin A
SN	supernatant
SNP	Single nucleotide polymorphism
ssRNA	single stranded RNA
Strep	streptavidin
Term	terminal
TetR	tet Repressor
TICAM1	TIR-domain-containing molecule 1
TICAM2	TIR-domain-containing molecule 2
TIR	Toll/interleukin-1 receptor (TIR) homology domain
TIRAP	TIR-domain-containing adaptor protein
TLR	Toll-like receptor
TNF α	tumor necrosis factor α
TRAF6	Tumor necrosis factor receptor-associated factor 6
TRAM	TRIF-related adaptor molecule
TRAF6	Tumor necrosis factor receptor-associated factor 6
TRIF	TIR-domain-containing adaptor protein inducing IFN-β
WT	Wildtype
Y	Tyrosine

1 Introduction

In the introduction, first, I will review the general mechanisms of the innate and adaptive immune system and highlight some specific details relevant to the gut mucosal immune system. Next, I will focus on TLR and NLR signaling and point out the role of, particularly, *TLR5* and *NLRP6* in the mucosal immune system. After, I will focus on current knowledge gained from *Tlr5* and *Nlrp6* KO mice models and further, reveal associations of individual *TLR5* and *NLRP6* SNPs, tested in this project, with human CRC. Finally, I will describe the aims of this study.

1.1 The Immune System

Human beings are regularly exposed to microorganisms, which can cause disease. The host has developed a sophisticated and remarkably effective system throughout evolution, to combat pathogens. The human immune system comprises the innate and adaptive immune system.

An innate immune response is present in plants, vertebrates, and non-vertebrates[1], responds rapidly and is not specific to a certain pathogen. It rather enables a fast immune evaluation and reaction to altered self-molecules or non-self molecules, such as conserved molecules deriving from microbes[2], i.e. LPS or flagellin, by a germ-line encoded range of receptors. The activation of these receptors triggers responses able to eliminate pathogens (e.g. phagocytosis) and foreign molecules in the system. Concomitant to the innate immune response, an adaptive immune response is initiated and mounted, providing a means to eliminate the pathogen should innate defenses not suffice to eliminate the invader[3].

The adaptive immune system is an elaborate system, present only in vertebrates[1,4]. The adaptive immune response is specific to a pathogen and usually requires several days to develop[2], at least when a pathogen is recognized for the first time. When an infection with a certain pathogen is encountered again, in many cases the adaptive immune response is able to recognize the pathogen and confer a rapid protective immunity upon any time of reinfection due to long-lived memory cells.[3]

However, the innate and adaptive immune system complete each other in protecting the host from invaders and are not strictly separated. Before the activation of the adaptive immune system, the innate immune system by itself has to control the infections and after activation of the adaptive immune system, the innate immune system still supports the adaptive immune system in the elimination of pathogens.[2,3]

1.2 The innate immune response

Innate immune defenses comprise physical and chemical barriers, such as epithelial cell lining, mucus layer covering the epithelium of i.e. the gastrointestinal tract or acidic pH in the stomach, as well as humoral and cell-associated recognition and effector functions[2]. Out of this array of defense mechanisms, Pattern recognition receptors and cellular responses triggered by these receptors are of great importance for this thesis and therefore focused upon here.

1.2.1 Pattern recognition receptors

Pattern Recognition Receptors (PRRs) are germline-encoded[5] and highly conserved among species, including plants, invertebrates and vertebrates[1]. Their major task is to sense the presence of microorganisms in the body thereby protecting the body from invading pathogens.

This is an enormous challenge considering the molecular diversity of pathogens and their tremendous replication and mutation rates. PRRs overcome this difficulty by recognising abundantly expressed microbe-associated molecular patterns (MAMPs) which are conserved among broad classes of microorganisms. These structures are critical for replication and/or survival of the microbe and unique to microorganisms. This allows the receptors to discriminate between self and non-self and initiate an effective immune response to invading pathogens.[6]

The redundant recognition of many patterns and activation of corresponding receptors ensures the sensing even in a state when the microorganism has evolved some escape mechanisms. The term 'microbe-associated molecular patterns' (MAMPs) has been suggested instead of pathogen-associated molecular patterns as the recognized patterns in microbes also are present in commensals, which are beneficial for the host[1]. In addition, some PRRs such as Nod-like receptors can also recognise endogenous molecules and toxins such as ATP, Nigericin and crystals released from damaged cells, termed damage-associated molecular patterns (DAMPs) indicating an infected, stress or otherwise altered cell[7,8].

PRRs can be divided so far in 6 major groups: Toll-like receptors (TLRs), C-type lectin receptors (CLRs), Retinoic acid-inducible gene (RIG)-I-like receptors (RLRs), AIM2-like receptors (ALRs), Nod-like receptors (NLRs)[5,9] and cytosolic DNA receptors such as cGAS[10]. Depending on the activated PRR and its localisation, PRRs are able to initiate an immune response in a context-specific manner by distinct expression patterns of inducible genes according to the situation. The main regulators of the inflammatory response are proinflammatory cytokines.

1.2.2 Cellular responses triggered by Pattern recognition receptors (PRRs)

PRRs are expressed in hematopoietic cells (e.g. phagocytotic macrophages and dendritic cells) and non-hematopoietic cells as in epithelial cells to detect foreign microbes in order to protect the host. Activation of these receptors leads to the secretion of proinflammatory or anti-inflammatory cytokines, which affect other cells carrying corresponding receptors and thereby lead to signal transduction. Further, chemokines are released and together with cytokines, they are involved in processes including activation, migration, and differentiation of immune cells.[3]

The process of inflammation, dilation and increased permeability of blood vessels enables the increased local blood flow and the leakage of fluid. Secreted chemokines attract cells bearing chemokine receptors, such as monocytes and neutrophils from the bloodstream to the site of infection. An inflammatory response leads to the recruitment of neutrophils into the inflamed, infected tissue in large numbers, which also carry PRRs and are crucial cells in engulfing and destroying the invading micro-organisms. Next, at the site of infection, monocytes arrive, which differentiate into macrophages. The inflammatory response increases the flow of lymph containing antigen and antigen-bearing cells into lymphoid tissue.[3]

1.3 The adaptive immune response

The main cell types involved in the adaptive immune response are B- and T-lymphocytes, which characterize the immune response through the specificity for a given pathogen conferred by their specificity through receptors[2].

Each of the B-cells carries antigen receptors with a single specificity, which is acquired during the selection between millions of different variants of genes encoding the receptor molecules[2]. In this process, a unique genetic mechanism during lymphocyte development in the bone marrow and thymus is employed. Throughout life, lymphocytes are naturally selected.[2,3]

When the lymphocytes encounter an antigen, only those which are capable with their provided receptor to bind to the antigen will be activated to proliferate and differentiate into effector cells. Binding of antigen on naïve B-cell initiates the division of the cell and produces many identical clones. These clones can thus secrete the same antibody, which was activated as a membrane-bound form on the activated naive B-cell. Clonal deletion is a process where self-reactive B-cells are removed in an early stage of lymphocyte development and thus are absent from the repertoire of mature B-cells before they can mature.[3]

B cells contribute to the adaptive immune response by generating antibodies, which function in various ways, i.e. to sensitize infected or tumor cells for antibody-dependent cellular cytotoxicity (ADCC), carried out by CTLs and NK cells, to opsonize microbes for phagocytosis, to activate the complement system or neutralize toxins[3].

The response of lymphocytes is well regulated and requires, besides the antigen binding to their receptor, a second signal from another cell. Naïve T-cells are generally activated by activated DCs, whereas B-cells receive their second signal from T-cells.[3] Antigens are presented on the cell surface on their major histocompatibility complex to T-cell receptors[11], which leads to T- cell priming, activation and differentiation and can lead to two different outcomes, depending on the type of T-cell activated.[2]

T-cells bearing co-receptor CD8 can recognize peptide sequences derived i.e. from viruses or intracellular pathogens, presented on MHC class I. Effector cytotoxic CD8 T lymphocytes (CTLs) leave the lymphoid organs and home to the site of infection and can induce cell death of infected cells through many mechanisms, i.e. by releasing cytokines such as interferon-γ (IFNγ) and tumor necrosis factor (TNF), expression of perforin and granzymes or via cell surface interactions between the so-called death receptors, at which Fas ligand (FasL) on CTLs binds to Fas on infected target cells.[3]

T-cells bearing the co-receptor CD4 can recognize peptides from extracellular pathogens, presented on MHC class II from APCs[3]. Activation of CD4 T cells induces a comprehensive production of cytokines which successively is able to activate a wide range of surrounding effector cells like macrophages, B lymphocytes and CTLs. CD4 T cells can be further classified depending on secreted cytokines as T helper cells (Th) 1, Th2, Th17 and Tfh. Th1 can produce i.e. IFN-gamma, which stimulates CTL cytotoxicity and IL-2, which induces CD4 T cell proliferation in an autocrine loop. Further, interferon γ (IFN- γ) is able to activate macrophages and to initiate the expression of MHC class II molecule. Th2 cells, on the other hand, produce cytokines as for example interleukin 4 and 5, which are crucial for B cell maturation and antibody response.[2,3]

1.4 The mucosal immune system

The surface of the gastrointestinal tract is one part of the body, which is covered with a mucus-secreting epithelium. This site is routinely exposed to harmless food antigens and harbors innocuous commensal microbiota[3,12]. Its main function in nutrient transport requires this barrier to be thin and permeable to the interior of the body[3]. It thus also represents an access route for invading pathogens[3,12].

The human body has developed an advanced system to react with an adequate response to harmless food antigens and commensals with tolerance or active suppression but also protects the body from invading pathogens by inflammatory responses[3,12].

To meet these requirements, the mucosal immune system is quite distinct in its structure and function from the systemic immune system as lymph nodes and spleen. The mucosal immune system, which includes the gut mucosal immune system, captures the largest part of the entire tissues of the immune system in the body. It comprises nearly 75 % of all lymphocytes and the majority of immunoglobulin is generated here[13].[3]

1.4.1 Gut structures and their functions

In this section, I will address the structures in the gut and their functions (as reviewed in[14]). For a better understanding of my thesis, in particular, I will briefly describe types of cells arising from gut epithelial stem cells (as reviewed in[15]) and highlight lymphoid tissues (as reviewed in[3,14]), which play an important role in the gut.

The intestine can be differentiated between the small and large intestines, which vary in their functions. Whereas the small intestine absorbs nutrients from digested food in the gut lumen, the main task of the large intestine is rather to reabsorb water and eliminate undigested food components. Moreover, the large intestine is the main habitat of commensal microbiota in the gut and plays an essential role in the health of the host.[14]

The small and large intestine form a continuous tube, which is internally separated from the gut lumen by an inner layer of epithelial cells. This layer serves as a highly selective physical barrier separating the gut lumen with all its antigens from host connective tissues. Below the epithelial lining in the gut, is a layer of connective tissue, termed lamina propria. The epithelium and lamina propria are distinct immunological compartments and their composition and function also vary throughout the intestine. The epithelium with the lamina propria and a thin muscle layer below the lamina propria, termed muscularis mucosa, form together the mucosa, which is the area where the main immunological processes in the gut take place.[14]

The gut epithelial cells derive from a common population of epithelial stem cells in the intestinal crypt of Lieberkühn[16] and are continuously renewed. These give rise to enterocytes, as well as enteroendocrine cells, Goblet cells, and Paneth cells. Among these, the enterocytes are the most abundant cells bordering the lumen and have metabolic and digestive function[17].[15]

On the other hand, secretory intestinal epithelial cells, among them for instance the Paneth cells, goblet cells and enteroendocrine cells are responsible to protect the epithelial barrier[18]. For instance, goblet cells, which are located at crypt surface, secrete mucus and thereby hinder microbes from attachment and direct contact to epithelium through its viscosity[19].[15]

Compared with this, the lymphoid tissue of the gut mucosal immune system can be divided in two parts: On the one hand, the organized gut-associated lymphoid tissue (GALT), in which combined with the draining lymph nodes, the intestinal adaptive immune response is initiated. On the other hand, a diffuse mucosa-associated lymphoid tissue, including lymphocytes and other immune cells, i.e. DCs and macrophages, distributed throughout the intestinal tract in the surface epithelium of mucosa and lamina propria, which is the effector site of the adaptive immune response.[3]

In the following, I will draw attention to the GALT for a better understanding of this thesis.

The GALT encompasses subepithelial lymphoid aggregates that are present in the mucosa and submucosa. These structures contain on top of them a follicle-associated epithelium (FAE). An important feature of this FAE is the presence of microfold (M) cells. M cells are enterocytes, which are ideally adapted to uptake and transport soluble and particulate antigens from the gut lumen into an underlying DC rich, subepithelial dome (SED) region. Here, these antigens can be presented to adaptive immune cells.[3,14]

In particular, aggregated follicles in macroscopically visible subepithelial dome-like structures, termed Peyer`s patches, are very characteristic in the structure of the small intestine. Peyer's patches are formed by numerous B cell lymphoid follicles, which are surrounded by small T cell areas along them[20]. Compared to lymph nodes, Peyer's patches are not enclosed and always contain germinal centers.[3] This suggests regular immune stimulation, most likely by luminal antigen. Equivalent structures are found in the large intestine, in caecal patches and in colonic patches throughout the colon and rectum[21,22]. Indications hint on an important role of caecal patches in the generation of IgA-producing plasma cells that migrate to the colon in response to the local microbiota[23]. By contrast, Peyer's patches seem to be the main source of small intestine-homing IgA plasmablasts[23].[14]
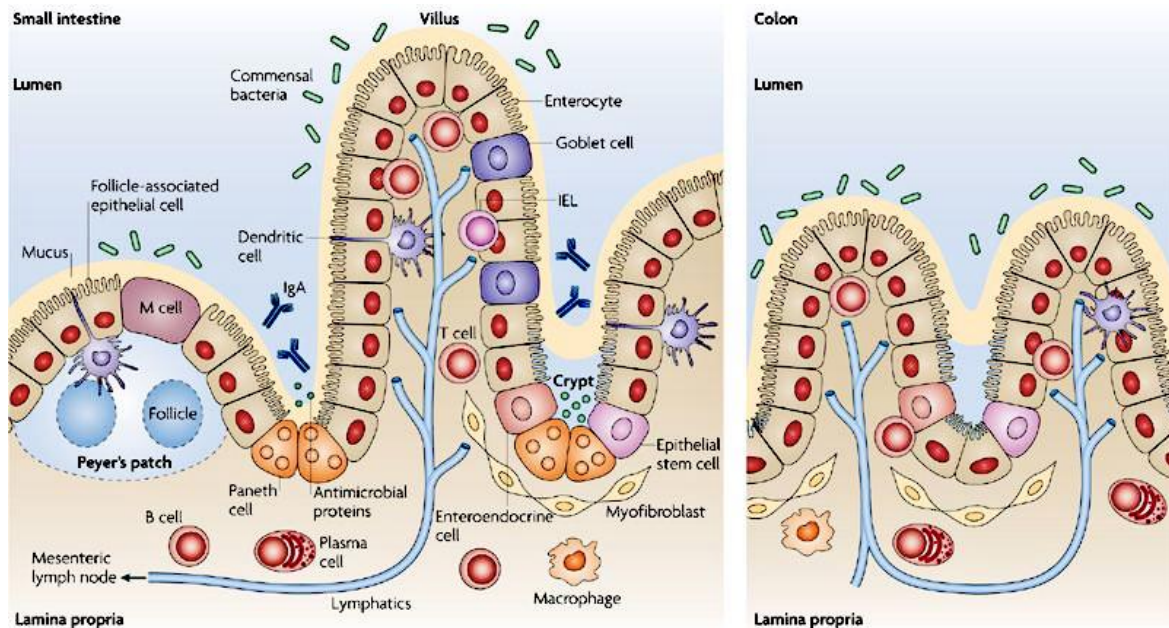
Figure 1-1 Anatomy of the intestinal immune system.
Figure and adapted legend from Abreu et al.[24]. A single layer of intestinal epithelial cells (IECs) serves as a physical barrier and protects the underlying lamina propria from commensal bacteria and antigens in the intestinal lumen. The IECs lining contains Goblet cells, which secret mucus and build an additional protective layer. Further, B-cells produce IgA and Paneth cells at the base of the small intestinal crypt in the IEC lining produce antimicrobial peptides, which are secreted into the intestinal lumen and regulate the microbial content. Beneath the IEC lining is a layer of stromal cells (myofibroblasts) termed Lamina propria, which contains large numbers of immune cells, i.e. dendritic cells, macrophages, B cells (especially IgA-producing plasma cells) and T cells. CD8+ T cells are further found between the IECs. The follicle-associated epithelium (FAE) and microfold (M) cells above the Peyer's patches allow through their specialized structure to sample the intestinal lumen and transport them into an underlying DC rich region, where they can be presented to adaptive immune cells.

1.4.2 The mucosal immune response

A mucosal immune response (as reviewed in[25]) is initiated, when an antigen is transported beyond the epithelial barrier. Through a paracellular uptake of an antigen, the antigen is straightforwardly transported to the basolateral surface of intestinal epithelial cells, where antigen-presenting cells can recognize it. Further, transcellular mechanisms like receptor-mediated or nonreceptor-mediated mechanisms, i.e. Microfold cell (M cell) dependent mechanisms, exist.[25] In the following, I have chosen to refer to a nonreceptor-mediated, M cell dependent uptake of antigens (as reviewed in [25]).

The basolateral surface of M cells is formed like an intracellular pocket. The uptake of antigens in the apical membrane of M cells occurs through endocytosis or phagocytosis, which results in the transport of antigens in endosomal vesicles and

subsequent release into the pocket by exocytosis. Dendritic cells and macrophages are located below the M cells. This localization allows them to sample transported antigens and subsequently present them to lymphoid follicles within the subepithelial dome, located in Peyer`s patches (PP). Primed lymphocytes in the PP leave via the lymphatics to the mesenteric lymph nodes and differentiate hereafter. Subsequently, antigen-specific IgA B plasmablasts proliferate and reach mucosal tissues via the bloodstream.[25]

A migration of primed lymphocytes in GALT is mediated by altered expression through selective upregulation of receptor $\alpha_4\beta_7$ integrin and loss of expression of L-selectin. Mucosal addressin cell adhesion molecule 1 (MAdCAM 1), a ligand of receptor $\alpha_4\beta_7$ integrin, is highly expressed by blood vessels of mucosal surfaces and thereby enables gut homing of immune cells.[26]

Here, the primed lymphocytes differentiate mainly into plasma cells, which produce dimeric or polymeric IgA antibodies. Transcytosis allows these antibodies to be delivered cross epithelial cells.[25]

1.4.3 Synthesis and secretion of secretory IgA

At intestinal sites, the primary function of B-cells is to continuously produce IgA[27], which are shed into the gut lumen. Here, secretory IgA (sIgA) acts as a barrier and protects the epithelium from pathogens. This is facilitated by the interaction of sIgA with manifold intestinal antigens, which include dietary antigens, self-antigens and intestinal microbiota[28]. This instance is of high relevance as it enables to contain intestinal antigens in the gut lumen and restrict their access to the bloodstream and additionally to regulate the intestinal microbiota. Interestingly, sIgA production by plasma cells is almost completely dependent on the presence of the microbiota. In addition, the polymeric immunoglobulin receptor (pIgR) reveals a similar microbiota-dependent pattern with enhanced expression found in the large intestine. (reviewed in [29])

As reviewed in[25], in an sIgA molecule, an intermediate joining (J) chain connects the alpha heavy chains of the two IgA molecules and forms a dimer. This complex is delivered to the intestinal lumen across the epithelial cells by the process of transcytosis. For this event, the J chain of an sIgA dimer binds to a pIgR, which is expressed by intestinal epithelial cells. Thereby the IgA together with the pIgR is endocytosed into a vesicle in enterocytes and the proteolysis of the receptor allows the release of the vesicle to the apical surface of the enterocyte. Here, a part of the receptor, the secretory component, is still joined to the immunoglobulin. While IgA is transported to the intestinal lumen, it is able to form an immunocomplex with antigens. These antigens have been formerly able to breach the epithelial barrier

and can now be transported back to the intestinal lumen. Beside these, also non-substrates of pIgR, as monomeric IgG or IgA, are able to form complexes and can thereby be carried out to the intestinal lumen.[25]

Under normal circumstances, IgA is the major immunoglobulin produced in the gut and at other mucosal surfaces. The total amount of sIgA produced daily in the average adult human gut is about 3-5 g every day[30]. About 80 % of the intestinal plasma cells secrete IgA, while other isotypes, such as IgG, IgM or IgE, are usually underrepresented in the gut and can be elevated, during inflammatory or disease setting, or in the case of IgA deficiency. In humans, but not in mice, two IgA isotypes exist and their relative proportions vary along the intestine, with most plasma cells in the duodenum and jejunum producing IgA1. The proportion of IgA2-producing cells then progressively increases from ~25% in the small intestine to >60% in the distal colon[31-34].[25]

1.4.4 Antimicrobial peptides

Paneth cells are found in the small intestine, at the base of crypts of Lieberkühn. They secrete antimicrobial peptides (AMPs) to keep the mucosal surface free from microbes[35]. AMPs are mostly cationic and form cell pores in the bacteria, leading to their death. Paneth cells retain a diversity of peptides and proteins, both utilized for host-defense. Among them, in particular, α-defensins (termed cryptdins in mice), C-type lectin human REG3α (=REG3γ in mice)[36], lysozyme C[37] and phospholipases[38] represent the major available components of the granules. Exposure to a stimulus, i.e. LPS[39], leads to degranulation of the cells and subsequently the distribution of these host-defense molecules into the mucus layer and intestinal lumen allows them to hinder microbes to invade the crypt[40]. As Paneth cells encounter regularly bacteria and their products, they are thought to secrete frequently antimicrobials, which are further believed to be enhanced upon stronger stimulation[39]. (reviewed in [15])

Within the AMPs, particularly, defensins are subjected in this study. This class is characterized by antimicrobial peptides, which are small in size (<50 amino acids), cationic and cysteine-rich. The mature peptides contain regiospecific disulfide bondages[41], based on which the classes of defensins are categorized. In humans, α- and β- defensins are produced, which are characterized by a triple-stranded β-sheet fold containing six cysteine residues connected in a specific way depending on the class of defensin[41]. So far, 6 α-defensins and 4 β-defensins have been found in humans and further β-defensin genes identified[42]. (reviewed in [15])

1.4.5 Commensal Gut Microbiota

Apart from providing a microbiological barrier against pathogens, the commensal gut microbiota is crucial for both: the development of the intestinal immune system[43] and its proper functioning[44,45]. Failure of a tolerated immune response in the gut to commensals is associated with several inflammatory conditions, including inflammatory bowel disease and intestinal cancer[46].

After birth, the gut is colonized by bacteria[47] and other microorganisms. Approximately, 10^{14} bacteria inhabit the human gut, which derive approximately from 500-1000 species[48]. As gut microbes often live in anaerobic conditions, a clear understanding of the gut microbiota was missing for a long time, as appropiate techniques to assess the gut microbiota in their entirety were limited[49]. But with the progress of DNA sequencing methodologies, the understanding of gut microbiota advanced. Studies have shown that the gut microbiota consists of two major groups, Bacteroidetes and Firmicutes[50-52]. Further, smaller groups i.e. Proteobacteria and Actinobacteria, Fusobacteria and Verrucomicrobia also are a part of the gut microbiota[52]. A comparison of gut microbiota between individuals shows that the general phylogenetic composition and metagenomics are similar, whereas differences occur on abundance and species level[53].

Microbiota fulfills different tasks in the host, such as maintenance of the intestinal mucosal barrier, immunomodulation, host metabolism including proper intake of food nutrients, biosynthesis of crucial vitamins for the body[54] and digestion of food[55,56]. Further, it prevents colonization of the habitat by pathogens by occupying these sites, secreting substances, such as bacteriocins or metabolic products, which are inhibitory or expending available nutrients[25]. Metabolites generated by microbiota enable its communication and influence the intestinal immune system.

A well-coordinated balance between microbial and immune system is crucial for gut homeostasis and further influenced by environment and host genetics. Disturbance in the gut microbiota (termed dysbiosis[57]) is associated with an imbalance of gut homeostasis and has been shown to result in diseases, i.e. obesity[58], type 2 diabetes[59] hypertension[60] and inflammatory bowel diseases[61]. In addition, it becomes more apparent that the composition of gut microbiota does not only influence intestinal health but also altered microbiota is associated with several other diseases, such as rheumatoid arthritis, asthma and atopic dermatitis[62-64].

However, much of what is known about changes in the microbiota has been gleaned from mouse models and there is great uncertainty about the applicability to humans; not least because there are distinct differences in murine versus human gut and intestinal microbiota[65]. Furthermore, it is difficult to assess whether in a natural setting disease causes an altered microbiota or vice versa or both.

In addition, the 16S rRNA sequencing technique, which is currently used in most of the studies to sequence bacterial strains, has limitations. For example, it has been shown that results can vary depending on the regions selected[66] and difficulties can occur in assigning operational taxonomic units (OUTs)[67,68]. Further, this technique does not allow to distinguish at species and strain level[68,69].

1.5 Toll-like receptors

In the following chapters, first, I will give an overview of TLRs and their signaling pathway and subsequently focus on TLR5. Thereafter, I will describe the phenotype of *TLR5* KO mice and elucidate human genetic associations of *TLR5* with diseases.

Toll-like receptors (TLRs) have a central role in early host defence against invading pathogens[4,70,71]. Discrimination of various microbial ligands depends majorly on the highly conserved family of TLRs, which are broadly expressed in many cell types, including nonhematopoietic cells, such as epithelial[24] and endothelial[72] cells. Regardless, only an exclusive subset of these receptors is expressed in most of the cell types. On the contrary, crucial immune cells in the early immune defence as haematopoietically derived macrophages, neutrophils and DCs, do express most of the TLRs. (reviewed in[73]) The TLR pathway can initiate a variety of immune responses, inflammatory and antimicrobial.

TLRs are type I transmembrane glycoproteins, which are expressed at the cell plasma membrane facing outward, recognizing extracellular ligands. TLRs are also expressed in subcellular compartments such as the endosome, where they can survey microbial ligands intracellularly. TLRs belong to the Interleukin-1 receptor (IL-1R) family. They consist of an N-terminal leucine-rich-repeat (LRR) for ligand binding, a single transmembrane domain, and a C-terminal intracellular signalling domain[71]. The N-terminal extracellular domain is characterised by 19-25 repeated copies of an LRR motif. Each repeat contains 24 – 29 amino acids, enriched with a characteristic leucine-rich sequence XLXXLXLXX, and another conserved sequence XØXXØX4FXXLX[74]. In these sequences, X indicates for any amino acid and Ø for a hydrophobic amino acid. This allows the formation of a horseshoe structure, where MAMPS are recognized on their concave surface. Remarkably, even though the LRR domain is highly conserved, each TLR can sense with its domain various ligands[6,75]. The C-terminal domain is involved in signal transduction and is homologous to the intracellular domain of IL-1R and thus referred to as the Toll/IL-1 receptor (TIR) domain[71]. (reviewed in[76])

1.5.1 The TLR family and their ligands

Although the number of existing TLRs is limited, they can recognize a wide array of ligands derived from bacteria[77,78], viruses[79,80], fungi[81], and protozoa[82] and thus are highly efficient in protecting the host from invading pathogens.

Many TLRs are able to recognize several structurally unrelated ligands. So far, 13 mammalian TLRs have been identified, 10 in humans and 13 in mice. TLR 1-9 are conserved among humans and mice. TLR 10 is uniquely present in humans, while TLR11 is only functional in mice. (reviewed in[73]) The specific ligand of TLR10 is not identified yet and the biological role of the receptor still under investigation[83,84]. TLR12 has been found to recognize profilin and protect from *Toxoplasma gondii*[85]. TLR13 in mice is an RNA sensor[86-88]. Below, TLRs expressed in humans and their ligands (reviewed in [70,73,89,90]) are summarized, in Table 1-1.

Table 1-1 Overview of human Toll-like receptors and their ligands.

TLR	Dimer-formation with TLR	Activating ligands	Cellular localization	TIR-containing adaptor	Comments
1	2	tryiacylated lipopeptides	surface	MyD88	
2	2	lipoteichonic acid, mycobacterial cell wall	surface	MyD88/Mal	
	1	triacylated lipopeptides			
	6	diacylated lipopeptides			
3		dsRNA	endosome	TRIF	activates IRFs
4	2	LPS	surface	MyD88/Mal,	LPS bound to co-receptor MD-2 is recognized
			endosome	TRAM/TRIF	→NF-κB activation →IRF activation
5		flagellin	surface	MyD88	
6	2	diacylated lipopeptides	surface	MyD88/Mal	
7		ssRNA	endosome	MyD88, Mal	
8		ssRNA	endosome	MyD88, Mal	
9		unmethylated CpG-rich DNA	surface or endosome	MyD88, Mal	highly expressed in B cells
10		unknown	surface		present only in humans; role unclear

1.5.2 TLR signaling pathway

TLR activation has a critical impact on the host and thus has to be stringently regulated. Ligand binding to corresponding TLRs, facilitates the dimerization of these receptors, inducing conformational changes required for the recruitment of adaptor proteins[90]. Signal transduction is mediated by the homotypic interaction of cytoplasmic TIR domains of TLRs and TIR domain-containing adaptor protein[91].

TLR signaling can lead to distinct target gene expression programs, including inflammatory cytokines, chemokines, major histocompatibility complex (MHC), and effectors such as inducible nitric oxide synthase and antimicrobial peptides. These are facilitated by the use of different adaptors in the TLR signaling of some TLRs, to modulate the immune response.[6] The most prominent and in so far known TLRs, except TLR3, mainly used adaptor protein is Myeloid differentiation primary response protein 88 (Myd88). Some of the TLRs, namely TLR2, TLR5, TLR7/8, TLR9, and TLR11 exclusively signal through Myd88[73].

As reviewed in[76] , Myd88 has a C-terminal TIR domain and an N-terminal Death domain. Activation of a TLR by binding of its respective ligand induces a conformational change of the C-terminal domain of the TLR. This enables the activated TLR and Myd88, which is recruited as a homodimer to the receptor[92], to interact through their TIR domains. Members of the Interleukin-1 receptor-associated kinase (IRAK) family, such as the serine/threonine IL-1 receptor-associated kinase-4 (IRAK-4), contain a death domain. Accordingly, downstream signaling occurs by interaction of Myd88 with (IRAK-4) by their respective death domains[93-96].

IRAK-4, in turn, recruits IRAK-1, which engages the kinase function of IRAK-1[97], leading to its autophosphorylation and recruitment of the tumor necrosis factor receptor-associated factor-6 (TRAF6) to the Myd88/IRAK-4/IRAK-1 complex. This enables IRAK1 and TRAF6 to disengage from the receptor complex and interact with another complex consisting of TAK1, TAB1, and TAB2 or TAB3. TAK-1 is important for IL-1/LPS, TNF- induced NF-κB signaling[98]. TAB 1-3 are TAK 1 binding proteins. TAB2 and TAB3 function redundantly and mediate the linkage of TAK1 to TRAF6, thereby promoting TAK1 activation[99,100]. This event results in phosphorylation of TAB2/3 and TAK1, followed by translocation of these components together with TAB1 and TRAF6 to the cytoplasm.[76]

Next, in the cytoplasm, TAK-1 is activated, which subsequently results in the activation of IKKs and is followed by their phosphorylation of IκBs. The phosphorylation results in the degradation of IκB and as a result release of NF-κB[101,102]. This enables NF-κB to translocate to the nucleus to its DNA binding sites and regulate transcription of a large number of genes. The activation of TAK1 also

facilitates the activation of activator protein 1 (AP-1) and MAPKs, including JUN N-terminal kinase (JNK).[76]

Further, activation of transcription factors (AP-1) and NF-κB activation result in transcription of genes encoding proinflammatory cytokines and chemokines such as TNFα, IL-6, IL-8, and IL-1β.[73,103-105].

The NF-κB family consists of several members, namely RELA (p65), NF-κB1 (p50;105), NF-κB2 (p52; p100), c-REL and RELB[106,107]. The commonly activated form of NF-κB consists of p65 and p50 or p52. Whereas p50 and p65 are widely expressed, other members are restricted in their expression location, i.e. REL B in regions of the thymus, lymph nodes and Peyer`s patches, c-REL hematopoietic cells, and lymphocytes. NF-κB signaling activation can impact many additional processes. Beside the above mentioned, these include, control of innate and adaptive immune response as for example induction of transcription of pro-inflammatory cytokines and chemokines, as mentioned above, but also of adhesion molecules, antimicrobial peptides, anti-apoptotic proteins and stress-response proteins and emerges to a wide range of stimuli, i.e. pathogens, stress signals and pro-inflammatory cytokines (reviewed in [108]). Thus, dysregulated NF-κB activation is associated with inflammatory diseases, i.e. rheumatoid arthritis, inflammatory bowel disease and cancer. (reviewed in[109,110])
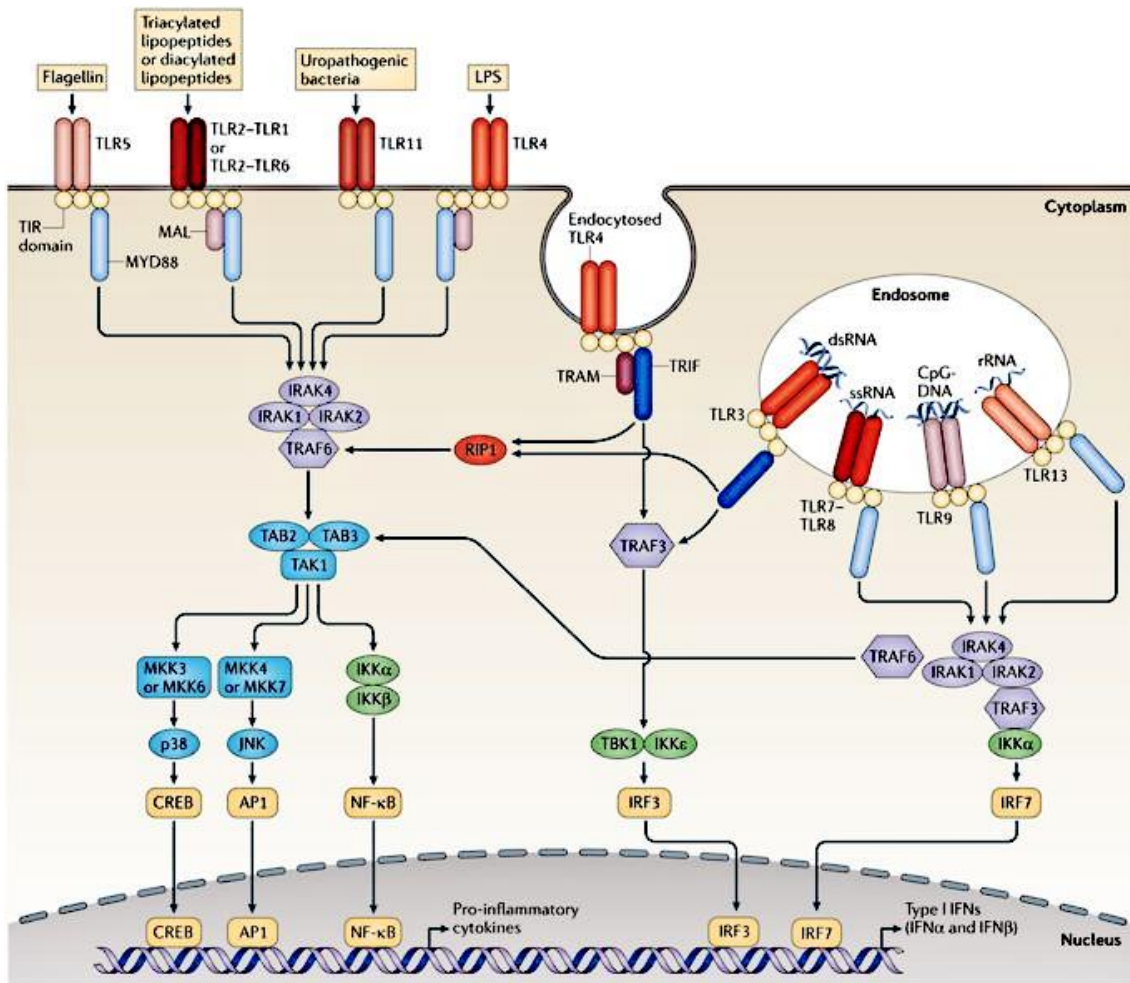
Nature Reviews | Immunology

Figure 1-2 Mammalian TLR signaling pathways.
Figure and adapted legend from O`Neill et al.[89]. TLRs are central Pattern recognition receptors, which recognize a variety of ligands. Corresponding to their recognized ligands, each TLR is placed at different compartments in the cell, i.e. TLR5, the heterodimers of TLR2–TLR1 or TLR2–TLR6, TLR11 (only functional in mice) and TLR4 are located at the cell surface, whereas TLR3, the heterodimer TLR7–TLR8, TLR9 and TLR13 are localized to the endosomes suitable to their task to sense nucleic acids derived from microbes and the host itself. TLR4, uniquely, is present at both sides, the plasma membrane and the endosomes. TLR signaling is initiated by recognition of ligand by its corresponding TLR and induces dimerization of respective receptors, which allows a conformational change. Subsequently, the Toll–IL-1-receptor (TIR) domains of each TLR interact with their specific homotypic TIR domain-containing adaptor protein (i.e. myeloid differentiation primary-response protein 88 (MYD88), MYD88-adaptor-like protein (MAL), TIR domain-containing adaptor protein inducing IFNβ (TRIF) or TRIF-related adaptor molecule (TRAM)). Hereby, TLR4, uniquely is able to utilize different adaptor proteins depending on targeted outcome, either inducing proinflammatory cytokines via Myd88 or IFNs via TRIF at the endosome. Activation of adaptor molecules leads to interaction with IL-1R-associated kinases (IRAKs) and the adaptor molecules TNF receptor-associated factors (TRAFs), which further initiate the activation of the mitogen-activated protein kinases (MAPKs) JUN N-terminal kinase (JNK) and p38, finally leading in activation of transcription factors, mainly nuclear factor-κB (NF-κB) and the interferon-regulatory factors (IRFs), but also cyclic AMP-responsive element-binding protein (CREB) and activator protein 1 (AP1). TLR signalling mediates induction of pro-inflammatory cytokines of cell surface TLRs or induction of type I interferon (IFN) of endosomal TLRs.

1.5.3 TLR5 and its role in intestinal homeostasis

TLR5 is expressed on the cell surface of many cells, including monocytes, macrophages, neutrophils, dendritic cells, lymphocytes, NK cells and intestinal epithelial cells[3,111-115], which enables it to recognize widely extracellular flagellin. Unlike most of the other TLRs, TLR5 is able to recognize a protein structure[78,90].

In particular, TLR5 recognizes conserved amino acids present on the N- and C-terminal domain of flagellin, namely in D1 domain[116]. The D0 domain links both flagellin molecules and thereby promotes the dimerisation of TLR5[117]. The D1 and D2 domains are further found to be important for proinflammatory signaling[118,119], whereby the D1 domain is in direct interaction with the receptor[120].

Flagellin is a major subunit of the bacterial flagellum, which consists of several thousand flagellin monomers[121,122] and is used for motility[123] by many kinds of bacteria. Since the activating domain in flagellin for TLR5 activation is buried, when existing as a flagellum, only monomeric flagellin is able to activate TLR5[115,124].

TLR5 activation can result in manifold responses, such as induction of proinflammatory cytokines, nitric oxide, H_2O_2, chemokines, genes with antiapoptotic or stress-induced genes and host defense proteins, i.e. β-Defensin 2[125-131]. The activation of this PRR facilitates two options for subsequent events. On the one hand, TLR5 activation can involve Myd88 mediated signaling and leads to NF-κB and AP-1 activation resulting in the induction of genes implicated in host defense[132]. Alternatively, TLR5 activation can lead to the formation of TLR5/TLR4 heterodimer and involve TRIF, which results in the induction of antiviral cytokine, IFN-β[133]. This event further induces the activation of STAT1, which promotes inducible NO synthase (iNOS) gene transcription and NO production[133].

The gut is exposed to many host and microbial products, microbes and antigens. Thereby, intestinal PRRs have important functions in the gut[24]. They allow to contain gut microbes in the mucosal immune compartment and intestinal lumen[24]. A lack of TLR signaling, on the other hand, results in mice in a higher number of bacteria contained in spleens[134,135]. Further, TLR engaged activation of the innate immune system prohibits exaggerated adaptive immune responses[135]. One of the innate immune receptors with a major role in the gut is TLR5[136,137,138].

PRR localization and expression in the intestinal epithelium and respective DCs are well regulated and distinct to other tissues. In general, the expression of many TLRs on IECs is low[24]. In colonic epithelial cells, TLR5 is particularly expressed on the basolateral surface compared to the apical surface of these cells[111]. This localization of TLR5 enables the receptor to recognize flagellin of cell invading microbes rather than of present co-existing microbes on the surface of the host cell and subsequent

overt inflammatory response. The importance of TLR5 in the gut is quite obvious as uncontrolled levels of flagellin could lead to invasion of bacteria in tissues and induce inflammation[139-141].

Among the commensal gut microbiota, many species do express flagellin[141], including *E. coli*. However, when the gut barrier is compromised, the commensal *E. coli* can become pathogenic[142]. Under normal conditions, TLR5 activation promotes the expression of antiapoptotic genes[128], which protects the cell and maintains epithelial homeostasis. In contrast, when TLR5 in cell lines is activated, a proinflammatory response is induced[111], which is also the case in human colonic mucosa[137].

1.6 Phenotype of *Tlr5* KO mice

1.6.1 *Tlr5* is associated with maintenance of inflammatory response, altered microbiota and diseases like metabolic syndrome, colitis and CRC

In a study by Vijay-Kumar et al.[141], *Tlr5* KO mice displayed different phenotypes. 10 % of mice developed severe colitis and 30 % of mice showed histopathologic evidence of colitis. Remaining 60 % of *Tlr5* KO mice in this study showed proinflammatory gene expression, i.e. IL-1β, IL-18, but didn`t fall into the classification of colitis. Latter mice displayed higher body masses. In a follow-up study[140], *Tlr5* KO mice were shown to develop obesity and metabolic syndrome with an increased level of triglycerides and cholesterol in the blood, higher blood pressure, and insulin resistance. Further, in *Tlr5* KO mice an altered microbiota was found, which upon transfer to WT germfree mice displayed hyperphagia, parameters linked to metabolic syndrome and higher levels of proinflammatory cytokines. In particular, metabolic syndrome in human and mice are associated with shifts in the relative abundance of Bacteroidetes and Firmicutes, whereas here a specific set of bacterial species is altered by loss of *Tlr5*. This emphasizes the role of *Tlr5* in regulating gut microbiota and metabolic homeostasis.

Similar results were found by Carvalho et al.[139], when *Tlr5* WT or KO offspring of heterozygous *Tlr5* carriers were tested to evaluate the impact of solely host genetics on gut microbiota. Sequencing of cecal bacteria at 12 weeks revealed an elevated level of Proteobacteria (and lower level of Bacteroidetes) in colitic *Tlr5* KO mice compared to non-colitic *Tlr5* KO or WT mice. A comparison of microbial composition from weaning to 11 weeks of age showed greater variability of microbiota in all *Tlr5* KO mice and delayed stabilization compared to WT mice. Enterobacteria were one family, but not alone, contributing to high variances in abundance during the time course. Other studies (Lupp et al.[143], Nagalingam et al.[144]) have also reported a

correlation between elevation in Proteobacteria and colitis. In colitic *Tlr5* KO mice, enterobacteria were observed to have penetrated the mucus layer and being close or in direct contact to the epithelium.

1.6.2 *Tlr5* activation regulates microbial flagellin expression and sIgA production in host.

Cullender et al.[145] showed in *Tlr5* KO mice that loss of *Tlr5* function results in a reduced anti-flagellin IgA response despite higher total IgA production. Further, when *Tlr5* was not functional, flagellin amounts were enhanced, indicating that reduced anti-flagellin IgA response allows bacteria to sense an absent recognition of flagellin and hence promote their upregulation

By recognition of flagellin, *Tlr5* is able to regulate the intestinal flagellin level and maintains gut homeostasis. An enhanced level of flagellin has been associated with a breach of the gut mucosal barrier and inflammation. Present microbial phyla in the gut include Bacteroidetes, Firmicutes, and Proteobacteria, where the latter ones are able to produce flagellin. Even though a broad diversity of gut commensals is genetically capable to produce flagellin, flagellin levels in the gut are controlled. TLR5 activation leads to the production of flagellin specific IgA in the gut. It has been shown that bacteria are able to regulate their gene expression in response to the environment.[145]

Cullender et al.[145] further showed in their study that *Tlr5* KO mice compared to WT produce lower flagellin specific IgA in ceca and fecal pellets despite higher total IgA levels. Further, stimulation of TLR5 HEK reporter cells, which allows to evaluate the activating flagellin content in samples used for stimulation, revealed enhanced intestinal flagellin levels in fecal samples of *Tlr5* KO mice compared to *Tlr5* WT mice. Both latter observations, resulted from the loss of TLR5 signaling. Further, comparison of WT and *Tlr5* KO mice showed no metagenomic differences indicating both genotypes are capable to encode for the same genes but were distinct in their metatranscriptome profile in ceca. Flagellin transcripts derived majorly from commensal members of the phyla Firmicutes, as for example of *Roseburia*, *Eubacterium*, and *Clostridium*. Additionally, a subset of flagellin transcripts elevated, were mapped to the phyla Proteobacteria, as for instance *Desulfovibrio spp.*.

In addition, they assessed the consequence of different IgA repertoire, KO mice had increased total IgA level with reduced flagellin-specific IgA level, on bacterial coating. Similar levels of bacteria in the cecum were found to be coated with IgA for WT and *Tlr5* KO mice. However, *Tlr5* KO mice resulted in overcoating of Firmicutes and undercoating of Proteobacteria compared to WT, while coating for

Bacteroidetes remained similar for both. It suggests that the IgA coating of Firmicutes is compensated by another IgA than flagellin specific IgA.[145]

In terms of diseases, which are associated with dysbiosis, where often the ratio between Bacteroidetes and Firmicutes is considered important, alterations in TLR5 signaling as in the case of SNPs may result in a different coating of gut bacteria of Firmicutes, and thus be a crucial factor. Further, even though attention is drawn to the ratio of Bacteroidetes/Firmicutes, a report has shown that genes from Proteobacteria, are among those highly adjustable to the environment[146].

IgA were thought to bind their antigen, leading to agglutination of bacteria and entrapment in mucus, which result in clearance from mucus. *In vitro* assays have shown that anti-flag sIgA have a distinct feature from anti-LPS sIgA by completely inhibiting motility of bacteria, whereas latter one only partially is able to. *Tlr5* KO mice further showed bacteria of Proteobacteria and Firmicutes penetrating the crypts and villi of small intestine and being present in the inner mucus layer (which is usually devoid of any bacteria) of the large intestine, thereby being in direct contact to epithelial cells. This was not the case in WT. Thus, TLR5 signaling and its induced flagellin specific IgA is crucial to avoid risk of developing chronic inflammation.[145]

1.6.3 Genetic association of *TLR5* with human colorectal cancer

In 2013 a study published by S. Klimosch et al.[147] (our laboratory group), demonstrated for the first time, associations of different *TLR5* SNPs to be associated with CRC survival.

Heterozygous, or heterozygous and homozygous, *TLR5* N592S SNP carriers were found to be associated significantly with both, worse CRC and overall survival. In contrast, homozygous, or heterozygous and homozygous, carriers of *TLR5* F616L SNP were shown to be significantly associated with better CRC survival. F616L and N592S both are missense SNPs, present in the ectodomain of TLR5, which may be crucial for dimerization of the receptor or signal transduction. Both TLR5 SNPs are unique for human. Different models were applied to elucidate their roles.

HEK FLP-IN™ T-REX™ 293T cells, stably expressing TLR5 WT or SNP constructs, were generated to evaluate their response in *TNF* induction and IL-8 secretion, after flagellin stimulation. TLR5 SNP R392X, which is also present in the ectodomain, encodes for a STOP codon leading to a hyporesponsive phenotype[148] and was used as a negative control. Whereas TLR5 N592S showed slightly different outcomes compared to WT, depending on the species, from which the flagellin for stimulation derived from, TLR5 F616L consistently showed low response after stimulation with any tested flagellin. However, no difference in signaling was observed stimulating

transiently transfected CRC cell lines as HCT116, DLD1 or HEK293 with corresponding SNP constructs and subsequent flagellin stimulation.

When analyzing whole blood of WT vs homozygous F616L SNP carriers, again a hyporesponsive phenotype was confirmed, resulting in reduced p38 phosphorylation, CD62L shedding, and proinflammatory cytokines, as IL-6 and IL-1β. The authors point out that elevated IL-6 levels in serum and tumor tissue are associated with a tumor-promoting role via STAT3[149], which could explain the ameliorated survival of homozygous F616L SNP carriers in CRC. The number of N592S carriers was not enough to test the effect of these carriers on immune response, but a hyperresponsive result was suggested.

Table 1-2 TLR5 SNPs N592S and F616L are associated with colorectal cancer
Figure adapted from Klimosch et al.[147] by A.Weber. Legend adapted from Klimosch et al.[147]. TLR coding variants with major allele frequency (MAF) > 0.05% were screened for associations in a case-control study of white Caucasians in Czech Republic, retrospectively analyzed (n=613). Heterozygous N592S carriers have significantly nearly twice higher probability to die from CRC, whereas homozygous *TLR5* F616L carriers reveal better survival in CRC. CRC (colorectal cancer), HR (hazard ratio).

SNP	Genotype		No.	Deaths (%)	HR (95% CI)	P value
					Cause of death: CRC	
SNP1 TLR5 (N592S)	AA		468	77 (16.45)	1.00	
	AG		135	36 (26.67)	1.92 (1.29-2.87)	0.001
	GG		5	1 (20.00)	1.13 (0.16-8.14)	0.90
SNP2 TLR5 (F616L)	TT		191	42 (21.99)	1.00	
	CT		278	50 (17.99)	0.73 (0.48-1.10)	0.13
	CC		128	17 (13.28)	0.51 (0.29-0.93)	0.03
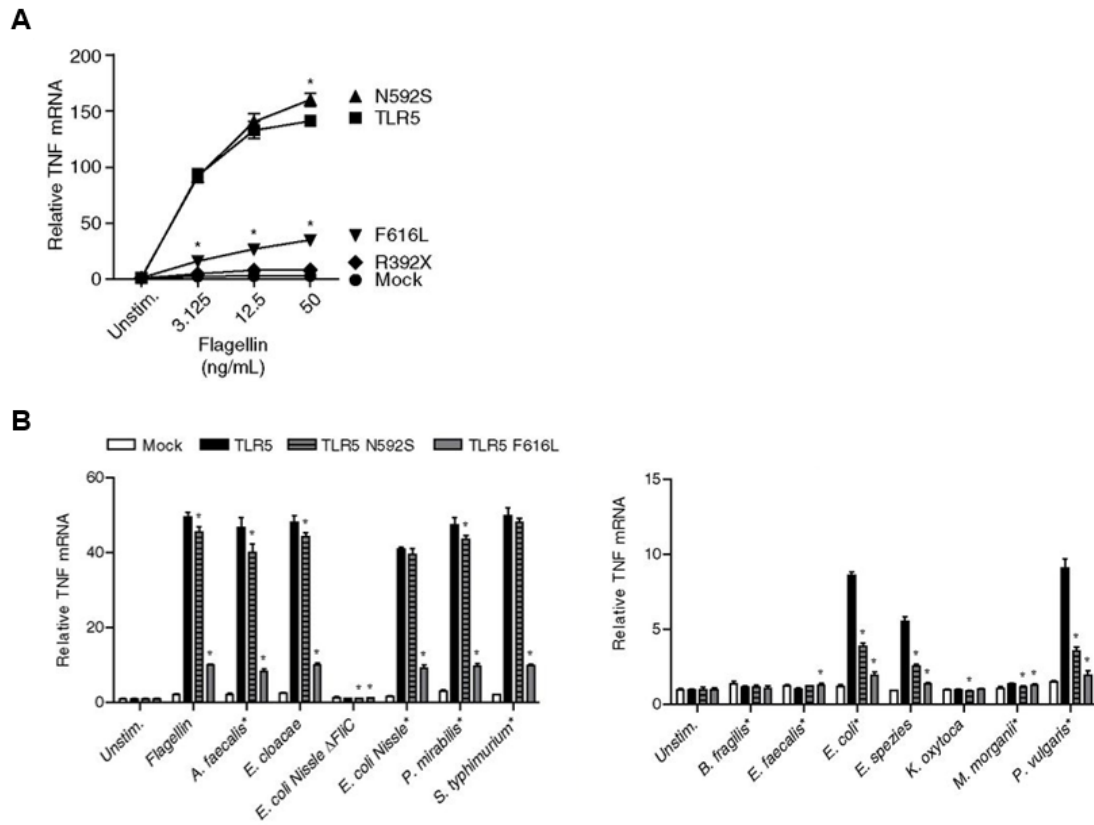
Figure 1-3 Coding *TLR5* SNPs modulate responsiveness to flagellin.
Figure and legend adapted from Klimosch et al.[147]. A) HEK FLP-IN™ T-REX™ 293T cells expressing Wildtype (WT) or TLR5 SNP (R392X), (N592S) and (F616L), which are all located in the ectodomain of TLR5, were stimulated with different amount of flagellin. TLR5 activation was assessed by analyzing induced *TNF* mRNA by qPCR. One representative experiment out of three (triplicate mean ± SD) was shown. Whereas N592S acts similar or significantly slightly elevated at higher tested amount, a hyporesponsive outcome is observed in F616L, whereas as expected in TLR5 signaling abrogated R392X SNP, no dose-dependent signaling is seen. B) TLR5 cell lines stably expressing tested TLR5 SNP were analyzed also for *TNF* mRNA upon stimulation with heat-killed bacterial preparations, mainly gut related. These show again a hyporesponsive outcome for F616L, whereas N592S reveal significant slight reduced or similar *TNF*-induction as WT. Depicted was one representative experiment out of two (triplicate mean ± SD). *, $P < 0.05$ (unpaired *t* test).

1.6.4 Genetic association of *TLR5* with other diseases

A study conducted by Sironi et al.[150] in a cohort of Saudi Arabians elucidated a role of genetic susceptibility of *TLR5* carriers in metabolic diseases, like Type 2 diabetes. They reported *TLR5* R392X being protective from obesity but predisposing to Type 2 diabetes, which is an altered result to *Tlr5* KO mice. They proposed metabolic diseases including Type 2 diabetes to be associated with immune dysregulation. All, and in particular female carriers, of R392X were significantly protected from obesity. Interestingly, they found female R392X carriers alone associated significantly with Type 2 Diabetes. Additionally, all, and in particular female carriers, of R392X of non-diabetic subjects revealed increased plasma glucose levels. Further, reduced

production of proinflammatory cytokines upon flagellin stimulation in PBMCs of heterozygous R392X carriers compared to homozygous were reported.

Other reports also exist stating gender-specific associations of human gut microbiota[151-153]. In line with the importance of TLR5 in recognition of flagellated bacteria, other studies have associated R392X to enhanced susceptibility to several diseases, including Pneumonia[154], Legionnaires disease[148], urinary tract infections[155] and bronchopulmonary dysplasia[156]. Besides, also in an Indian population R392X carriers were associated significantly with a higher risk for UC whereas N592S was associated with a lower risk for UC[157]. Further, in another study TLR5 F616L was found to be modestly associated with CD[158].

Further, a study[159] revealed, TLR5-dependent commensal bacteria increase systemic IL-6, thereby driving malignant progression at extra mucosal locations. In TLR5-unresponsive tumor-bearing mice, IL-17 was found to be upregulated and only accelerates malignant progression, when tumors were not responsive to IL-6. Differences in tumor growth based on *TLR5* were abrogated when commensal bacteria were depleted.

1.7 Nod-like receptors (NLRs)

In the next chapters, I will first give an overview of NLRs and the inflammasome complex as a signaling pathway. Then, I will focus particularly on NLRP6, describe the phenotype of *Nlrp6* KO mice and state human genetic associations of *NLRP6* with CRC.

Nod-like receptors (NLRs) are innate immune receptors, which survey the cytosol and thus are a critical line of defense. They are able to sense cell threats, such as microbial invasion and environmental or endogenous noxious substances upon whichh they mediate protective responses to the host[7]. NLRs can act synergistically with TLRs[160], which allows an effective immune response of the host. The importance of NLRs can be seen in its conservation among plants to humans[161]. They maintain inflammatory processes through the initiation of cytokines, chemokines, and anti-microbial genes[162]. Some NLRs can act through a complex, termed inflammasome[163], activating e.g. caspase signaling while others activate NF-κB and MAPK signaling without the formation of this complex[162]. NLRs are linked to several human diseases as infections, cancer, autoimmune and inflammatory disorders[164].

NLRs have three characteristic domains: An N-terminal domain, which enables protein-protein interaction and is responsible for signal transduction, a central NACHT (or nucleotide binding domain (NBD)) domain, which is necessary for self-

oligomerization and a C-terminal LRR domain, allowing ligand recognition[165]. In case of missing receptor stimulation, another important function carried out by the LRR domain is the suppression of NLR signaling, which is fulfilled by disguising the N-terminal domain with the LRR domain[163].

NLRs are categorized into subfamilies according to their N-terminal domain[165]. Up to date, 23 human NLRs are known [162,166]:
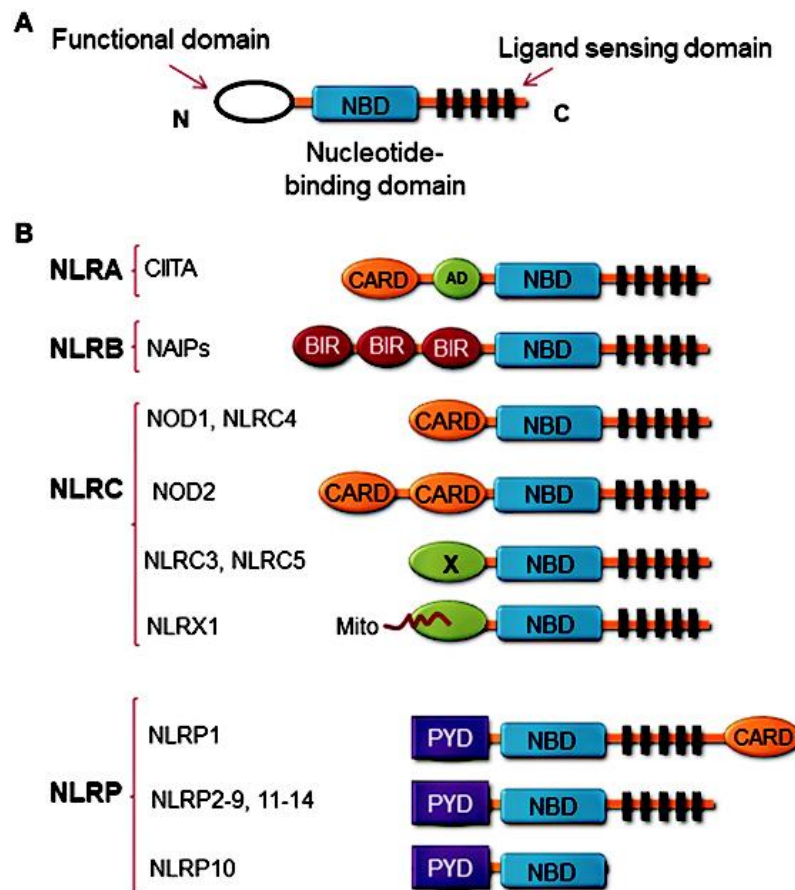
Figure 1-4 The structure of Nod-like receptors (NLRs).
Figure from Gharagozloo et al.[166]. (A) NLRs contain an N-terminal functional domain, a central nucleotide binding and oligomerization domain (NBD), and a C-terminal ligand sensing domain (LRR). (B) NLRs are categorized based on their functional domain: NLRA or Class II transactivator (CIITA) carry an acidic transactivation (AD) domain and function as transcriptional regulators of MHC class II antigen presentation, NLRBs or neuronal apoptosis inhibitor proteins (NAIPs) contain a baculoviral inhibitor of apoptosis protein (IAP) repeat (BIR), NLRCs have a caspase-activation and recruitment domain (CARD) and NLRPs are characterized by their Pyrin domain (PYR). A subfamily of NLRC, namely NLRX, contain an unknown domain (X).[7] Further, NLRX1, contains an N-terminal sequence targeting it to the mitochondrial membrane (Mito)[166].

NLRP1, NLRP3, NLRP7, NLRP12, NLRC4, and NAIP are known to form so-called inflammasomes. NLRP10, NOD1, NOD2, NLRC3, NLRC5, NLRX1, and CIITA fulfill their tasks by regulating NF-κB and MAPK pathways, or by serving as transcriptional regulators in the nucleus.[167]

1.7.1 The inflammasome complex as signaling platform

Several NLR proteins are known to be able to form multiprotein platforms[7], which are termed `inflammasomes`[163]. These complexes consist of an NLR protein, ASC and a Caspase[163,168]. Caspases are cysteine proteases and available as an inactive zymogen[169], pro-caspase. Inflammasome activation leads to maturation of pro-caspase to Caspase by autoproteolytic cleavage, which is essential for inflammasome activity[163]. In humans, Caspase-1, but also Caspase-4, Caspase-5, and Caspase-12 (Caspase-1, -11, and -12 in mice) are recognized to play a role in inflammatory processes[169,170]. In the canonical inflammasome activation, mainly Caspase-1 is involved in processing of pro-IL-1 and pro-IL-18 into their mature forms upon inflammasome activation, leading consequently to the release of these cytokines out of the cell and induction of inflammation[163,171,172]. The role of Caspase-4, -5 and -11, on the other hand, is found to rather interact with and activate Caspase-1[173,174]. Further, Caspase-8, which plays a role in apoptotic processes and regulation of inflammatory processes, has been found to promote directly or indirectly the processing of pro-IL-1 and pro-IL-18[169,175]. Usually, after inflammasome activation, the cell itself undergoes pyroptosis[176] a form of programmed cell death. Inflammasome activation can lead to an extremely effective, inflammatory environment, which includes a strong migration of immune cells, such as neutrophils and natural killer cells[177].

Inflammasome formation is promoted by diverse substances that occur during infections, metabolic imbalances or tissue damage[177]. It can be activated by i.e. uric acid crystals[178], extracellular ATP[179] and oxidized phospholipids[180], which are danger-associated molecules from the host and allow to sense cellular death without direct detection of products deriving from the pathogen[181]. The best studied inflammasome to date is NLRP3. Based on data of NLRP3, inflammasome activation has been shown to depend on two signals[182]. Signal I is provided by TLR activation and downstream NF-κB activation, upon which the transcription of inflammasome components are upregulated. Signal II derives from microbe or danger-associated molecular patterns, which results in inflammasome assembly.[182,183] Inflammasome formation is conducted through the Pyrin-Pyrin interaction of NLRP and ASC, and CARD-CARD interaction of ASC and pro-caspase[184].

1.7.2 NLRP6

NLRP6 (previously termed PYPAF5) is an innate immune receptor, which is still intensively researched and particularly has drawn attention due to its role in the regulation of gut homeostasis found in mice. Knowledge of NLRP6, so far, mainly derives from studies in mice models and in *in vitro* models.

In mice, NLRP6 has been found to be highly expressed in duodenum, ileum, and colon whereas in human it is expressed to a lesser extent in the gut, in the duodenum, jejunum, and ileum[185]. Further, NLRP6 has been found to be expressed in hematopoietic cells in the colon but also in non-hematopoietic cells in lamina propria cells of granulocytic and monocytic lineage, in mice[186].

NLRs can be involved in different functions as inflammasome activation, negative regulation of NF-κB and MAPK pathways involving cytokine and chemokine expression and regulation of antiviral immunity[164]. Intriguingly, whereas other known NLRs have been shown to be involved in one of the three functions, NLRP6 is suggested to participate in all three functions[187-189]. NLRP6 has been shown to activate NF-κB when co-expressed with ASC in HEK cells *in vitro*[189], thereby indicating a role as an activator or regulator of NF-κB. Interestingly, it has been reported that in rats, NLRP6, ASC, Caspase-1, and pro-IL18 and processed IL-18 are only detected in the gut at embryonic day 20 during the postnatal period, coinciding with the colonization of the gut ecosystem[190].

NLRP6 is thought to function as an inflammasome, even though no direct evidence exists. During the compilation of my thesis, NLRP6, ASC and Caspase-1 interaction was indirectly shown by IP[191]. Further, similarities in phenotypes of mice lacking one of the inflammasome components in microbial composition were considered as an indication for the inflammasome formation of NLRP6[192]. However, the formation of an inflammasome by NLRP6 is controversial. Intriguingly, even though *in vitro* NLRP6 has been shown to generate IL-1β[189], in contrast, in mice models, in particular, an effect of NLRP6 on the regulation of IL-18 is found[187,191].

Further, microbial metabolites were suggested to be activators of NLRP6 inflammasome and thereby modulate the microbial environment[191]. However, results on NLRP6 determining intestinal microbial composition are controversial and studies by Mamantopoulos et al. claim that respective differences found in mice models employed in the study by Elinav et al. do not derive from host genetics and are based on experimental design[193].

Recently, after completion of the experimental work of my thesis, lipoteichoic acid (LTA), a major component of the cell wall of gram-positive bacteria, was found to bind and activate NLRP6. Thereby, it was shown that caspase-11 and caspase-1

are recruited by ASC and their processing leads to IL-1β and IL-18 maturation in macrophages. Intriguingly, the production of IL-18 was found to worsen systemic gram-positive pathogen infection.[194]

Mice models have revealed, NLRP6 to be of great importance and have versatile functions in regulating gut homeostasis, being involved in mucus secretion[195], generation of antimicrobial peptides[191] and containing gut microbiota[191,192]. Further NLRP6 has been shown to be involved in containing proliferation and to have an important role in wound healing in intestinal epithelial cells[186].

Key factors initiating carcinogenesis are exceeding inflammation, as well as dysregulated pathways in apoptosis and autophagy. NLRs are involved in these pathways and therefore can intervene in processes of cancer development and progression. Particularly, they play great roles at sites of intestinal host-microbiome interaction.[196]

In mice, NLRP6 expressed in non-hematopoietic cells, the intestinal epithelial cells, were found to play an important role in promoting tumorigenesis[186]. In humans, two *NLRP6* SNPs, namely, M163L and F361Y, have been found to be associated with risk for CRC[197].

1.8 Phenotype of *Nlrp6* KO mice

1.8.1 Role of NLRP6 in intestinal mucus secretion

Colonic Goblet cells (GC) continuously secrete Muc2, and thereby form mucus layers[198]. They express TLRs and NLRP6 inflammasome[199,200]. In mice, the deletion of Muc2 results in absent mucus, which subsequently enable bacteria to invade and occupy the crypts and promote inflammatory and carcinogenic processes[201,202]. To protect the mucus layer from invading bacteria, `sentinel GC`, which are situated at the beginning of the crypt are identified to sample unspecifically luminal content by endocytosis and secrete mucus upon recognition of TLR2, TLR4 and TLR5 ligands by ROS production and subsequently induced NLRP6 inflammasome activation, independent of IL-1β and IL-18. TLR5, however, was also found to be activated in a Myd88/TRIF independent pathway. This leads to Muc2 secretion of sentinel GC and release from the endoplasmic reticulum of Ca^{2+} generates Calcium-dependent signaling through gap junctions. This event, in turn, initiates mucus secretion of the sentinel GC neighboring GC in the upper crypt and respective GCs are ejected, which altogether leads to the expel of bacteria from the crypt opening, and protects the lower crypt and intestinal stem cells.[195]

1.8.2 NLRP6 is important for wound healing and is associated with colitis and tumorigenesis

Nlrp6 deficient mice resulted in incomplete mucosal regeneration and were prone to colitis[186]. *Nlrp6* KO mice models have revealed several functions of NLRP6 and shown its versatile role in maintaining gut homeostasis and its role in colitis and colorectal cancer. Interestingly, in this model and in a colitis-associated CRC model, NLRP6 expression was found to be significantly reduced after DSS treatment in the first model or in adenocarcinoma compared to nontumoral colonic tissue in the second model. This indicates for NLRP6 a protective role in intestinal inflammation and tumorigenesis. Additionally, DSS treated *Nlrp6* KO mice showed enhanced proliferation upon injury and upregulated transcripts linked to tumorigenesis. Further, non-hematopoietic cells (rather than immune cells in lamina propria) of *Nlrp6* deficient mice were found to promote tumors. Therefore, NLRP6 in non-hematopoietic cells are protective in colitis-induced tumorigenesis.[186]

1.8.3 Microbiota in *Nlrp6* deficient mice render susceptibility to dysbiosis

In a study[192], Elinav et al. found *Nlrp6*^{-/-}, *Asc*^{-/-} and *Caspase 1*[-/-] mice harbor similar microbiota. The microbiota of these mice was colitogenic when mice were treated with DSS and could be transferred to neonatal or adult WT, where it induced colitis as well. These microbiota compositions were characterized by an elevated abundance of Prevotellaceae (Bacteroidetes) and TM7, and reduction in Lactobacillus (Firmicutes). *IL18* [-/-] mice microbiota was also colitogenic and could be transferred to WT, inducing colitis, but were slightly different in composition from NLRP6 inflammasome deficient mice. The colitogenic microbiota was seen to be dominant and sustainable in the recipient for prolonged times.

However, another study claimed differences seen in microbial composition in *Nlrp6*^{-/-}, *Asc*^{-/-} and *Caspase 1*[-/-] mice compared to WT in this study do not derive from their genetic background and are influenced by the study design[193].

Further, in the previously mentioned study[192] by Elinav et al., NLRP6 inflammasome deficient mice were outlined by spontaneous colonic crypt hyperplasia, the formation of germinal centers with enlarged Peyer`s patches, elevated serum IgG2c, and IgA, inflammatory cell recruitment and DSS induced colitis. Antibiotic treatment of *Asc*^{-/-} mice reduced colitis severity compared to WT. Further *Nlrp6*^{-/-} and *Asc*^{-/-} mice showed multiple bacteria in crypt basis that according to its monomorphic phenotype was suggested to be *Prevotella* species. ASC and Caspase1 were found to be expressed highly in gut epithelial cells but also CD45$^+$ cells. NLRP6, on the other hand, mainly was expressed in epithelial cells, described to appear primarily within speckled cytoplasmic aggregates and barely detectable in CD45$^+$ cells. Thus,

NLRP6 inflammasome is crucial to maintain microbial balance. Further, NLRP6 inflammasome induced IL-18 is a critical (but not only factor) for colitogenic microbiota.[192]

It has been proposed that the function of the inflammasome in epithelial cells and immune cells might be different, in that in epithelial cells IL-18 is important to maintain gut barrier and regeneration whereas in immune cells it promotes proinflammatory responses[203].

1.8.4 NLRP6 inflammasome determining intestinal microbial composition

In vitro, transfection of NLRP6 inflammasome components and pull-down showed an interaction of NLRP6, ASC, and Capase-1, in a further study by Elinav et al.[191]. *In vivo*, *Nlrp6*^{-/-} mice displayed a reduced level of processed Caspase-1 compared to WT, which indicates a contribution in Caspase-1 processing by NLRP6 inflammasome. Further, Elinav et al. found microbial or host-derived metabolites to be activators (signal II) of NLRP6 inflammasome. These metabolites determine, via IL-18 derived from colon tissue, antimicrobial peptide (AMP) secretion, i.e. ITLN1, RELMβ and Angiogenin in colonic mucosa and thereby modulate gut microbial composition. In particular, IL-18 alone was sufficient to induce AMP, thereby allowing microbial balance.[191]

Additionally, inflammasome components deficient microbiota was shown to be dysbiotic and this microbiota was also found to be dominant over non-dysbiotic microbiota. Further, dysbiotic microbiota was shown to influence its persistence via modulated IL-18 secretion. Bile acid conjugate taurine, carbohydrates, and long-chain fatty acids have been found as potential microbiota-associated NLRP6 inflammasome activators. In contrast, host or microbiome-derived histamine and spermine suppress NLRP6 inflammasome activation. Moreover, it has been shown that taurine can rescue the inflammasome suppressive phenotype. Thus, the balance of inflammasome activators and suppressors determine the NLRP6 inflammasome outcome. Therefore, metabolite administration can be an important therapeutic tool, as it can form inflammasome signaling, which influences the microbial composition, host physiology and disease susceptibility.[191]

However, according to Mamantopoulos et al., NLRP6 do not shape the gut microbial composition and results found by Elinav et al. are based on the experimental design of the study[193,204].

1.8.5 Genetic association of *NLRP6* in human CRC

41 non-synonymous single nucleotide polymorphisms in 21 NLR genes, among these also 3 *NLRP6* SNPs, were systematically analyzed in a Czech cohort of sporadic colorectal cancer (CRC) (1237 cases, 787 controls), for their association with CRC risk and survival in a study by Huhn et al.[197]. The patient cohort was characterized as n=1237, median age: 63, 61.7 % males with malignancy in colon or rectum and healthy blood donors n=787, median age 47 years, 55.4 % males, cancer-free at the time of sampling. Hereditary-nonpolyposis colorectal cancer patients were excluded from this study. At the stage of the study, only *NOD1*, *NOD2,* and *NLRP3* have been directly associated with human CRC and were linked to susceptibility, progression and treatment of sporadic CRC, colitis and/or colitis-associated CRC[205,206]. This study showed six NLR SNPs to be significantly linked with risk for CRC, among these *NLRP2* rs1043673, *NLRP3* rs35829419, *NLRP6* rs6421985 (=L163M), *NLRP8* rs306457, *NLRP11* rs299163, and *NLRP13* rs303997.[197]

Table 1-3 Association of rectal and colon cancer with *NLRP6* SNPs.
Table and legend adapted from Huhn et al. [197]. *NLR* SNPs were systematically analyzed for their association with CRC in a Czech cohort of sporadic colorectal cancer (CRC) (1237 cases, 787 controls). Among *NLR* SNPs, *NLRP6* SNP L163M was one of the candidates found to be associated significantly with higher risk for rectal or colon and rectal cancer.

| Gene | | Risk of CRC | | | |
SNP	Genotype	Cases	Controls	OR (95%CI)	P Val
NLRP6 rs56159585 (F361Y)	T/T	927	630	1	
	T/A	221	118	1.30 (0.95-1.77)	0.1047
	A/A	19	7	0.98 (0.37-2.56)	0.9629
	T/A + A/A	240	125	1.27 (0.94-1.71)	0.1249
NLRP6 rs6421985 (M163L)	G/G	924	629	1	
	T/G	252	128	1.36 (1.01-1.83)	**0.0421**
	T/T	-	-	-	-
	T/G + T/T	252	128	1.36 (1.01-1.83)	**0.0421**

1.9 Aims of this study

NLRP6 SNPs M163L and F361L have been shown to be associated with a higher risk for colon and rectal cancer[197], whereas *TLR5* SNP N592S is associated with worse probability to die from colorectal cancer[147], while *TLR5* SNP F616L with better probability to survive from colorectal cancer[147]. With this background, our hypothesis is that SNPs of important intestinal PRRs, as in the case of *TLR5* and *NLRP6*, may alter gut immune parameters and microbial balance and thereby render carriers of these SNPs susceptible to diseases, such as obesity, colitis, and cancer.
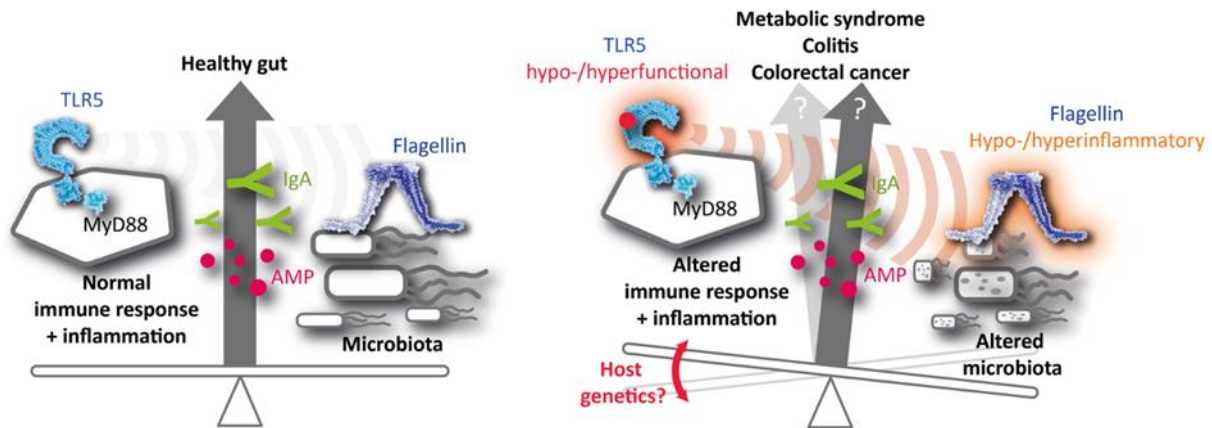
Figure 1-5 Hypothesis of thesis

Figure from Weber and Försti[207]. Pattern recognition receptors (here shown TLR5), which are important for gut immune and microbial balance in healthy status, may lead by alterations, i.e. in the case of SNP to an altered phenotype, i.e. hypo or hyper-responsive. Thereby, they can render intestinal immune parameters and microbial balance, which can result in associated diseases i.e. metabolic syndrome or CRC.

An understanding of basic mechanisms and functions of NLRP6 itself, which are not well understood to date, and the effect of *NLRP6* and *TLR5* SNPs on gut immune parameters and microbiome is central for the development of new therapies that specifically target malignant innate signaling and microbiome in human disease. Further, current knowledge is mainly based on functional studies conducted in mice and thus, many aspects of TLR5 and NLRP6 function in humans remain unclear. Therefore, this dissertation addresses the following questions in human:

- How do the *NLRP6* SNPs affect NF-κB activation in a cell system?
- Are *NLRP6* SNPs physiologically functional in terms of a functional effect of individual alleles on immune parameters in blood cells or stool?
- How do *TLR5* and *NLRP6* SNPs affect gut immune parameters and microbiota in otherwise healthy allele carriers?

Results on these questions will give us basic understanding and ideas on therapeutic strategies against diseases induced by these *TLR5* and *NLRP6* SNPs.

2 Materials and Methods

2.1 Molecular biology methods

2.1.1 Mutagenesis design for *NLRP6* constructs

The amino acid Leucine (defined as Wildtype) at position 163 in the NLRP6 protein sequence is encoded by the nucleotide codon CTG. Mutation to ATG results in the amino acid Methionine (SNP). The amino acid Phenylalanine (defined as Wildtype) at position 361 is encoded by the nucleotide codon TTC. A mutation to TAC or TAT both results in the amino acid Tyrosine (SNP). Here, we chose a mutation to TAC, which has a higher codon usage in mammals (https://www.genscript.com/tools/codon-frequency-table). The mutation for each amino acid was carried out sequentially. For mutations designed to probe the effect of Tyrosine at different amino acid positions (357-361) multiple mutations to TAC or TTC were used to generate Tyrosine or Phenylalanine mutants.

Table 2-1 Overview mutagenesis reactions for *NLRP6* construct generation.
SNPs are indicated in red. Primer sequences are given in Table 5-3. For further information on plasmids see Table 5-5.

Template	Aminoacid at 163_361	5`primer	3`primer	Resulting construct	Aminoacid at 163_361
Pex484 (NLRP6)	L_F	-	-		
Pex484 (NLRP6)	L_F	AWm525	AWm526	pTS1	L_Y
Pex484 (NLRP6)	L_F	AWm523	AWm524	pTS4	M_F
pTS1	L_Y	AWm523	AWm524	pTS6	M_Y
pTS4	M_F	AWm525	AWm526	pTS5	M_Y

Template	Aminoacid at 163_357-361	5`primer	3`primer	Resulting construct	Aminoacid at 163_361
Pex484 (NLRP6)	L_YFYKF	AWm527	AWm528	pTS2	L_**FFF**KF
pTS2	L_**FFF**KF	AWm523	AWm524	pTS7	M_**FFF**KF
pTS4	M_YFYKF	AWm527	AWm528	pTS41	M_**FFF**KF
pTS1	L_YFYKY	AWm531	AWm532	pTS3	L_**FFF**KY
pTS3	L_**FFF**KY	AWm523	AWm524	pTS8	M_**FFF**KY

2.1.2 Site-directed mutagenesis
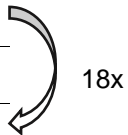
Site-directed mutagenesis was carried out to generate mutations in *NLRP6* using Stratagene QuickChange II Site-Directed Mutagenesis Kit XL by Agilent with a scaled-down protocol (Table 2-2) of the manufacturer. Mutagenesis primers were designed by the web primer design tool QuikChange Primer Design from Agilent Technologies (http://www.genomics.agilent.com/primerDesignProgram.jsp.), purchased from biomers.net GmbH and diluted in sterile DNase free H_2O. Quiksolution, reaction buffer, dNTP mix and enzyme were provided by the kit. DNA was amplified in peqSTAR 2x Gradient Thermocycler supplied by Peqlab (Table 2-3).

Table 2-2: Site-directed mutagenesis used to generate *NLRP6* mutated constructs.

Reagents	Volume	Final concentration
Reaction buffer (10x)	2 µl	1x
Template plasmid (10ng/µl)	0.4 µl	4 ng/20 µl
Primer Forward (100 ng/µl)	0.5 µl	50 ng/ 20 µl
Primer Reverse (100 ng/µl)	0.5 µl	50 ng/ 20 µl
dNTP mix (10 mM)	0.4 µl	0.2 mM
QuikSolution	1.2 µl	
ddH₂O	14.8 µl	
PfuTurbo DNA polymerase (2.5 U/µl)	0.2 µl	0.5 U
Final volume	20.2 µl	

Table 2-3: Thermocycler protocol to amplify mutated constructs in PCR.

Step	°C	Duration	
Heat lid	110		
1. Initial denaturation	95	1 min	
2. Denature	95	50 s	
3. Anneal	60	50 s	18x
4. Extend	68	6 min (1 kb/min)	
5. Final extension	72	10 min	
Hold	4	∞	

2.1.3 Mutation procedure and verification

The mutation is based on the amplification of the parental template DNA with the designed mutagenesis primer, resulting in a parental and a mutation harboring strain after each amplification cycle. At the end, DpnI is added to this reaction to digest the methylated parental supercoiled dsDNA, resulting in the mutated strain only. Electrocompetent cells were transformed with each of these reactions containing each of the mutated plasmid, inoculated in medium and plated on Kanamycin containing Agar plates. In the following, for each mutation reaction, three of the clones were picked and cultured for Miniprep of DNA. The plasmid was then first subjected to sequencing of the targeted mutation area in an automated sequencing process by GATC to confirm the desired mutation, and after sequence analysis by Geneious software and verification of the mutation, the rest of the plasmid from one clone of each mutation harboring the mutation was sequenced to verify the whole construct and ascertain no further, unwanted, mutations were carried by the plasmid.

2.1.4 Sequencing

Sequencing primers (AWs148-150) to verify *NLRP6* insert were designed according to the guidelines of GATC primer design (criteria: melting temperature should be between 52-55° C, primer length 17-19 bp, optimal GC content, at 3`end G or C but not more than continuous 3 x G or C, all 4 bases should be there but not more than 4 same bases in a row) using the following tool in Geneious Pro software: Primerdesign. Additionally, primers were checked at the webtool OligoCalc[208] (http://biotools.nubic.northwestern.edu/OligoCalc.html), especially in respect of melting temperature and self-complementarity of the designed primer. Primers have been chosen the way that they cover a specific mutation position. Automated sequencing usually leads into reads of around 1000 bp, where around 800 bp are reliable. Therefore, primers have additionally been designed in a way, that two primers have some overlapping reads. For sequencing primers used and their binding site see Table 2-4. For sequencing from the backbone into the beginning of *NLRP6*, a commercial standard GATC primer UP-2 or UP-40 were selected, which anneal 153 bp or 169 bp upstream of *NLRP6* in the backbone.

Table 2-4 Designed sequencing primers and their binding sites.
Listed are commercially available GATC primer for sequencing backbone or designed sequencing primer (sequence listed in Table 5-4) for *NLRP6* and noted, if reads with this primer encompass mutation sites.

Sequencing primer	From	Mutation verification
UP-2	153 bp upstream *NLRP6* in backbone	L → M
UP-40	169 bp upstream *NLRP6* in backbone	L → M
Aws148	673 bp in *NLRP6*	
Aws149	1456 bp in *NLRP6*	(Y → F), F → Y
Aws150	2266 bp in *NLRP6*	

Sequencing was conducted by automated sequencing at GATC. 20 µl of plasmid at a concentration of 35 ng/µl and 20 µl of sequencing primers at 10 µM were sent. Standard GATC primers as UP-2/UP-40 were provided by the company. Gene sequences were retrieved from NCBI (https://www.ncbi.nlm.nih.gov/gene). Sequencing results were analyzed in Geneious Pro software (version 5.5.6).

2.1.5 Transformation of *E.coli*

Plasmids were propagated in *E.coli*, usually, DH5α cells or when propagated plasmid contained a *CCDB* gene (i.e. destination vectors for GATEWAY cloning: pex117, pex118, pex145, pex146, pex147) in DB3.1 cells. 1 µl of plasmid DNA was added to 50 µl of competent cells in a precooled tube and incubated 30 min on ice. To induce bacterial cell transformation with an added plasmid, a heat-shock treatment was performed by placing the cells in the tube in a water bath at 42 ˚ C for 45 s and subsequently on ice for 5 min. 120 µl of pre-warmed S.O.C or NZY⁺ medium was added to the tube to cultivate the cells in a shaker at 160 rpm, 37 ˚ C for 1 hour. All of the cell suspension was plated on agar plates containing appropriate antibiotics and incubated inverted at 37 ˚ C over night in an incubator.

2.1.6 Plasmidisolation from transformed *E.coli*

For Miniprep clone were picked from agar plate of transformed *E.coli* and propagated in 3-5 ml LB medium supplemented with appropriate antibiotics or for Midiprep a small fraction of glycerol stock containing transformed *E.coli* with plasmid of interest propagated in 150 – 250 ml LB medium supplemented with appropriate antibiotics and incubated in a shaker at 160 rpm, 37 ˚ C over night.

Cells were pelleted at maximum speed (3220 g) for 10 min and the pellet resuspended in 600 µl DNase/RNase free H_2O for Miniprep. DNA was isolated utilizing Promega kits PureYield^{TM} Plasmid Miniprep or Midiprep System according to manufacturer`s instruction. For Midiprep System 5 ml of cell resuspension solution, 5 ml of Cell lysis solution and 8 ml of Neutralization solution was used for 150 – 250 ml bacterial culture. Extracted DNA via Miniprep was resuspended in 60 µl of DNase/RNase free sterile H_2O.

2.1.7 Cryopreservation of bacteria

Glycerol stocks of bacterial culture harboring plasmid with gene of interest were generated by adding 150 µl of glycerol to 850 µl of O.N. in LB medium with appropriate antibiotics cultured bacterial cells and stored immediately at -80˚ C.

2.1.8 Quantification of DNA/RNA

DNA and RNA concentrations were determined by NanoDrop 1000 Spectrophotometer by Peqlab Biotechnologie GmbH, Erlangen.

2.1.9 Gateway Cloning LR reaction

In brief, an LR reaction allows targeted recombination of a gene of interest in a Gateway entry clone (at specific sites, from attL1 and attL2) to a destination vector (at the recombination sites, attR1 and attR2). LR reactions were performed using Invitrogen Gateway™ LR Clonase™ II Enzyme Mix according to the manufacturer`s protocol with half of the recommended volumes. For entry clone and destination vector, 1 µl of each plasmid diluted in TE-buffer (pH 8,0) to a final concentration of 75 ng/µl were employed. The transformation of DH5α cells was performed as described in section 2.1.5. 250 µl of S.O.C. medium was used to culture cells, and all or half of the bacterial culture plated on LB agar plates supplemented with Ampicillin at a concentration of 100 µg/ml. This enables the selection of clones that have successfully undergone LR reaction (to generate differently tagged expression clones, see Table 5-1), which will harbor Ampicillin resistance and have lost *ccdB* gene. Three clones of each LR onset were picked to conduct Miniprep of the plasmid and examine for the success of the generation of the desired expression clone.

The Gateway Cloning LR reaction employs the following method: The entry clone harbors *NLRP6*, flanked by the recombination sites, attL1 and attL2, and additionally carries the bacterial resistance gene for Kanamycin. The destination vector is an expression clone, harboring the gene for the toxic CcdB protein, flanked by the recombination sites attR1 and attR2, with an additional desired tag subsequent to the attR2 site and carries a bacterial resistance gene for ampicillin.

A **LR**-reaction, where recombination takes place specifically from the att**L**1 **to** att**R**1 and att**L**2 to att**R**2 sites, results in an expression clone containing *NLRP6*, flanked by the recombination sites attB1, attB2, with the respective tag and the bacterial resistance gene for Ampicillin and a donor vector, with the recombination sites attP1, attP2, flanking the *ccdB* gene, which inhibits DNA Gyrase in *E.coli* and thereby inhibit cell proliferation, for negative selection, and containing the bacterial resistance gene for kanamycin. Proteinase K is a serine protease and renders the enzyme clonaseII inactive by digestion.

2.1.10 BsrgI digest

As it cuts in the att sites and can thus release the insert of completed expression clones, BsrgI digestion (Thermo Fisher) was used to confirm the successful generation of LR clones. Digests were performed according to the manufacturer`s protocol using half of the reagent volumes and 300 ng DNA in 3 µl. The digest was performed by incubation at 37 ˚C for around 2 hours. After digest, DNA was separated in gel electrophoresis.

2.1.11 Seperation of DNA

DNA was separated on a 0.8 % (w/v) agarose (Roth) sodium borate buffer gel containing SERVA DNA Stain according to the manufacturer`s instructions. DNA was supplemented with a final concentration of 1 x loading dye (NEB) and electrophoresis conducted at 100 V for about 90 min in agarose gel chambers (Peqlab). The 2-log DNA Ladder (NEB) standard or 1 kb DNA Ladder (BIORON) standard was used as a marker depending on expected sizes. Separated DNA fragments were visualized by UV light exposure using Peqlab Fusion SL charge-coupled device (CCD) system.

2.1.12 Gene expression analysis of differently tagged *NLRP6* constructs generated in LR reactions by immunoblot

All *NLRP6* expression vectors generated by Gateway cloning (see Table 5-1) were verified for respective protein expression by transfection and immunoblot of lysates. HEK cells were transfected with 200 or 100 ng respective plasmid and lysed 48 hours later in 60 µl RIPA or Passive Lysis buffer (Promega) for 15 min. Lysates were transferred to 1.5 ml tubes and pelleted at maximum speed, at 4 ° C for 10 min to get rid of cellular debris. Lysates were used to separate protein in an SDS-PAGE and immunoblotted for proteins carrying specific tags with respective antibodies.

2.1.13 RNA isolation and Quantitative RT-PCR

Total RNA from HEK cells were isolated employing RNeasy Mini Kit, from HEK FLP-IN^{TM} T-REX^{TM} 293T cells stably expressing TLR5 WT employing RNase-Free DNase I treatment, which combines DNase I treatment and RNA isolation or from whole blood using QIAamp RNA Blood Mini Kit were all conducted on a Qiacube Robot (kits and machine from Qiagen) according to the manufacturer`s protocol.

To further remove contaminating genomic DNA from RNA, DNA-free Kit (DNase Treatment and Removal Reagents) (ambion, Thermo Fisher) is applied. This kit further removes used rDNase (recombinant DNase) and divalent cations, i.e. Mg^{2+}, Ca^{2+} from the samples, which upon heating of RNA can catalyze its degradation. 700 ng RNA were supplemented with a final concentration of 1 x DNase I Buffer, 1 µl rDNase (2 Units/µl) and DNase/RNase-free H_2O in a 22,5 µl reaction volume and DNase I treatment conducted according to manufacturer`s protocol. Alternatively, for HEK Flp-In$^{TM}$ T-REx$^{TM}$ 293T cells stably expressing TLR5 WT stimulated with stool supernatant from the cohort, RNase-Free DNase Set was employed according to the manufacturer`s protocol, which combines RNA isolation and DNase I treatment in a single step on a Qiacube Robot. In this case, RNA concentration was measured afterwards and 1000 ng used for RT.

20 µl of RNA samples from a manual DNase I digest or 1000 ng of RNA DNase I treated on the Qiacube were transferred into a fresh tube and reverse transcription conducted by employing High-Capacity RNA-to-cDNA^{TM} kit from Thermo Fisher according to the manufacturer`s protocol. cDNA was diluted 1:10 with DNAse/RNAse free sterile H_2O. Subsequently, the mRNA abundance of human *TBP* (housekeeper), *TNF-α*, *TLR5, IL-8, IL-6* and *IL-1β* was assessed by qPCR using Applied Biosystems 7500 Fast or a QuantStudio8 instrument in 96 or 384 well plate. QuantStudio^{TM} Real-Time PCR Software v1.0 or 7500 Software v2.0.6 from Thermo Fisher were used for analysis.

To analyze the expression of different mRNA relative to a housekeeping gene (*TBP*), TaqMan Gene expression Assays were performed to the manufacturer`s protocol with half of the recommended volume for Simplex PCR Setup in a 96 or 384 well format. Data were plotted using $2^{-\Delta CT}$ or $2^{-\Delta \Delta CT}$.

Table 2-5 Detection of gene expression by qPCR.

Analyzed mRNA expression	TaqMan Gene Expression Assay (Thermo Fisher)	Experiment
TNF-α	Hs00174128_m1	HEK, HEK FLP-IN™ T-REX™ 293 cells stably expressing TLR5 and whole blood stimulation
IL-8	Hs00174103_m1	Whole blood stimulation
IL-6	Hs00985639_m1	Whole blood stimulation
IL-1β	Hs01555410_m1	Whole blood stimulation
TBP	Hs00427620_m1	all as housekeeping gene expression

Analyzed mRNA expression	TaqMan Gene Expression Assay (TIB Molbiol)	Experiment
TLR5	provided by company on request, no assay number	HEK cell stimulation

2.1.14 Genotyping

Genotyping was performed to determine the genotype of donors for *TLR5* SNPs (F616L, N592S, R392X) and *NLRP6* SNPs (L163M, F361Y) using allele-specific TaqMan SNP Genotyping Assays according to the manufacturer`s protocol in 10 µl set-up for 96 well format or 5 µl set-up for 384 well format.

In brief, to determine genotype of donors of our cohort, we isolated DNA from a saliva sample provided by the donor on Qiacube according to manufacturer`s protocol and ran a qPCR with specific primers, either for WT or SNP with individual fluorescence marker, upon which carriage of WT or SNP heterozygous or homozygous can be evaluated. In case of *NLRP6* SNP F361Y, genotyping was linked with melting curve analysis, identifying WT or SNP by melting temperature of their product. Genotyping of all donors in our cohort was conducted by our technician, Sabine Dickhöfer.

Table 2-6 Genotyping assays used to detect SNPs.

Analyzed mRNA expression	TaqMan Gene Expression Assay ID (Thermo Fisher)	SNP ID
TLR5 SNP F616L	C_25608809_10	rs5744174
TLR5 SNP N592S	C_22273027_10	rs2072493
TLR5 SNP R392X	C_25608804_10	rs5744168
NLRP6 SNP L163M	C__29062478_10	rs6421985

Genotyping for *NLRP6* SNP F361Y was performed using *NLRP6* LightSNiP (TIB MOLBIOL) based on the melting temperature of the product with or without SNP. Genotyping is performed similarly to TaqMan SNP Genotyping according to the manufacturer`s protocol in 10 µl set-up but in 384 well format.

Table 2-7 Genotyping assay for SNP assay by melting curve analysis.

Analyzed mRNA expression	TaqMan Gene Expression Assay ID (Thermo Fisher)	SNP ID
NLRP6 SNP F361Y	rs56159585 NLRP6	rs56159585/7482965

96 well format was run in TaqMan (Thermo Fisher) or QuantStudio Real-Time PCR. 384 well format was run in QuantStudio Real-Time PCR. Results were analyzed according to software TaqMan 7500 Software version 2.0.6 or QuantStudio™ Real-Time PCR Software (version 1.0). Internal wildtype, heterozygous or homozygous controls were run along.

2.2 Biochemical methods

2.2.1 Determination of protein concentration

The protein concentration of cell lysates was determined by a colorimetric assay, employing Pierce™ BCA Protein Assay Kit (Thermo Fisher), according to manufacturer`s instructions. 10 µl of lysate was employed and protein concentration of each lysate measured in duplicates in a 96 well microplate reader (BMG Labtech, Fluostar Optima).

2.2.2 SDS PAGE and Western Blot

In general, cells were lysed in RIPA buffer or for Co-IP experiments in lysis buffer (see Table 5-2) and lysates prepared for separation by molecular weight by sodium dodecyl sulfate polyacrylamide gel electrophoresis (SDS-PAGE) by adding NuPAGE 4x LDS loading dye (Invitrogen) and 10 x Sample Reducing Agent (Invitrogen) to a final concentration of 1x and samples boiled 5 min at 95˚ C. According expected molecular weight of tested proteins (NLRP6, ASC), 8 % gels were used which give the best separation range for these proteins and proteins along with a marker PageRuler™ Prestained Protein Ladder (Thermo Fisher) separated in SDS running buffer (see Table 5-2) at 120 V in a Mini Cell chamber system (Invitrogen Xcell Surelock) for 90 minutes.

To immunoblot the proteins, proteins were transferred on 0,45 µm nitrocellulose blotting membranes (GE Healthcare) by semi-dry blot in a Bio-Rad Trans-Blot® Turbo™ Transfer System, applying protocol `STANDARD SD´, transfer 35 min, using NuPAGE Transfer Buffer (20x) (Thermo Fisher), containing 20 % Methanol. Following the transfer, blots were automatically processed in a BlotCycler™ (Precision Biosystems) at 4˚C. The nitrocellulose membranes were first blocked by incubating the membrane 90 minutes in blocking buffer, containing TBS, 0,05% Tween®20, 5% w/v powdered milk (Roth). Subsequently, the membrane was incubated in the primary antibody for 7 hours, in secondary antibody for 4 hours with three washing steps for 15 min after each antibody incubation. Antibodies were used in following working dilutions (see Table 2-8), diluted in blocking buffer. As the secondary antibodies are conjugated with horseradish peroxidase (HRP), the addition of chemiluminescent substrate AceGlow™ results in a signal which was captured and if needed, quantified on Peqlab Fusion SL charge-coupled device (CCD) system.

Table 2-8 List of used antibodies in immunoblot analysis.

All antibodies were diluted in TBS-based blocking buffer.

Antibody	Raised in species	Working dilution	Manufacturer (catalogue number)
Anti-mouse HRP conjugated	Goat	1:5000	Promega (W4028)
Anti-rabbit HRP conjugated	Goat	1:5000	Vector Laboratories (PI-1000)
Anti-rabbit conformation specific HRP conjugated	Mouse	1:2000	Cell Signaling (L27A9)
Anti-rat HRP conjugated	Goat	1:2000	Cell Signaling (7077)
Anti-HA (hemagglutinin) C29F4 monoclonal	Rabbit	1:1000	Cell Signaling (3724)
Anti-Protein A	Rabbit	1:625000	Sigma Aldrich (P3775)
Anti-Renilla Luciferase clone 1D5.2	Mouse	1:2500	Merck Millipore (MAB4410)
Anti-Tubulin clone TUB 2.1	Mouse	1:5000	Sigma Aldrich (T5201)
Anti-GFP	rabbit	1:5000	Sigma Aldrich (G1544)

2.3 Cell Biology Methods

2.3.1 Cell lines and cultivation

Table 2-9 Cell lines and cultivation parameters.
All cell lines were cultivated at 37°C and 5% CO_2 in a humidified incubator

Cell line	medium	Selection antibiotics
HEK	Dulbecco`s modified Eagle medium minimal (DMEM) (Sigma Aldrich) + 10 % heat-inactivated fetal calf serum (FCS) +1 % Penicillin/Streptomycin + 1 % Glutamine (Invitrogen)	
HEK Flp-In™ TREx™ 293T (Thermo Fisher SCIENTIFIC)	DMEM +10% heat-inactivated Tet-free FCS +1 % Penicillin/Streptomycin + 1 % Glutamine (Invitrogen)	Zeocin 100 µg/ml Blasticidin 15 µg/ml
HEK Flp-In™ TREx™ 293T (stably expressing TLR5 or NLRP6)	DMEM +10% heat-inactivated Tet-free FCS +1 % Penicillin/Streptomycin + 1 % Glutamine (Invitrogen)	Hygromycin B 100 µg/ml Blasticidin 15 µg/ml
HEK-Dual™ hTLR5 (InvivoGen)	DMEM +10% heat-inactivated FCS +1 % Penicillin/Streptomycin + 1 % Glutamine (Invitrogen) + 100 µg/ml Normocin	Hygromycin B 100 µg/ml Zeocin 50µg/ml
HEK-Blue™ hTLR4 (InvivoGen)	DMEM +10% heat-inactivated FCS +1 % Penicillin/Streptomycin + 1 % Glutamine (Invitrogen) + 100 µg/ml Normocin	1 x HEK BLUE selection

2.3.2 HEK Flp-In™ T-REx™ 293T cell line system

In brief, the Flp-In™ T-REx™ 293 cell line and its system allows to integrate a gene of interest in an expression vector at specific Flp Recombination Target (FRT) site to the same locus in every cell by a Flp recombinase and control expression of the protein of interest by tetracycline or its derivates.

In this system, genetically modified HEK293T is used, in which an FRT site was introduced at one position in the genome into the HEK cell line. Further, these cells are transfected with a plasmid, coding for a tet repressor to control tetracycline dependent expression. Via an FRT site containing expression vector, any gene of interest under a CMV promoter regulated by tetracycline or its derivates with the help of an FLP recombinase can then be introduced in the HEK Flp-In™ T-REx™ 293T cell line. This recombinase from *Saccharomyces cerevisiae* can recognize FRT sites and enables the homologous recombination of the FRT containing sites. It leads to the targeted integration of the expression vector to the same locus in every cell. Thus, this system allows a rapid generation of stable cell lines with homogenous expression of the protein of interest. As *tetR* is also expressed in the cell line, this leads to inactive expression of the gene of interest. By treating the cells with the antibiotic Tetracycline or the derivate Doxycycline, these can bind to TetR and in this way, the expression of the gene of interest can be controlled.

2.3.3 Generation of HEK Flp-In™ T-REx™ 293T cells stably expressing the gene of interest (GOI) and verification of expressed protein

HEK Flp-In™ T-REx™ 293T cells stably expressing NLRP6 mutants were generated according manufacturer`s protocol (InvivoGen). To verify and compare expression levels of different NLRP6 constructs introduced in HEK Flp-In™ T-REx™ 293T cells for stable expression, 1 ml of 500000 cells were seeded for about 3 hours in a 24-well format and induced with 100 µl Doxycycline with a final concentration of 1 µg/ml or as control 100 µl selection medium only overnight. The next day, the medium was discarded and cells lysed in 60 µl RIPA buffer containing phosphatase inhibitor and protease inhibitor. Cells were stored at -20°C for 20 min. Lysate was transferred to 1.5 ml Eppendorf tube, centrifuged at max. speed for 3 min at 4 ° C to clear cell debris and protein concentration determined, based on the Pierce™ BCA Protein assay (see section 2.2.1). Same amount (approximately 10 mg) of each NLRP6 protein was separated in an 8 % SDS PAGE and Western Blot conducted immunoblotting for HA to verify and compare HA-tagged NLRP6 construct or Tubulin as a loading control.

2.3.4 Whole blood stimulation

20 ml of whole blood was drawn from healthy donors and heparinized. Whole blood was inverted several times before 1.5 ml was transferred for each stimulation condition in a 24 well plate. Blood was stimulated with 5 µg/ml R848, 100 ng/ml Flagellin, 100 ng/ml LPS or as a control not-stimulated for 3 hours at 37 ° C, 5 % CO_2. Cells were harvested by centrifugation at 2000 rpm (796 g), 5 min at room temperature. After plasma was removed as far as possible, to remove erythrocytes, which are approximately 1000 times more apparent in whole blood than leukocytes, cells were transferred to 7.5 ml precooled erythrocyte lysis buffer (Qiagen) and inverted immediately. Cells were incubated with erythrocyte lysis buffer for 15 min by inverting the tube every 5 min. Cells were centrifuged at 1600 rpm (509 g) for 4 min at 4 ° C. The supernatant was removed and cells in the tube scraped on a metal frame and placed on ice. 3 ml erythrocyte lysis buffer was added to the pellet, vortexed and centrifuged again at 1600 rpm (509 g), 4 min at 4 °C. The supernatant was removed, and cells were resuspended well in 600 µl RLT buffer containing β-mercaptoethanol and frozen at – 80 ° C until RNA isolation.

RNA isolation was conducted employing QIAmp RNA blood Mini Kit according to manufacturer`s protocol and processed on a Qiacube robot. RT (see 2.1.13) was conducted and *IL-1β*, *IL-6*, *IL-8,* and *TNF-α* assessed by qPCR (see 2.1.13).

Dataset analyzed (see section 3.4): Dataset of my experiments was pooled together with a previous dataset generated by Dr. Klimosch from samples of different donors measured using an identical protocol. Therefore, data of whole blood stimulation experiments from Dr. Klimosch were retrospectively analyzed by stratifying for *NLRP6* genotype. Of note: No homozygous *NLRP6* SNP carriers were among the donors studied by Dr. Klimosch. Further, in his experiments, *IL-8* expression upon LPS and R848 stimulation and *TNF-α* expression in general, were not determined. Therefore, data in aforementioned categories derive only from my experiments.

2.3.5 Dual luciferase reporter assay (DLA)

NF-κB dependent activation of signaling pathways by NLRP6 or ASC or both together were analyzed using Dual-Luciferase® Reporter Assay System (Promega). The reporter plasmid contains an inducible Firefly luciferase gene upon NF-κB activation and a constitutively expressed Renilla luciferase to monitor equal cell numbers and control transfection.

HEK293T cells were transfected with expression clone encoding for WT or different mutants of HA-tagged NLRP6 and GFP-tagged ASC, together with 100 ng NF-κB reporter plasmid, 10 ng Renilla luciferase (pRL-TK, Promega) (pEX351) and 100 ng

eGFP (pEX008; for monitoring transfection efficiency) in triplicates in a 24 well format with calcium phosphate method (see Table 2-10).

48 hours post transfection, cells were lysed on ice in 1 x 60 µl Passive Lysis Buffer (Promega) and immediately frozen at -80˚ C. On day of analysis, lysates were thawed and centrifuged at 2500 g, 4 ˚ C for 10 min and 10 µl of the cleared supernatant transferred to a white 96-well plate (Nunc).

The analysis was conducted with the aid of a Fluostar Optima device (BMG Labtech). Sequentially, 50 µl of Luciferase Assay Reagent II (LAR II, Promega), which allows the quantification of firefly luminescence, and subsequently 50 µl of Stop & Glo® Reagent (Promega), which stops the first reaction and simultaneously allows to assess the Renilla luminescence signal from Renilla luciferase, were added using automated injection in the luminometer. Luminescence signals were assessed for both luciferases separately every 0.5 s in a timeframe of 10 s and shown as relative light units (RLU). Firefly reporter RLU were normalized to control reporter Renilla RLU.

Table 2-10 Calcium phosphate transfection in HEK cells for DLA.
Plasmid 1 and 2 can be adjusted in volume according to their concentration for end concentration of each plasmid.

Additive	Concentration	Volume added (final conc.)
NLRP6 (plasmid 1)	100 ng/µl	1 µl (100 ng end conc.)
ASC (plasmid 2)	10 ng/µl	1 µl (100 ng end conc.)
NF-κB luciferase reporter plasmid	100 ng/µl	1 µl (100 ng end conc.)
Renilla reporter plasmid	10 ng/µl	1 µl (10 ng end conc.)
EGFP-plasmid (if proteins analyzed not GFP tagged)	100 ng/µl	1 µl (100 ng end conc.)
$CaCl_2$ (2.5 M, -80°C)		1.2 µl
H_2O		3.8 µl
2x HBS (Sigma HEPES buffered saline, -80°C, 500 µl aliquots)		10 µl
Total		20 µl

2.3.6 Luminescence-based mammalian interactome mapping (LUMIER)

To study the protein interaction of NLRP6 and ASC, the LUMIER technique was applied. In brief, the interaction of two proteins are tested by expressing these proteins with different tags (one of them tagged with Renilla) and assessing after addition of luciferin the Renilla luciferase activity to determine the expression of the Renilla tagged protein before (control of protein expression) and after pull down of the other tagged protein. In case of an interaction of both tested proteins, the pull down of the other tagged protein by magnetic beads will result in a co-immunoprecipitation with the Renilla tagged protein and therefore its presence in the complex detectable via its luciferase activity after pull down. NLRP and ASC are shown to interact via their N-terminal Pyrin domain. Therefore, to avoid disturbance of the interaction assay, generated C-terminal ProA tagged ASC (pMS24) and C-terminal Renilla tagged NLRP6 constructs (see Table 5-1) were tested.

10^4 HEK293T cells were seeded in 100 µl in a 96 well format and transfected with 20 ng plasmid (diluted 1:10 in Optimem) encoding for Renilla tagged ASC or Protein A tagged NLRP6 each (Lipofectamine® 2000, Life Technologies). 48 h post transfection cells were lysed on ice for 15 min in 10 µl lysis buffer (composition lysis buffer LUMIER see Table 5-2). The lysis buffer includes magnetic Dynabeads® M-280 Sheep Anti-Mouse IgG slurry (Life Technologies), which allows later the precipitation of Protein A fusion proteins and in case of interaction, the co-precipitation of their respective interaction partners. Lysates were diluted with 100 µl PBS and 10 % of the suspension was used to measure the raw Renilla luciferase activity in the sample (Fluostar Optima, BMG Labtech). The rest of the lysate were washed with ice cold PBS on a magnetic plate washer (Hydro Flex plate washer, Tecan), which allows the purification of Protein-A fusion proteins and possible interaction partners. Coelenterazine (PJK GmbH), the substrate for Renilla luciferase, was prepared with Renilla assay buffer (see Table 5-2) to a final concentration of 3 µM and 70 µl used for each sample. Signals measured immediately every 0.5 s in a timeframe of 1,5 s in (Fluostar Optima, BMG Labtech). To evaluate specific interactions, as a negative control, cells were additionally transfected with NLRP6-Renilla and a ProA tagged backbone (pEX140) for pulled down, which thus shows non-specific binding of the Renilla-tagged prey to the beads and allows for excluding unspecific binding.

To determine interaction capacity, the activity of bound Renilla luciferase was divided by the amount of raw Renilla activity for each transfection, following subtraction of the result from a signal gained of the negative control (Protein-A only in this case, pEX140). Only when bound/expressed Renilla activity for each

construct normalized to 1 negative control (ProA only negative control) results in at least three-fold higher value, this is considered as a true interaction[209].

2.3.7 Co-Immunoprecipitation (Co-IP)

1.5×10^6 HEK cells or 1×10^6 HEK Flp-In™ T-REx™ 293T cells stably expressing NLRP6 were seeded in 10 ml appropriate medium (150 000 cells/ml or 100 000 cells/ml) in 10 cm dishes for at least 2-4 hours. Cells were transfected as listed in Table 2-11. 2 days post transfection, transfection efficiency was confirmed by GFP signal and cells were washed carefully with pre-warmed 5 ml PBS and lysed on ice in precooled 850 µl lysis buffer (composition lysis buffer Co-IP see Table 5-2) for 15 min. Cells were scraped off and transferred to a 1.5 ml Eppendorf tube and rotated at 4˚ C for 30 min for thorough lysis. Cells were centrifuged at max speed, at 10000 g for 5min at 4˚C to remove cell debris. Supernatant was transferred to fresh 1.5 ml Eppendorf tubes and placed on ice. 50 µl of lysate was transferred to determine gene expression later, supplemented with 4 x loading dye and 10 x reducing agent, boiled at 95° C for 5min and stored until analysis at -20˚ C.

2.5 µg of monoclonal anti-HA antibody (Sigma-Aldrich H9658. clone HA-7 dynabeads were equilibrated in precooled 40 µl lysis buffer, and in between beads vortexed several times. 40 µl of beads per sample were added and the sample incubated at 4˚ C 3-6 hours in end-over-end mixing. Magnetic stand holder was placed on ice and samples washed 5 times with 500-1000 µl lysis buffer by adding buffer and 5 min rotation after each wash. Samples were centrifuged at 2500 g, 4 ° C, 2 min and the supernatant removed. Remaining beads with immunoprecipitated proteins were prepared for SDS PAGE (see section 2.2.2). Samples were spun down at maximum speed for 2 min before loading and supernatant loaded.

Table 2-11 Co-IP set-up of transfection.
Preferentially add reagents in following order: H_2O, plasmids, eGFP, $CaCl_2$., then mix by vortexing and finally add 500 ul 2X HBS, mix gently and pipette carefully on cells and rotate dishes, followed by incubation at 37 °C, 5% CO_2.

Additive	Concentration	Volume added (final conc.)
NLRP6 c-term Strep-HA (plasmid 1)	100 ng/µl	50 µl (5 µg end conc.)
ASC c-term GFP (plasmid2)	100 ng/µl	50 µl (5 µg end conc.)
EGFP-plasmid (if proteins to test not GFP tagged)	100 ng/µl	10 µl (1 µg end conc.)
$CaCl_2$ (2.5 M, -80°C)		61 µl
H_2O		329 µl
2x HBS (Sigma HEPES buffered saline, -80°C, 500 µl aliquots)		500 µl
Total		1000 µl

2.4 Stool methods

2.4.1 Cohort description and set up

Following ethical approval of the study protocol and after obtaining written informed consent, 250 healthy donors were recruited for our study to donate saliva, blood and/or stool sample. The population was characterized by age, sex and *TLR5,* and *NLRP6* genotype, we are interested in. From this cohort, 51 donors from age 20-48, median 26, 68% female participated in stool donation. Along with stool donation, participants completed a questionnaire on information related to their dietary and medical status.

2.4.2 Study design and stool collection

During enrollment of participants, general data of study participants were documented and an identification number assigned to each donor. Additionally, without food intake of the donor for about 30 min before, roughly 500 µl saliva was collected from the donor for DNA isolation to determine the genotype (see 2.1.14). Stool was collected in total one time from each donor during one of four collection periods in 07/2015 – 11/2016. Participants in the study were informed about the general procedure and time of sample collection.

Before sample collection, the interior container (Commode Specimen collection, Thermo Fisher Scientific, see 5.6), for collection of stool sample was treated for 10 min with UV-light in the laminar airflow cabinet and provided. During the stool collection time, all materials to participate in this study were deposited in a public restroom, in a designated cool box. According to our instructions, participants were asked to deposit their stool sample in the provided pre-treated container and store it in the set up cool box. Participants further were asked to complete a questionnaire for prospective, advanced analysis of samples. The time of message received from a participant on deposit of stool sample was listed as sample deposition time.

2.4.3 Workflow and processing of stool collections

Deposited stool containers by donors were picked up and stored at 4° C in the fridge until samples were processed (processing of samples was conducted within 24 hours, exceptionally maximum within 48 hours, after deposition). Samples were processed in a laminar airflow cabinet, specifically designated for stool processing. Container was placed on ice in the laminar airflow cabinet and for each sample, the ID of the donor, time of sample deposition and time of processing was documented. General description of stool, in particular, color, form, general amount, presence of non-digested particles and consistency, were further documented and a picture of

the sample taken (not shown). Sterile, one-time use spoon (Roth) was used to mix the stool sample well, ensuring an equal distribution. The sample was further processed for microbial analysis (PowerSoil® DNA Isolation kit, Mo Bio Laboratories, Inc.) (see 2.4.5), glycerol stocks (see 2.4.4), and aliquots (see 2.4.4) prepared.

2.4.4 Stool aliquots and glycerol stocks

Stool was filled in a sterile 5 ml syringe (Eppendorf) and aliquoted into sterile cryovials (Nerbe Plus). Filled cryovials were immediately incubated on ice and stored at – 80° C. For glycerol stocks, 0.5 g of stool was transferred into cryovials and 1 ml of TBS/Glycerol added for preservation. For resuspension, stool was mixed and incubated 10 min on ice and then stored at – 80° C.

2.4.5 Microbial analysis preparation

2.5 g of sample was weighed in a 50 ml falcon tube and kept on ice. 6 ml of PowerLyzer PowerSoil Bead Solution (Dianova GmbH) was added in the prepared falcon tube and incubated 20-30 minutes on ice, while time to time vortexing, to homogenize sample as far as possible. Samples were centrifuged in a precooled centrifuge (Eppendorf) at 1500 rcf, 4°C for 5 min.

800 µl of supernatant were transferred to (Power Soil Power Bead Tubes, Dianova GmbH (prefilled or manually prefilled with lysis buffer: 750 µl PowerLyzer PowerSoil Bead Solution (Dianova GmbH)), 4-5 tube per sample, and tube inverted several times and spun down shortly. In parallel 800 µl of PowerLyzer PowerSoil Bead Solution (Dianova GmbH) as control (blank) were run along. Garnet tubes were incubated for 10 min at 95°C in a heating block and subsequently transferred to a heating block at 65° C for another 10 min. Subsequently, samples were stored at - 80° C. Samples were further processed by our collaboration partners.

2.4.6 Dry weight determination

One cryovial of the stool sample of each donor was slowly thawed overnight at 4° C on the previous day. Next day stool sample was mixed well with a sterile spatula and weight of petri dish determined. Generally, around 100 – 600 mg stool for each donor was distributed on a 2 cm Petri dish (Greiner Bio-one) and kept closed on ice until further procedure. Petri dish with stool was then placed without lid in a dehydrator (Bielmeyer BHG 601) under a hood and run for 12 hours at maximum stage 3 (equals 20 °C above room temperature) overnight.

Next day, the stool was dry and petri dishes closed and dry weight including petri dish weight measured to determine dry weight.

1. (Dry weight/Fresh weight) x 100 = percentage of stool content.
2. Percentage of stool content from 100 mg plotted to compare the stool of each donor

2.4.7 Preparing stool samples for following assays: TLR5, HEK-Dual^{TM} hTLR5, HEK-Blue^{TM} hTLR4, and sIgA ELISA

To determine TLR5 activation by TLR5 assay or HEK-Dual^{TM} hTLR5 assay, TLR4 activation by HEK-Blue^{TM} hTLR4 assay and sIgA content by sIgA ELISA, in stool samples, stool supernatant was prepared as described in the following: 100 mg fresh weight (avoiding undigested material) of stool was weighed in a precooled 15 ml falcon and incubated on ice. According to manufacturer`s instruction (Ridascreen, sIgA ELISA) 5 ml of extraction buffer, previously diluted with Millipore H_2O 1:10, was added to the sample. The sample was homogenized by incubation on ice for about 20 – 30 min and in between vortexing. Stool sample was centrifuged at max speed 4000 rpm (3220 g) for 12 min and five aliquots of 500 µl supernatant in 1.5 ml Eppendorf tubes generated and immediately stored in -80 °C.

2.4.8 TLR5 assay

To determine TLR5 activation potential by stool samples, indicating the flagellin content in each sample, in brief, TLR5 expression is induced by Doxycycline in generated HEK Flp In^{TM} TREx^{TM} 293T cells stably expressing TLR5 WT and stimulated with stool supernatant to assess TLR5 dependent *TNF-α* expression in mRNA. HEK Flp In^{TM} TREx^{TM} 293T cells stably expressing TLR5 WT had been generated earlier by Dr. Sascha Klimosch[147] and were used to determine the flagellin-associated inflammatory potential of stool samples, similar to HEK-Blue hTLR5 reporter cell assay utilized by Cullender et al.[145].

To do so 200,000 cells were seeded in 500 µl selection medium in a 24 well plate for about 3 hours and treated with 100 µl Doxycycline for a final concentration of 1 µg/ml Doxycycline to induce TLR5 expression, or with 100 µl selection medium as a control without induction of TLR5 expression. Doxycycline induced and non-induced cells were stimulated with 100 µl of stool supernatant extracted previously in section 2.4.7. Further, cells were stimulated with following controls: 50 ng/ml *S.typhimurium* flagellin (positive control), extraction buffer (Ridascreen) 1:10 diluted in Millipore H_2O according to manufacturer`s protocol (negative control), selection medium (negative control) and sample Elch025 (pseudonymized sample) was used for stimulation in all plates of the experiment to assess variability in plates (internal control). After 3 hours of stimulation of cells with stool supernatant at 37 ˚C, 5 % CO_2, cells were harvested in 350 µl RLT buffer containing 1% v/v

β-mercaptoethanol. Cells were immediately frozen at -80 ˚C until complete lysis and RNA isolation.

2.4.9   sIgA ELISA

100 mg stool was homogenized in 5 ml extraction buffer (sample preparation see section 2.4.7). SIgA in stool was determined according to the manufacturer`s protocol. For the assay following controls were added: sample Elch025 (internal control for plate variation determination), extraction buffer (negative control), H_2O control (negative control), Kit High and Low control provided in used sIgA kit (Ridascreen). To have a standard, purified human sIgA was purchased from BioRAD and prepared according to manufacturer`s instruction in Millipore H2O at a concentration of 1000 ng/ml. The highest standard used in our assay was 800 ng/ml and prepared in a serial dilution by initial dilution 1:100 in Milipore H2O and second dilution 1:12.5 in Diluent A (provided by kit Ridascreen, sIgA ELISA). Values were measured in triplicates in a microplate reader (BMG Labtech, Fluostar). Samples were analyzed by determination of mean of triplicates and subtraction from extraction buffer (negative control) by software.

2.4.10 HEK-Dual^{TM} hTLR5 assay

In brief, to assess TLR5 activation potential by stool samples, HEK DUAL^{TM} hTLR5 reporter cells were stimulated with stool supernatant and upon TLR5 activation, NF-κB induced SEAP expression and IL-8 dependent luciferase activity determined.

50000 HEK DUAL^{TM} hTLR5 cells in 180 µl were seeded per well in a 96 well format and stimulated for about 22 hours with 20 µl stimuli in triplicates. Stool samples for stimulation (preparation see 2.4.7) were diluted 1:5 in ddest H2O. Further, flagellin at concentrations 1 µg/ml and 100 ng/ml (positive control of TLR5 activation), Tri-DAP at concentrations 10 µg/ml and 1 µg/ml (positive control of cell line, NOD1 agonist), sample E025 1:5 diluted in ddest H2O (internal control of all plates) were employed in the assay. Afterwards, plates were centrifuged at 1600 rpm (509 g) to get rid of cells and supernatant harvested. 20 µl of supernatant was used for NF-κB induced SEAP assay by adding to it 180 µl Quanti-Blue and OD measured after 3 hours in a microplate reader (BMG Labtech). For analysis of IL-8 induced luciferase, to 10 µl of previously harvested supernatant, 50 µl Quanti-Luc was added by machine and measured in white Nunc plate using Fluo-optima. Kinetic luminescence measurement was selected (30 intervals, kinetic interval time 0.10 s, measurement start time 2 s, measurement interval time 0.10 s) and the sum of range calculated by the machine.

2.4.11 HEK-Blue^{TM} hTLR4 assay

In brief, to measure TLR4 activation potential by stool samples, indicating the LPS content in each sample, HEK-Blue^{TM} hTLR4 cells were stimulated with stool supernatant and, upon TLR4 activation, NF-κB induced SEAP expression assessed.

25000 HEK-Blue^{TM} hTLR4 cells in 180 µl were seeded per well in a 96 well format and stimulated for about 22 hours with 20 µl stimuli in triplicates. Stool samples for stimulation (preparation see 2.4.7) were diluted 1:5 in ddest H2O. Further, LPS at concentrations 100 ng/ml and 10 ng/ml (positive control of TLR4 activation), TNF-α at concentrations 200 ng/ml and 50 ng/ml (positive control of cell line, TNF receptor agonist), sample stud203 1:10 diluted in ddest H2O (internal control of all plates) were employed in the assay. Afterwards, plates were centrifuged at 1600 rpm (509 g) to get rid of cells and supernatant harvested. 20 µl of supernatant was used for the assay by adding to it 180 µl Quanti-Blue and OD measured after 3 hours in a microplate reader (BMG Labtech).

2.4.12 β-Defensin and Calprotectin ELISA

β-Defensin in stool was measured in β-Defensin ELISA (Immundiagnostik) and Calprotectin respectively in Calprotectin ELISA (Immundiagnostik) according to the manufacturer`s instruction. One stool sample for one donor was prepared simultaneously for both ELISAs. Stool aliquots (previously prepared in 2.4.4) were thawed slowly (to protect from cell burst, which will increase Calprotectin level) overnight at 4 ˚C. Stool extracts were prepared by homogenizing 15 mg of stool for both assays in 1.5 ml (1:2.5 in Millipore H_2O diluted) extraction buffer in 1.5 ml Eppendorf tubes for about 15 min. Subsequently, samples were shortly centrifuged for 30 s at 5000 rpm and 1 ml of supernatant, avoiding any disturbing particles, was transferred from the top in a fresh Eppendorf tube and mixed well. Afterwards, 40 µl of the stool supernatant was transferred to 1.5 ml Eppendorf tube for Calprotectin ELISA and 300 µl transferred to another 1.5 ml Eppendorf tube for β-Defensin ELISA and stored at - 20 ˚ C, until these ELISAs were conducted. One day after, β-Defensin-ELISA was run in duplicates, 2 days after Calprotectin ELISA was run in triplicates. For both ELISAs, values were measured in a microplate reader (BMG Labtech, Fluostar) and analyzed by its software.

2.5 Statistical Analysis

Data were analyzed with Microsoft Excel 2016 and GraphPad Prism 6. For statistical analysis, GraphPad Prism 6 was used. If Gaussian distribution did not apply according to D'Agostino-Pearson, Shapiro-Wilk, and Kolmogorov-Smirnov tests, Mann-Whitney-U test of unpaired samples was conducted.

Exception: DLA results (Figure 3-6) tested for Gaussian distribution showed unclear results (the outcome of above mentioned tests not equal and some require a higher number of replicates) and therefore, exceptionally, for these DLA results Gaussian distributions were assumed and tested for the paired t-test. Same DLA results pooled for M- and L- alleles (Figure 3-7), since unclear, if Gaussian distribution applies, were tested for Wilcoxon-test of paired samples.

Throughout, * indicates statistical significance at the 5% level, i.e. $p < 0.05$, ** at 1% level, i.e. $p < 0.01$. Ns indicates non-significant results.

3 Results

Based on the aforementioned aims, I pursued the following three-pronged strategy. Firstly, *in vitro* experiments were conducted to study NLRP6 variants in cellular systems and discover new functions of NLRP6. For this, I started my work by generating the aforementioned *NLRP6* constructs by Gateway cloning experiments and generated a HEK FLP-IN™ T-REX™ 293T system stably expressing NLRP6, induced by doxycycline. Next, we tested these constructs in overexpression assays in HEK cells and analyzed the interaction of NLRP6 and ASC by a) LUMIER and b) Co-IP (in HEK and HEK FLP-IN™ T-REX™ 293T cells stably expressing NLRP6). Secondly, in order to evaluate the physiological role in primary immune cells from healthy carriers of these *NLRP6* SNPs, stimulation assays in whole blood were carried out. Specifically, the influence of *NLRP6* variants on TLR4, 5 and 7/8 mediated gene transcription was analyzed. Thirdly, I sought to investigate the effect of the aforementioned *TLR5* and *NLRP6* SNPs on the intestinal immune function. To this end, stool samples from healthy donors carrying SNPs associated with CRC were analyzed for soluble well-known mediators such as sIgA, β-defensin and calprotectin level as well as the TLR activating potential assessed. Specifically, the potential to elicit TLR4 or TLR5 activation was assessed using cell-based reporter assays. The three approaches will be described in turn.

3.1 Generation of *NLRP6* SNP constructs and HEK Flp-In™ 293T cells stably expressing NLRP6 mutant for *in vitro* analysis

3.1.1 Selection of two *NLRP6* variants for further study

A CRC association study in a Czech cohort of sporadic colorectal cancer by Huhn et al. showed that an *NLRP6* SNP, M163L (rs6421985), was associated with CRC risk in Caucasians (OR=1.36, p=0.0421)[197]. Another *NLRP6* SNP, F361Y (rs56159585), was analyzed in the study, which revealed in our study to be mostly present along SNP M163L. However, SNP F361Y did not reveal a significant association with CRC in the aforementioned study (OR=1.27, p=0,1249)[197]. Less is known about the role of *NLRP6* in CRC and a potentially functional phenotype of these variants. One aim of this study was therefore to generate constructs harboring each of the respective *NLRP6* SNP alone and a construct harboring both of the SNPs together. Our aim was to characterize their effect in *in vitro* overexpression, reporter and interaction assays, and determine if the SNPs result in altered function.

3.1.2   Generation of *NLRP6* SNP constructs by mutagenesis

To generate constructs with respective mutations in *NLRP6*, we used a Gateway Entry Clone (NCBI Accession: AF479748.1; pEX484) containing the open reading frame (ORF) of the human wildtype (WT) *NLRP6* without a STOP codon. This enabled us to subclone *NLRP6* using the Gateway cloning system and tag NLRP6 C-terminally depending on the purpose of the experiment.

A mutation from leucine (defined as Wildtype, WT) to methionine (SNP) was carried out at position 163 in the protein sequence. A mutation from phenylalanine (defined as Wildtype) to tyrosine (SNP) at position 361 was carried out. The mutation for each amino acid was introduced sequentially. A schematic overview of the positions of SNPs and the respective nucleotide mutation conducted is given in Figure 3-1.
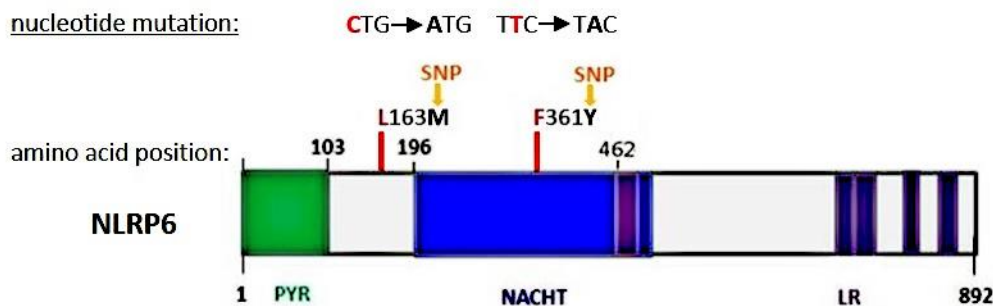
Figure 3-1 *NLRP6* SNPs and corresponding nucleotide mutations.
NLRP6 is shown with its domains (PYR: Pyrin, NACHT: NACHT, LR: leucine-rich repeat) based on information from the database UniProt (https://www.uniprot.org/uniprot/P59044). Single nucleotide polymorphism (SNP) mutations (WT in red, SNP in black, bold) and corresponding nucleotide mutations are illustrated.

We further wanted to generate an additional set of mutated *NLRP6* constructs. The purpose was to investigate possible phosphorylation targets in NLRP6 and their impact in *in vitro* assays. Based on a prediction by a bioinformatic tool from our collaborator Prof. Mathias Chamaillard in France and by submitting the protein sequence of NLRP6 to a web phosphorylation site prediction tool kinasephos[210] (http://kinasephos.mbc.nctu.edu.tw.), we predicted amino acid tyrosine 357 to be a target of Janus Kinase with prediction specificity of 90 %. The amino acid sequence before the SNP position 361, from amino acid 357-361, is **YFYKF**. To evaluate an impact of tyrosine at position 357, 359 and in the case of SNP 361, we wanted to generate different combinations of mutations from tyrosine to phenylalanine at these positions by site-directed mutagenesis (section 2.1.2). Phenylalanine was chosen as it has a similar size but cannot be phosphorylated. A schematic figure is shown below Figure 3-2.
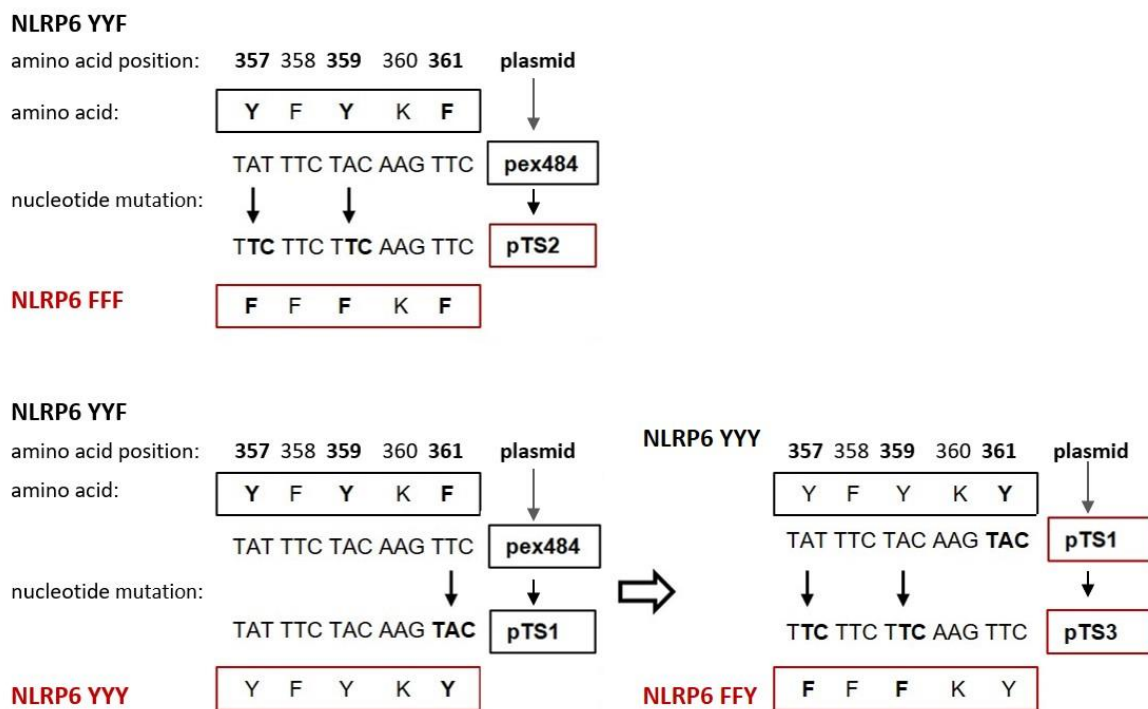
Figure 3-2 Mutations conducted in *NLRP6* to generate constructs to test impact of tyrosine at position 357, 359 and in case of SNP 361.
Amino acids (in boxes) in NLRP6 at indicated amino acid positions and respective nucleotide sequences with plasmid name (on the right) are shown with targeted nucleotide mutations and resulting amino acid (bold) and resulting construct.

The sequencing of generated constructs confirmed the expected sequence and the respectively targeted mutation(s). An overview of the generated and employed NLRP6 constructs and their abbreviations used in this thesis are summarized below in Table 3-1.

Table 3-1 Employed *NLRP6* constructs and their abbreviations in this thesis.

NLRP6 constructs	amino acid at position						abbreviation in thesis	characterization
	163	357	358	359	360	361		
L_YFYKF	L	Y	F	Y	K	F	L_YYF	Wildtype (WT)
L_YFYKY	L	Y	F	Y	K	Y	L_YYY	SNP F361Y
L_FFKF	L	F	F	F	K	F	L_FFF	mutation Y357F, mutation Y359F
M_YFYKF	M	Y	F	Y	K	F	M_YYF	SNP L163M
M_YFYKY	M	Y	F	Y	K	Y	M_YYY	SNP L163M, SNP F361Y
M_FFKF	M	F	F	F	K	F	M_FFF	SNP L163M, mutation Y357F, mutation Y359F

To generate tagged expression clones of all *NLRP6* constructs (list of generated clones see Table 5-1), we conducted a LR reaction of Gateway cloning (for methods see section 2.1.9) and each of the LR reactions were verified by BsrgI digest. Further, the expression of each of the constructs was also verified by immunoblot (see 5.1.1.)

3.1.3 Generation of HEK Flp-In™ TRex™ 293T cells stably expressing NLRP6 or TLR5 WT or mutants for *in vitro* studies

To investigate the role *of NLRP6 and TLR5* and their SNPs, we thought to utilize, additionally, the Flp-In™ TRex™ 293T cell system from Thermo Fisher. This system allows a controlled induction of a gene of interest and study its impact. Specifically, the Flp-In™ TRex™ 293 cell system enables to integrate, a gene of interest in an expression cassette, at specific Flp Recombination Target (FRT) site to the same locus in every cell. Further, a tet repressor (TetR) is continuously expressed in HEK Flp-In™ TRex™ 293 cell line and controls the Tetracycline dependent expression of the gene of interest, in this case of *NLRP6* or *TLR5*. By the addition of Tetracycline or its derivative Doxycycline (DOX), which binds to TetR, the expression of the gene can be induced. Thereby, this system ensures similar expression levels of the gene of interest.

HEK Flp-In™ TRex™ 293T cells stably expressing TLR5 WT were generated by our former post-doc, Dr. Sascha Klimosch and the cells expressing NLRP6 WT or mutants were generated by myself. (For generation of NLRP6 expressing HEK Flp-In™ TRex™ 293T cells see section 2.3.3, for verification of similar expression level of each NLRP6 protein in generated HEK Flp-In™ TRex™ 293T cells see immunoblot in Figure 5-2. Generated cell lines show comparable expression of respective NLRP6 constructs after induction with DOX. These cell lines enable us to study the effect of different NLRP6 SNPs at a similar level of expression (avoiding altered transfection efficiencies) and are employed in this present work to determine the presence and level of interaction of NLRP6 SNPs with ASC in section 3.3.

3.2 NLRP6 SNP F361Y and surrounding tyrosines at amino acid positions 357 and 359 in NLRP6 reveal elevated NF-κB activation in presence of ASC *in vitro*

In a screening of different NLRPs, Grenier et al. found that NLRP6 in the presence of the adaptor protein ASC, activates NF-κB and has an important function in proinflammatory signaling. Further, they showed by immunostainings that the Pyrin domain in NLRP6 is essential to recruit the Pyrin domain-containing ASC in punctate

structures in the cytoplasm. However, they were not able to show direct interaction of NLRP6 and ASC in immunoprecipitation assays.[189]

Taking into account that NLRP6 is able to induce NF-κB, we thought to determine the NF-κB activation potential of (our generated) *NLRP6* mutated constructs. We started by using, in this case, the *NLRP6* M_YYY construct, bearing both of the SNPs, to test NF-κB activation. We assessed the activation of NF-κB by different amounts of NLRP6 together with or without ASC using a NF-κB reporter in HEK293 cells, in a Dual-Luciferase Reporter Assay (DLA) (Figure 3-3). As a positive control we used MYD88, which is employed as a main adaptor in most of the TLR signaling pathways; its overexpression drives a strong activation of NF-κB[211].

NLRP6 alone did not activate NF-κB, but together with ASC, in amounts where ASC alone did not activate NF-κB, induced NF-κB activation. This is in line with observations by Grenier et al.[189]. In this setting, the use of 400 ng of NLRP6 did not show increased activation in comparison to 100 ng as expected. This could mean that the system is saturated.

Myd88	50	-	-	-	-	-	-
ASC	-	-	-	-	10	10	10
NLRP6 M_YFYKF	-	-	100	400	-	100	400
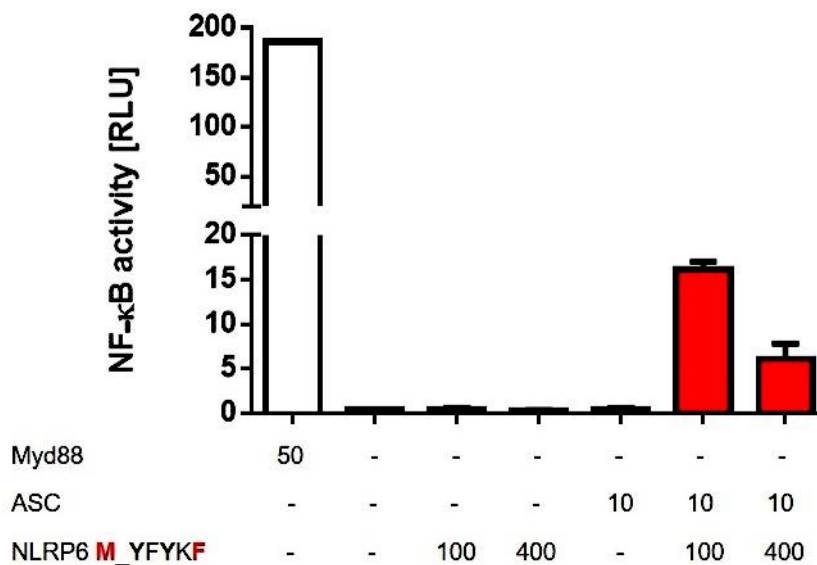
Figure 3-3 NF-κB is activated by NLRP6 only in the presence of ASC
HEK cells were transfected with 50 ng MYD88 as control or indicated amounts of NLRP6, together with or without 10 ng ASC, and 100 ng NF-κB reporter plasmid, 10 ng Renilla and eGFP. After 2 days NF-κB dependent luciferase activation was assessed by DLA. Data show the mean of values with SD representative of technical triplicates from one experiment.

Thus, to find the optimal amount of NLRP6 in the system, we performed titrations from 25 – 200 ng (see section 5.1.3 and Figure 5-3). We, further, narrowed down the titration of these constructs from 1 – 25 ng.

Upon optimization of plasmid amounts, we focused on the generated NLRP6 constructs, which are resembling naturally occurring genotypes as in the case of *NLRP6* L_YYF, *NLRP6* L_YYY, *NLRP6* M_YYF, and *NLRP6* M_YYY. Additionally, we selected NLRP6 L_FFF, carrying in all our targeted positions phenylalanine. If tyrosine is crucial for NF-κB activation, as for instance by being a target site for phosphorylation, this construct should show an effect.

First, I will exemplarily show one DLA experiment and results, on verification of DNA amount for each employed *NLRP6* construct and expression level of respective NLRP6 protein and eGFP, for this assay. Then, I will show a combined analysis of all DLA, which includes the exemplary DLA as well.

Figure 3-4 shows NF-κB activation by the different NLRP6 constructs in a dose-dependent manner from **one** exemplary DLA.

Results showed that 1 ng plasmid of the gene of interest is not enough to show an effect, whereas 5, 10 and 25 ng were able to induce NF-κB activity in a ligand-independent manner. In comparison to WT, mutation at the position 361 from phenylalanine to tyrosine (NLRP6 L_YYY) at construct amounts of 5, 10 and 25 ng clearly demonstrated enhanced NF-κB activation. This is also the case when mutations at positions 357 and 359 from phenylalanine to tyrosine (NLRP6 L_FFF) occur. The results indicate that tyrosine at these (targeted) positions promote a higher NF-κB activation. However, these results are based on one experiment.
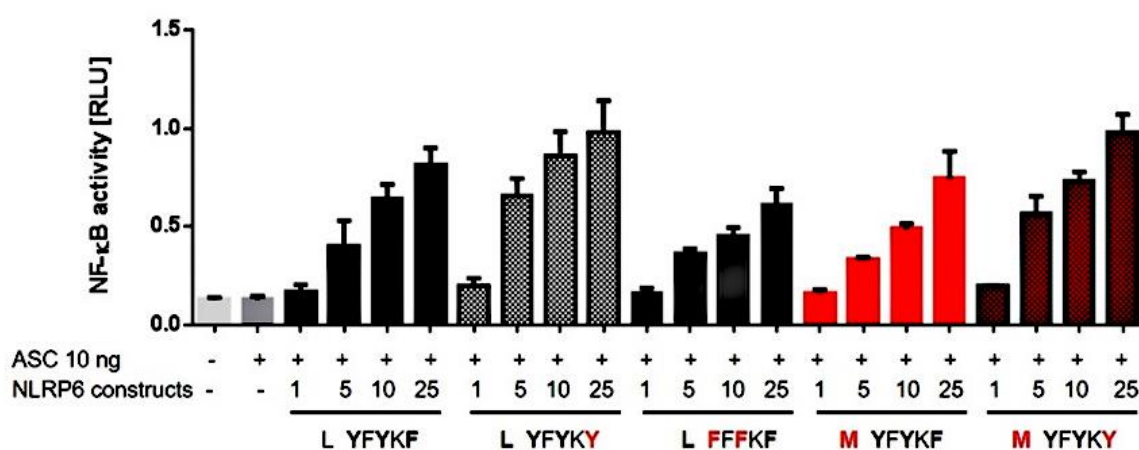
Figure 3-4 Titration of NLRP6 WT and mutants and their ability to induce NF-κB activation.
HEK cells were transfected with indicated amounts of NLRP6 construct together with ASC, NF-κB reporter plasmid and Renilla. After 2 days NF- κB dependent activation was assessed by DLA. Data show the mean of values with SD representative of technical triplicates from one experiment. Statistical testing was not conducted for this representative experiment, but in a combined analysis shown in Figure 3-6 and Figure 3-7.

We intended to rule out that the observed effects of the different constructs in our DLA are based on technical issues, as unequal amounts of DNA in the transfection or different transfection efficiencies. Hence, the same amount of DNA for each of the tested *NLRP6* constructs, before transfection, from one experiment was separated in an agarose gel. DNA level of the constructs were similar (not shown). Additionally, the same volume of (cell) lysate from each set of *NLRP6* transfection (in triplicate) was pooled and immunoblotted for NLRP6 and GFP. To be able to compare expression levels, signals were quantified. As shown in Figure 3-5, the GFP level, which reveals the transfection efficiency, and NLRP6 protein expression level of each construct have slight variances. Thus, the effect of tested NLRP6 constructs carrying tyrosine residue at amino acid positions 361 or 357 and 359 on NF-κB activation may partly be due to differences in expression level or the transfection efficiency of the constructs. However, they do not explain the results completely.
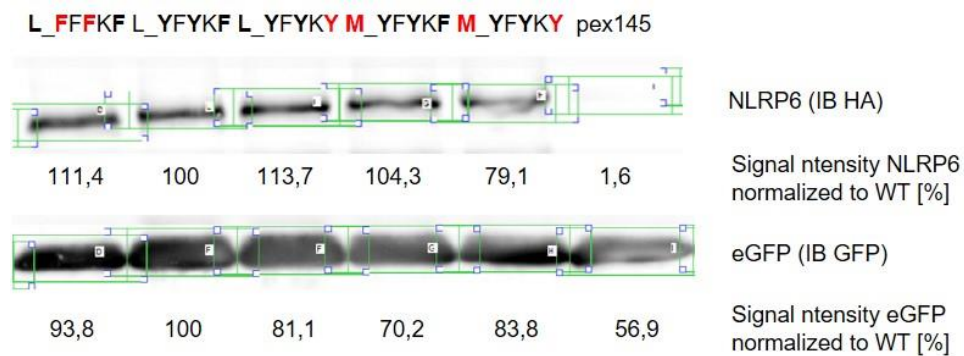
Figure 3-5 Differences in NF-κB activation by NLRP6 constructs may partly be affected from alterations of protein expression or transfection efficiency.
Immunoblot analysis for NLRP6 and eGFP from pooled cell lysates of triplicates of each 25 ng *NLRP6* transfection of previously shown DLA (Figure 3-4). Data show calculated % of quantified band intensity (by Fusion software), setting NLRP6 L_YYF (WT) as 100 % and is representative of technical triplicates from one experiment. Overlapping boxes (green) in the software were utilized to define signal beginning and end.

Further, we wanted to evaluate the statistical significance of the observed effect in previous DLA, where tyrosine at tested positions revealed enhanced NF-κB activation. Therefore, DLAs with the optimized plasmid amounts of 10 ng ASC and NLRP6 1 – 25 ng, were repeated. Below, Figure 3-6 shows NF-κB activation for several repeats (including previously shown exemplary experiment) in a <u>combined analysis</u>.

In line with our previous observation, NLRP6 SNP F361Y (L_YYY and M_YYY) clearly enhances NF-κB activation at 5, 10 and 25 ng. Moreover, NF-κB activation is enhanced by tyrosine residue at amino acid positions 357 and 359 at 10 and 25 ng (evaluated for L_FFF). Protein expression level for NLRP6 and eGFP were also tested (not shown). However, they do not explain the observed effects.

ASC 10 ng	+	+	+	+	+	+	+	+	+	+	+	+	+	+	+	+	+	+	+	+	+	+	+	+	+	+	+	+	+	+
NLRP6 L_YFYKF	1	-	-	-	-	5	-	-	-	-	10	-	-	-	-	-	25	-	-	-	-	-
NLRP6 L_FFFKF	-	1	-	-	-	-	5	-	-	-	-	10	-	-	-	-	-	25	-	-	-	-
NLRP6 L_YFYKY	-	-	1	-	-	-	-	5	-	-	-	-	10	-	-	-	-	-	25	-	-	-
NLRP6 M_YFYKF	-	-	-	1	-	-	-	-	5	-	-	-	-	10	-	-	-	-	-	25	-	-
NLRP6 M_FFFKF	-	-	-	-	-	-	-	-	-	-	-	-	-	-	10	-	-	-	-	-	25	-
NLRP6 M_YFYKY	-	-	-	-	1	-	-	-	-	5	-	-	-	-	-	10	-	-	-	-	-	25
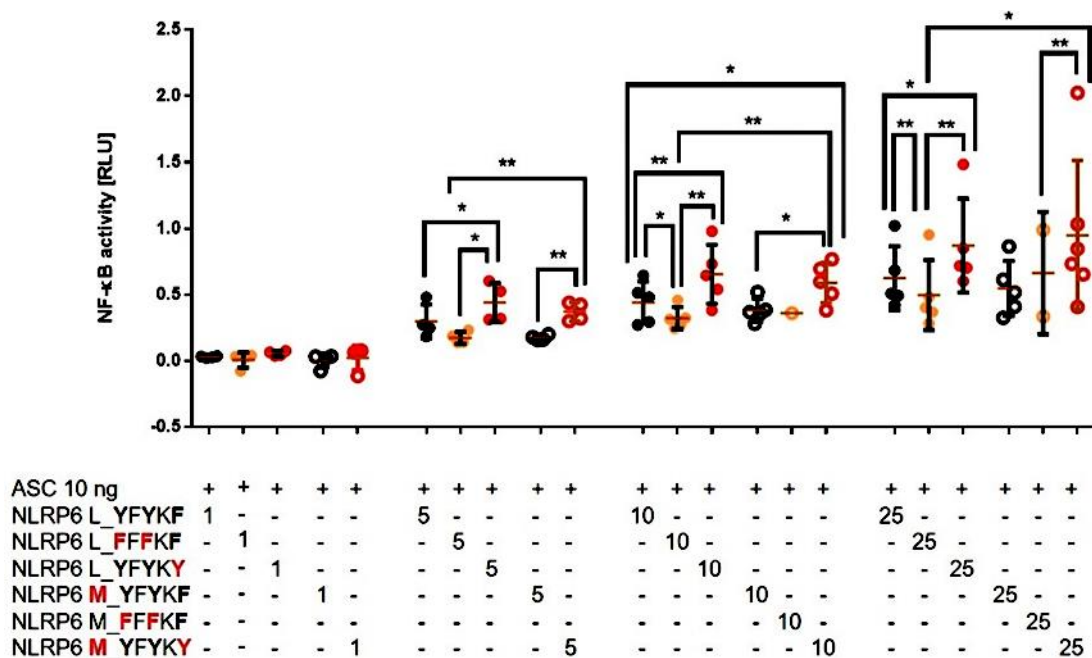
Figure 3-6 NLRP6 SNP F361Y and surrounding tyrosine at amino acid 357 and 359 result in significantly elevated NF- κB activation (when Gaussian distribution is assumed).
HEK cells were transfected with indicated amounts of NLRP6 construct together with ASC, NF-κB reporter plasmid and Renilla. After 2 days NF-κB-dependent activation was assessed by DLA. DLA values were subtracted from blank (10 ng ASC) transfection. Data show mean of values with SD representative of technical triplicates from a minimum 3 - 6 experiments depending on the amount tested. (1 ng n=3, 5 ng n=4, 10 ng n=5 except M_FFF, 25 ng n=5 except M_FFF n=2). Significance for 10 and 25 ng M_FFF could not be tested as data derive from less than 3 repeats. The amount of replicates is too small to test Gaussian distribution and a Gaussian distribution was assumed here (for further details see section 2.5). Differences were tested using a paired Student's t-test. *p< 0.05, **p< 0.01.

For an additional meta-analysis on the effect of SNP F361Y, we pooled results of M and L alleles at position 163 together, to have a larger data pool. The test resulted in no Gaussian distribution and hence, Wilcoxon-test was applied.

As observed previously, tyrosine at position 361 significantly enhances NF-κB activation nearly two-fold for 5 ng and 1.5-fold for 10 and 25 ng. Also, tyrosine at positions 357 and 359 elevate NF-κB activation compared to NLRP6 constructs carrying phenylalanine at these positions, which is significant at 25 ng construct tested.
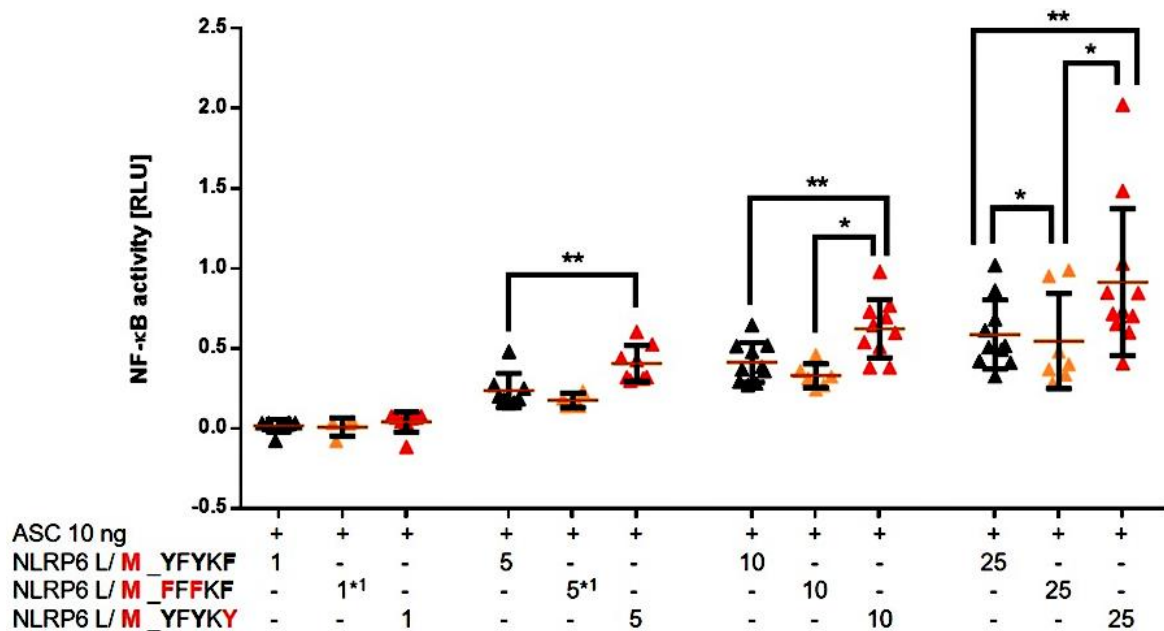
Figure 3-7 Reanalysis of effect of NLRP6 SNP F361Y and surrounding tyrosine at amino acid 357 and 359 pooling M- and L- alleles together reveal significantly induced NF- κB activation. Data from Figure 3.6 were reanalyzed by combining the results for L and M (amino acid 163) together for YYF, FFF and YYY (amino acid 357, 359, 361). *[1] For M_FFF no data on 1 ng and 5 ng are available. Differences were tested using Wilcoxon-test. *$p < 0.05$, **$p < 0.01$.

In agreement with Grenier et al.[189], we found that NLRP6 alone is not sufficient to induce NF-κB, and therefore needs ASC. In our experimental setting, 10 and 25 ng of *NLRP6* construct were suitable amounts to compare different constructs. Interestingly, tyrosine compared to phenylalanine at position 361 resulted in slightly enhanced NF-κB activation showing the strongest effect compared to WT. On the other hand, phenylalanine at positions 357 and 359 seemed to have lower signal potency. The effect of elevated NF-κB activation of tyrosine at the aforementioned positions is independent of the amino acid leucine (WT) or methionine (SNP) at position 163. Overall, although effects are small, they reveal a clear trend of tyrosine in inducing NF-κB activation, reaching significance when M- and L- alleles are pooled together.

3.3 NLRP6 mutant M_Y shows elevated interaction with ASC *in vitro* in IP

Next, we wanted to evaluate whether the observed increase in NF-κB activation by tyrosine in our tested constructs might be due to a higher interaction of respective NLRP6 constructs with ASC. Therefore, our next step was to look for the interaction of NLRP6 and ASC. Here, again we focused on the generated NLRP6 constructs, which are resembling naturally occurring genotypes. This applies to the constructs NLRP6 L_YYF, NLRP6 L_YYY, NLRP6 M_YYF, and NLRP6 M_YYY.

Direct interaction of NLRP6 and ASC had been suggested but not been shown at the time of our investigation. NLRP6 and ASC are thought to interact via their N-terminal Pyrin domains similar to other NLR inflammasomes[212], which was further confirmed after the experimental work of my thesis[213]. Therefore, C-terminally tagged constructs were generated for NLRP6 and ASC (see section 5.2), to avoid steric hindrance of the interaction by a tag. We first tested interaction employing a Luminescence-based mammalian interactome mapping (LUMIER) assay, but no interactions were detectable with this method (see section 5.1.6). However, results in our laboratory employing LUMIER have indicated weak interactions are as oftentimes not detectable via this method.

Therefore, our next step was to conduct a co-immunoprecipitation (Co-IP) assay. For this purpose, we transfected HEK cells with HA-tagged NLRP6 and GFP-tagged ASC and lysed cells 2 days post-transfection. A part of cell lysate was stored to immunoblot gene expression of NLRP6 and ASC. Further tubulin was immunoblotted to ensure similar loading. The rest of lysate was incubated with magnetic HA dynabeads to pull down HA-tagged proteins in the lysate.

In the assay, interaction of NLRP3 and ASC (positive control) was confirmed, detectable by ASC pulled down in the IP. Negative controls for unspecific binding of HA beads (transfection of pex145 (HA-EV) + ASC-GFP) and for unspecific binding of NLRP6 (transfection of NLRP6 L_YYF + pex193 (GFP-EV)) display no pull down in IP, in the GFP immunoblot. All conducted IP repeats (Figure 3-8 A) reveal an interaction of each of the tested NLRP6 construct with ASC. Interestingly, we found that the intensity of interaction of NLRP6 carrying both SNPs, namely NLRP6 M_YYY, is markedly stronger than WT NLRP6 and other tested NLRP6 constructs. Additionally, the minor difference in expression does not account for this result.

We intended to evaluate the interaction intensity and, further, consider the fact that transfection levels can vary between experiments. Thus, we analyzed the ratio of pulled down ASC to the transfection level of ASC.

Plotting these values normalized to NLRP6 WT, as shown in Figure 3-8 B), they display a consistent elevated interaction of NLRP6 M_YYY with ASC and a slightly elevated interaction intensity for NLRP6 L_YYY and M_YYF compared to WT.
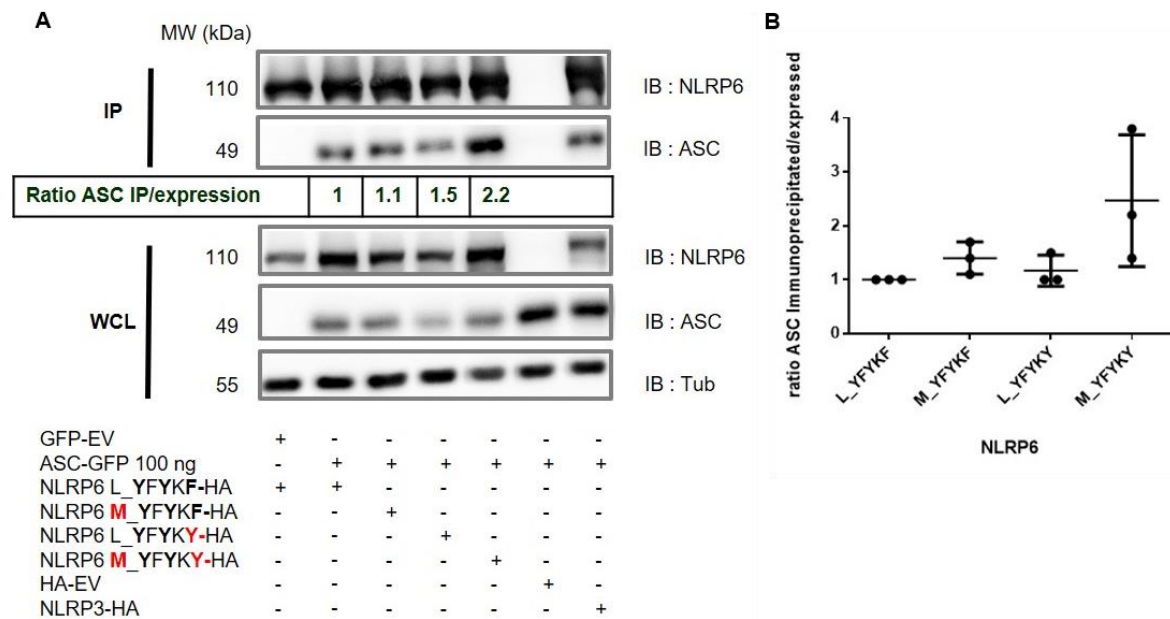
Figure 3-8 Interaction of NLRP6 and ASC in IP assays revealing elevated interaction of NLRP6 construct harboring both SNPs (M_YYY).
Co-IP was conducted with anti-HA beads (Pierce™ Anti-HA Magnetic Beads) for pull down of HA-tagged proteins from lysates of transfected HEK293T cells. (A) Immunoblot analysis for NLRP6, ASC and Tubulin (loading control) of whole cell lysate (WCL) and for NLRP6 and ASC after pull down of residual lysate with anti-HA beads. The signal of a band was quantified using Fusion software and the ratio of immunoprecipitated to expressed ASC normalized to NLRP6 WT deduced. Immunoblot is representative of three experiments. B) Ratios of determined immunoprecipitated/expressed ASC normalized to NLRP6 WT with SD from 3 experiments were plotted in a graph. EV, empty vector.

For an additional confirmation, the generated HEK Flp-In™ TRex™ 293T cells stably expressing different HA-tagged NLRP6 constructs (see section 3.1.3) were utilized to determine the interaction of NLRP6 and ASC. The advantage of this system is an induction of a similar expression level of each of the different NLRP6 constructs. This is because each of the generated cell lines (1 per construct) contains the *NLRP6* expression cassette in the same identification genomic integration site and expression of the protein can be controlled by Tetracycline and its derivates. Thus, the expression levels should be identical in theory. Since binding of similar levels of NLRP6 to beads is essential to allow subsequent binding of respective amounts of ASC, the application of this system can minimize variations in the readout and, therefore, allows for generating more dependable results.

An interaction for each of the employed NLRP6 construct with ASC was confirmed in Doxycycline-treated HEK Flp-In™ TRex™ 293T cell lysates (Figure 3-9 A). Distinctly, M_YYY co-precipitated with ASC over 3 times higher than WT and also L_YYY reveals almost 3 times higher interaction with ASC (Figure 3-9 B). M_YYF only shows slightly elevated interaction. Although this is in keeping with the results obtained from transient transfections, this assay was performed once and contrary to expectations, expression of NLRP6 was not entirely equal between cell lines. Thus, further repeats are required to verify the results and enable also to test for significance.
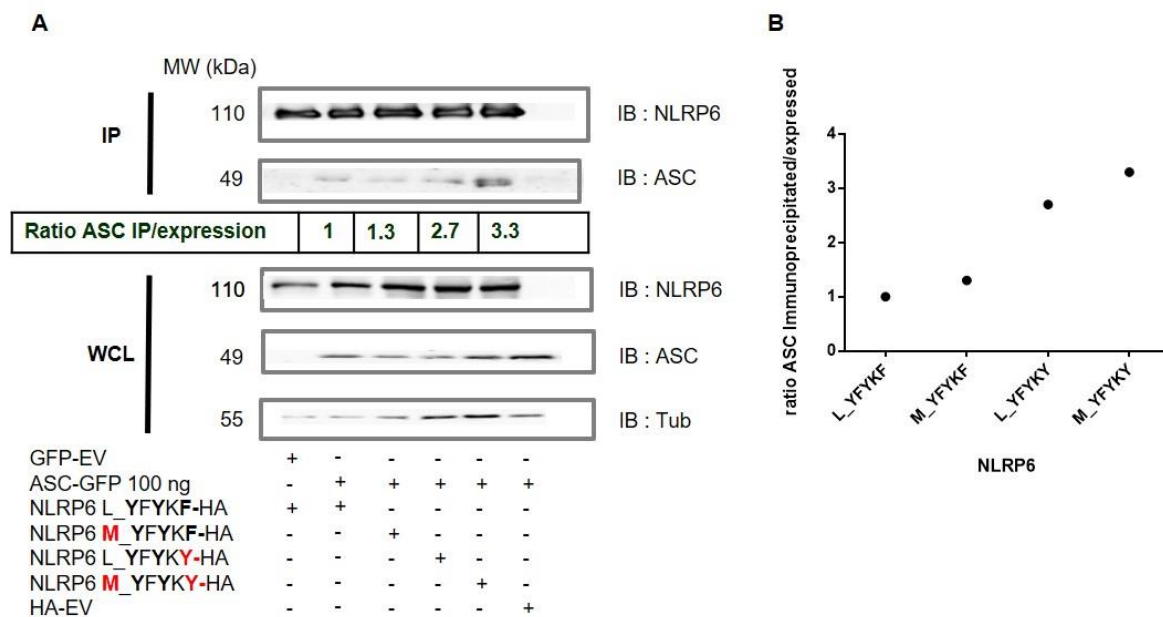
Figure 3-9 HEK Flp-In™ T-REx™ 293T cells stably expressing NLRP6 constructs confirm interaction of NLRP6 and ASC and increased interaction of NLRP6 harboring both SNPs or F361Y.
Co-IP assay of generated HEK FLP-IN™ T-REX™ 293T cells stably expressing Strep-HA tagged NLRP6 construct transfected with GFP-tagged ASC, were carried out with monoclonal anti-HA antibody (Pierce™ Anti-HA Magnetic Beads) as previously conducted in HEK cells. A) Immunoblot analysis for NLRP6, ASC, and Tubulin of whole cell lysate (WCL) together with immunoblot analysis for NLRP6 and ASC after pull down of residual lysate with a monoclonal anti-HA antibody. The signal of a band was quantified using Fusion software and the ratio of immunoprecipitated to expressed ASC normalized to NLRP6 WT is included (n=1). B) Ratios of determined immunoprecipitated/expressed ASC normalized to NLRP6 WT were plotted in a graph. EV, empty vector.

Taken together, in *HEK cells* NLRP6 M_YYY shows a tendency for induced interaction with ASC, whereas in *HEK Flp-In™ 293 T-REX™ 293T cells* stably expressing NLRP6, NLRP6 M_YYY and L_YYY clearly reveal an elevated interaction with ASC, compared to other tested NLRP6 constructs.

This result suggests that higher interaction of these NLRP6 constructs may result in elevated NF-κB activation, as observed previously, in our DLA assays. That the level of ASC binding might impact on the level of induced NF-kB activity had not been suggested before. However, since we observed that both tested *NLRP6* SNPs seem to occur together in our cohort, the determined effect of NLRP6 construct carrying both SNPs (NLRP6 M_YYY) in our *in vitro* systems is more relevant, physiologically. NLRP6 harboring both SNPs clearly revealed stronger interaction with ASC. This result suggests that a higher interaction of NLRP6 harboring both SNPs with ASC may result in an elevated NF-κB activation. Therefore, carriers of these *NLRP6* SNPs may thereby promote proinflammatory conditions and correlate with a higher risk for CRC.

3.4 *NLRP6* SNPs do not affect TLR4, 5 and 7/8-mediated gene transcription in whole blood

Since overexpression of NLRP6 and ASC in HEK cells is sufficient to induce NF-κB activation and additionally, molecular mechanisms of NLRP6 are hardly known, we wondered if *NLRP6* can function as a regulator of an NF-κB-dependent pathway, i.e. via TLR signaling.

We wanted to evaluate a physiologic role and potential impact of different *NLRP6* SNPs on TLR signaling via TLR4, 5 or 7/8 and proinflammatory signaling (an analysis system that was probably inadequate as discussed later). On these grounds, whole blood of WT, heterozygous or homozygous *NLRP6* SNP carriers, were stimulated with the TLR ligands R848 (TLR7/8), Flagellin (TLR5) or LPS (TLR4) and expression of proinflammatory cytokines determined by qPCR. Since both SNPs (M163L) and (F361L) always are found together in donors of our cohort, the term heterozygous or homozygous carriers refer to both *NLRP6* SNPs.

Whole blood stimulation with indicated TLR ligands and assessment of cytokine expression revealed no significant effects (Figure 3-10). Flagellin stimulation shows similar cytokine expression among all tested *NLRP6* genotypes. To rule out differences in tested *NLRP6* SNP categories due to impact of known *TLR5* SNPs, which may have a higher impact on flagellin response, we considered the *TLR5* status in the experimental design. The donors employed for all whole blood stimulations with R848, LPS and flagellin were the same. Selected donors for WT, heterozygous and homozygous *NLRP6* SNP carriers, represent equal numbers of F616L or N592S SNP carriers. R392X SNP carriers were excluded. However, for *NLRP6* homozygous carriers, only 1 FF carrier and 3 hypo-responsive LL carrier for *TLR5* F616L were available. Thus, our results suggest that *NLRP6* SNPs do not have an effect on TLR5 signaling.

However, upon R848 and LPS stimulation, there is a trend towards reduced cytokine expression (10-65%) for tested cytokines for homozygous *NLRP6* SNP carriers compared to heterozygous SNP carriers. The induced NF-κB activation in DLA by NLRP6 harboring both SNPs previously observed would suggest accordingly higher cytokine activation in respective donors. However, after LPS and R848 stimulation, we observed a reduction in cytokine transcription. Albeit this the effect of *NLRP6* SNP carriers on TLR4 or TLR7/8 signaling is not significant and the number of donors possibly too small to detect small differences. Several explanations for this apparent discrepancy between DLA and whole blood analysis can be given, for example, the experimental setup and the stimulating agonist. Both are discussed in section 4.1.3.
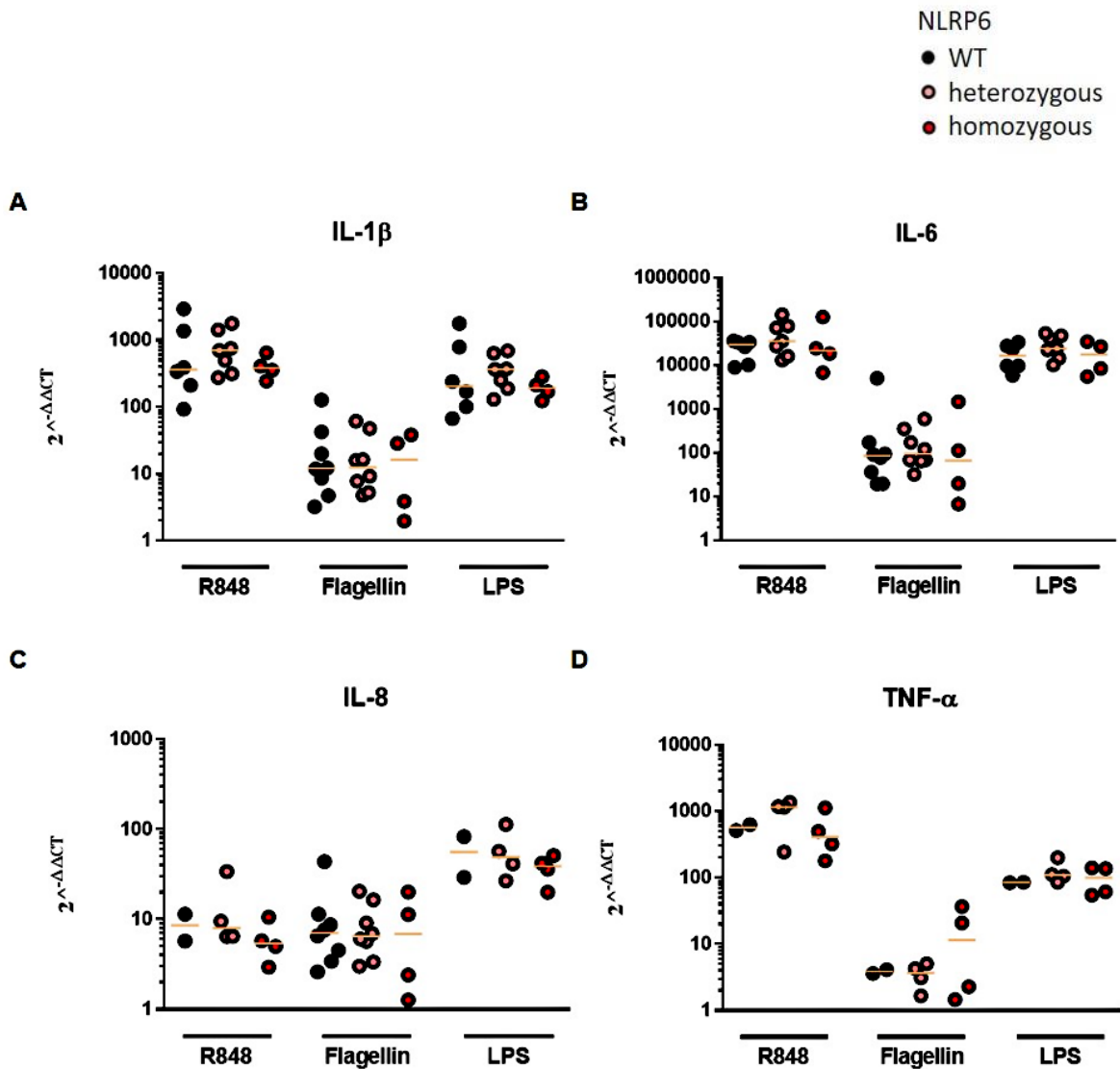
Figure 3-10 Homozygous carriers of both *NLRP6* SNPs (L163M, F361Y) reveal a slight trend towards reduced cytokine expression compared to heterozygous carriers upon LPS and R848 stimulation.

Whole blood of healthy *NLRP6* WT, heterozygous or homozygous *NLRP6* SNP carriers (M163L, Y361F) were stimulated with 5 µg/ml R848, 100 ng/ml Flagellin or 100 ng/ml LPS for 3 hours. Transcript levels of *IL-1β*, *IL-6*, *IL-8,* and *TNF-α* were assessed by RT-qPCR and normalized to *TBP* and shown as $2^{-\Delta\Delta CT}$. Data show the median of values representative of technical triplicates from each experiment. WT (black), heterozygous (rose) homozygous (red) donors for *NLRP6*. Each dot represents one donor. Data points were generated by Dr. Klimosch[147] (retrospective analysis) and me (see 2.3.4). Differences were tested using the Mann-Whitney U test. All tested differences were non-significant.

3.5 Role of *TLR5* and *NLRP6* SNPs in gut immune parameters analyzed in stool samples

3.5.1 *TLR5* and *NLRP6* SNPs impact gut immune parameters

According to mouse models, TLR5 and NLRP6 are crucial intestinal PRRs and to our knowledge, no systematic analysis on their physiologic role in the human gut immune and microbial parameters exists. We wanted to explore the impact of our *TLR5* and *NLRP6* SNPs on different parameters in human gut, utilizing stool samples of healthy donors.

The following part of my thesis is based on our hypothesis that alterations in important intestinal PRRs, as in the case of *TLR5* and *NLRP6* SNPs, may alter gut immune parameters and microbial balance and thereby render carriers of these SNPs susceptible to diseases, i.e. obesity, colitis, and cancer.

Supporting this idea, *Tlr5* knock out mice have been associated with adiposity and parameters of metabolic syndrome, including elevated body mass, higher cholesterol, blood pressure and glucose levels in the blood, compared to *Tlr5* WT mice by Vijay-Kumar et al.. Additionally, *Tlr5* deficiency has been linked to an altered microbiome in mice.[140]

Studies on *TLR5* SNPs, in human, by S. Klimosch et al. revealed alterations in the immune response: They employed HEK FLP-IN™ T-REX™ 293T cells stably expressing respective TLR5 SNP or whole blood from respective SNP carriers and assessed the cytokine response on mRNA level to TLR5 stimulation. TLR5 SNP F616L showed a hyporesponsive phenotype to flagellin stimulation. TLR5 SNP N592S, on the other hand, was significantly lower or similar responsive to flagellin (depending on flagellin strain employed for stimulation) compared to WT in HEK FLP-IN™ T-REX™ 293T cells expressing this SNP, whereas donor numbers were too low to investigate the immune response of *N592S* SNP carriers in whole blood. Additionally, these SNPs displayed remarkable associations with CRC. Heterozygous *TLR5* F616L SNP carriers were significantly associated with almost two times higher probability to survive from colorectal cancer (hazard ratio=1.92) compared to WT, whereas carriers of homozygous *TLR5* SNP N592S were significantly associated with two times worse survival in CRC (hazard ratio=0.51).[147]

Looking at *Nlrp6* KO mice, these have been associated with altered microbiota[191,192] and modified mucus secretion[200] and moreover were perceived to be prone to colitis and CRC[186,192].

Further, a human *NLRP6* association study by Huhn et al. revealed that heterozygous carriers of *NLRP6* SNP M163L were significantly associated with

nearly two times higher risk for rectal cancer and higher risk for colon and rectal cancer together. No significant association of *NLRP6* SNP F361Y for risk for colon or rectal cancer was found in the aforementioned study.[197] However, in our studies, we found *NLRP6* SNP F361Y usually linked to M163L. Therefore, we considered that SNP F361Y may thereby influence the function of M163L.

3.5.2 Study approach

To study immunologic and metagenomic parameters, we established a cohort of around 250 healthy donors, out of which 51 donors (age 20-48, 68 % female) participated in stool donation (for further cohort description, see 2.4.1 and for study design, see 2.4.2). The dry weight of samples (assay conditions and dry weight assessment, see 5.1.4, detailed method, see 2.4.6) may impact measured values, and therefore considered for each parameter. A metagenomic final analysis was conducted by collaboration partners and not included in this thesis work as they were in progress at the time of thesis writing.

3.5.3 Association of *TLR5* and *NLRP6* SNPs with intestinal sIgA level

Tlr5 KO mice have been shown to result in reduced flagellin specific, despite higher total sIgA levels by Cullender et al.. In addition, loss of *Tlr5* function in *Tlr5* KO mice resulted in enhanced bacterial flagellin expression, indicating lower anti-flagellin IgA response allows bacteria to sense a missing recognition of flagellin and thus, leads to an upregulation of flagellin.[145]

First, we wanted to evaluate, if the *TLR5* and *NLRP6* SNPs have an impact on intestinal sIgA level in humans. To this end, we employed a sIgA ELISA kit (Ridascreen) and developed a sIgA standard with purified human sIgA (Bio-Rad) for the kit to quantify sIgA level (for methods see 2.4.9).

Intriguingly, stool samples of donors, heterozygous for both *NLRP6* SNPs M163L and F361Y, reveal clearly significantly (up to 1.5 times) elevated sIgA level compared to WT (see Figure 3-11). This is also true for heterozygous carriers, with higher variances in upper values, after normalization. Stool samples of donors, heterozygous for *TLR5* SNP R392X in contrast to WT have a clear tendency towards elevated sIgA level (p=0.07), which is significantly up to two-fold higher after normalization to dry weight. Nearly 40 % of values in WT are below the lowest value measured (around 2700 before normalization) for heterozygous R392X carriers. On the other hand, *TLR5* F616L and N592S SNP carriers show no significant effect on the assessed human sIgA level.

In healthy individuals, the normal range of sIgA in the stool is 100-1200 µg/g according to the kit reference of the sIgA ELISA (r-biopharm AG). Here, donors in the category of homozygous F616L carriers have sIgA values close to 1200 µg/g, whereas, surprisingly, heterozygous *NLRP6* SNP carriers and heterozygous R392X carriers have sIgA values up to approximately 3500 or 4000 µg/g.
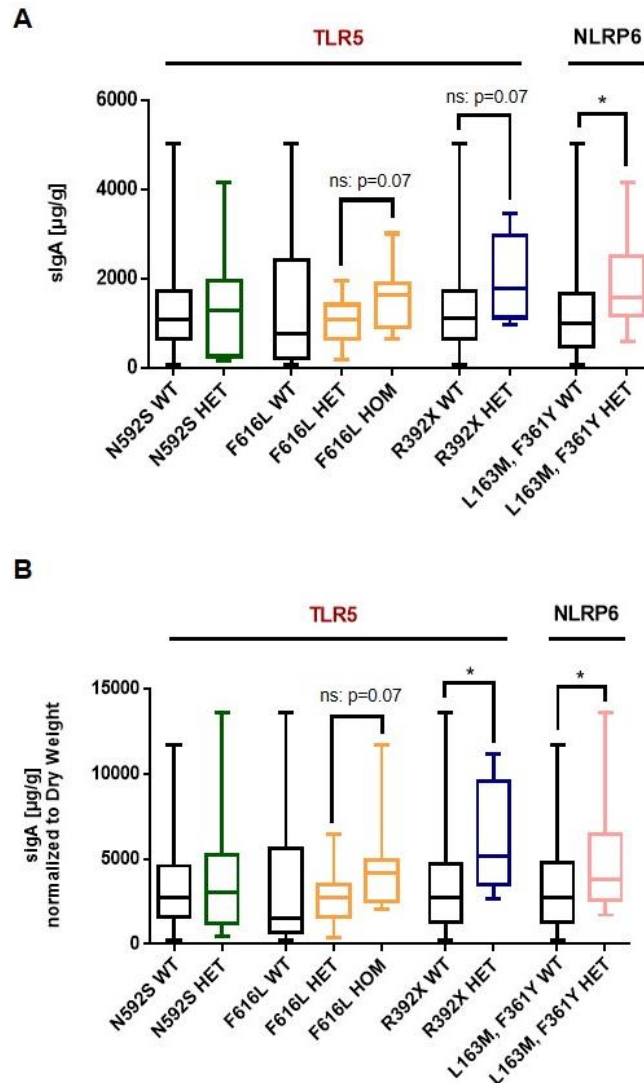
Figure 3-11 *NLRP6* SNPs and *TLR5* SNP R392X shape intestinal sIgA level.
ELISA of human sIgA in stool supernatant of donors stratified for *TLR5* and *NLRP6* genotype status. Data derive from triplicates of 1 experiment and are illustrated as min-to-max box-and-whisker plots with differences tested using the Mann-Whitney U test. *p< 0.05. A) raw data B) data normalized to dry weight.

The results suggest that NLRP6 may have a role in intestinal homeostasis, i.e. by regulation of sIgA secretion. Based on the previously observed phenotype in our *in vitro* studies, they further support the idea that induced NF-κB activation, by NLRP6 SNPs and ASC, may result in elevated sIgA level. Probably, NLRP6 SNPs may be activated by microbial ligands or metabolites, however, the molecular pathway for NLRP6 activation is not fully understood yet.

Further, R392X carriers, who have abrogated TLR5 signaling, displayed elevated total sIgA levels. This observation suggests an upregulation of other types of sIgA than flagellin-specific upon abrogated flagellin sensing. Additionally, *TLR5* R392X and *NLRP6* SNP carriers revealed up to two times higher levels of sIgA than WT, indicating highly inflammatory conditions for these SNP carriers in the gut.

3.5.4   Association of *TLR5* and *NLRP6* SNPs with intestinal MAMP levels

Levels of bioactive flagellin or LPS in stool samples determined by TLR5 or TLR4 activation, respectively, may give further indications and characterization on previously assessed sIgA content in different genotypes.

3.5.4.1 TLR5 activation by stool samples

Cullender et al. have shown that the absence of a functional TLR5 in *Tlr5* KO mice alters flagellin expression and results in an upregulation of flagellin content.[145] Elevated levels of intestinal flagellin have been associated with a breach of the mucosal barrier and inflammation[145]. In addition, a reduced flagellin recognition can be promoted during disease, such as IBS, by decreased TLR5 expression[214]. Thus, if the level of flagellin is not regulated or its recognition altered by corresponding receptors, in humans by TLR5 or NLRC4[215], it may predispose flagellated bacteria to invade the mucus layer and underlying cells and thereby induce inflammatory processes. This effect may be further enhanced in disease setting. Here, we wanted to test the effect that *TLR5* and *NLRP6* SNPs have on flagellin content in the human gut, examining stool samples.

To evaluate TLR5 activation in stool samples of our cohort, we conducted different activation reporter assays. First, we employed, generated HEK Flp-In™ T-REx™ 293T cells (Invitrogen) stably expressing TLR5, whose TLR5 expression can be regulated and induced by addition of Tetracycline or Doxycycline (for cell line description see 3.1.3). These cells were treated with Tetracycline or Doxycycline, for TLR5 expression, and then stimulated with stool supernatant or medium as control. Upon TLR5-dependent stimulation, cells were lysed, and *TNF-α* was assessed by RT-qPCR (for the establishment of the assay see 5.1.5).

Secondly, we employed HEK-Dual™ hTLR5 cells (InvivoGen), which allow to monitor NF-κB and AP-1 activation by an inducible secreted embryonic alkaline phosphatase (SEAP) reporter and a Lucia luciferase reporter under IL-8 promoter (for methods see section see section 2.4.10). This method allows us to confirm our result from HEK Flp-In™ T-REx™ 293T cells stably expressing TLR5 and gives further information on TLR5 activation on transcriptional and translational level.

3.5.4.1.1 TLR5 activation by stool samples determined by TLR5 assay

Using HEK Flp-In^{TM} T-REx^{TM} 293T cells stably expressing TLR5, we carried out stimulation with stool supernatant of all donors and stratified results for the respective genotype. When stratifying for *TLR5* wildtype, N592S and F616L, heterozygous or homozygous carriers, donors carrying *TLR5* R392X SNP were excluded (n=6).

Surprisingly, the stool supernatant of heterozygous carriers of *TLR5* SNP N592S revealed a pronounced and significantly reduced activation of TLR5 in HEK Flp-In^{TM} T-REx^{TM} 293T cells stably expressing TLR5 (see Figure 3-12). This was also true after normalizing the results to dry weight of corresponding stool samples. 75 % of the measured values for heterozygous N592S carriers lie between 0.00025 – 0.02, hardly showing any TLR5 activation or at a minimal level.

In comparison, nearly 75 % of values of WT donors are above this range with most values ranging from 0.036 – 0.07, approximately 2 to 3 times higher. Nevertheless, heterozygous N592S carriers show a wide distribution, having outliers even higher than WT points. Stool samples of heterozygous carriers of *TLR5* R392X SNP compared to WT have a tendency for elevated TLR5 activation, however, this result is not significant. In contrast, other tested genotypes do not show any significant effect on TLR5 activation.
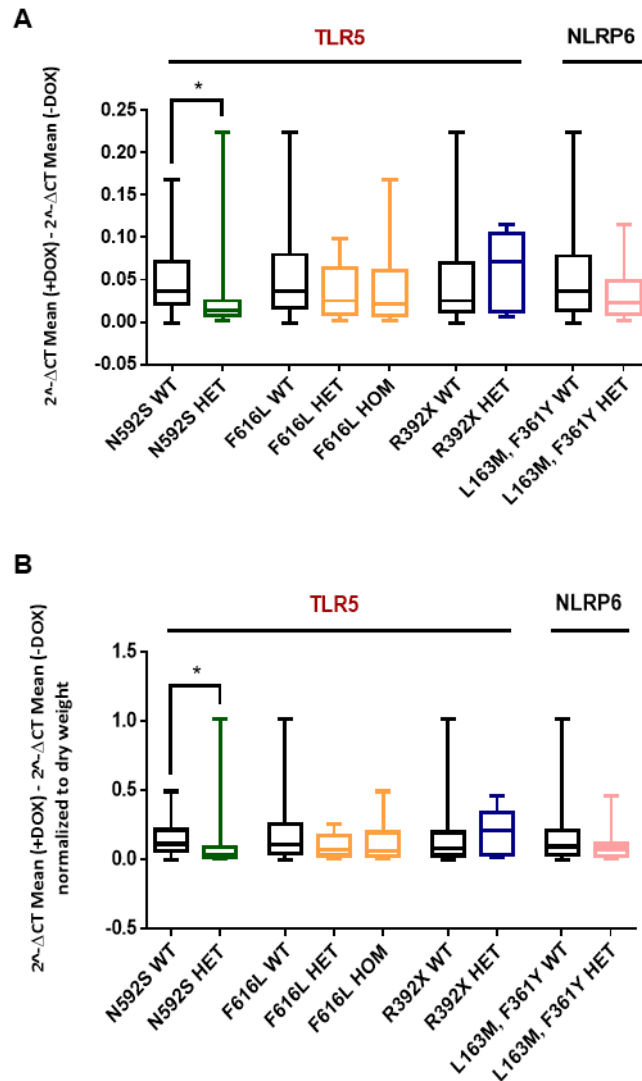
Figure 3-12 Heterozygous N592S carriers reveal remarkably reduced TLR5 activation in the gut compared to WT in TLR5 assay.
Doxycycline induced, or as a control for internal TLR5 activation non-induced, HEK FLP-IN™ T-REX™ 293 cells stably expressing TLR5 were stimulated for 3 hours with stool supernatant from donors and *TNF-α* was measured by RT-qPCR. Induction of TLR5 activation by each sample was assessed by subtraction of relative $2^{-\Delta\Delta CT}$ of Doxycycline induced from a non-induced sample and stratified for *TLR5* and *NLRP6* genotypes. Data derive from triplicates of 1 experiment and are illustrated as min-to-max box-and-whisker plots with differences tested using the Mann-Whitney U test. *p< 0.05. A) Data before normalization. B) Data normalized to dry weight. Stimulation assay was conducted by me, qPCR run by Sabine Dickhöfer.

3.5.4.1.2 TLR5 activation by stool samples determined by HEK-Dual™ hTLR5 assay

Looking at NF-κB activation in the HEK-Dual™ hTLR5 reporter system, we could find very consistent and significantly elevated values (up to 4 times higher than WT) for heterozygous R392X carriers (see Figure 3-13). Remarkably, we can see this phenotype for 6 donors in total for heterozygous R392X, which emphasizes its strong effect.

On the other hand, heterozygous N592S carriers hardly show any difference compared to WT, before and after normalization of the result to dry weight. No significant changes are found for *TLR5* F616L and *NLRP6* SNP carriers.
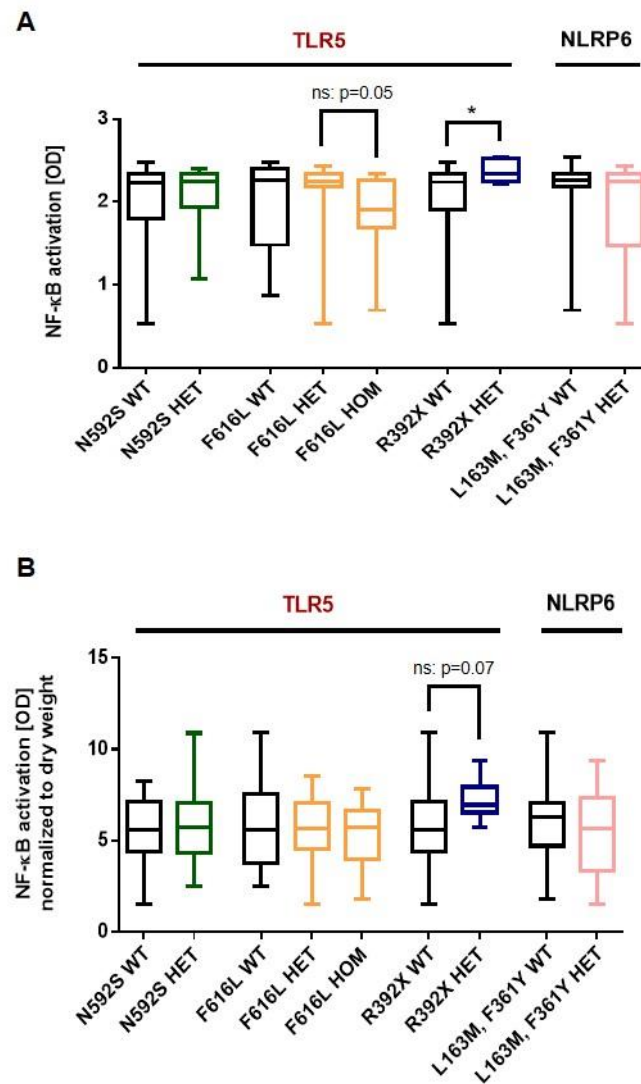
Figure 3-13 TLR5-dependant NF-κB activation is significantly elevated in stool samples of heterozygous R392X carriers in HEK-Dual™ hTLR5 cells.
HEK-Dual™ hTLR5 cells stably expressing TLR5 were stimulated with stool supernatant from donors for about 22 hours and NF-κB dependent SEAP expression was assessed in the supernatant by spectrophotometric analysis. Results were stratified for tested *TLR5* and *NLRP6* genotypes. Data derive from triplicates of 1 experiment and are illustrated as min-to-max box-and-whisker plots with differences tested using the Mann-Whitney U test. *p< 0.05. A) raw data. B) data normalized to dry weight. These experiments were conducted by our technician Sabine Dickhöfer.

IL-8 dependent luciferase activity in HEK-Dual™ hTLR5 cells displays drastic effects in tested *TLR5* SNPs carriers on TLR5 activation (see Figure 3-14).

IL-8 dependent luciferase activity in HEK-Dual™ hTLR5 cells reveals a pronounced significant decrease in TLR5 activation for heterozygous carriers of *TLR5* SNP N592S compared to WT, which is also confirmed when the result is normalized to dry weight. For example, 75 % of data for heterozygous N592S carriers are below around 23000, while 75 % of WT data are distributed up to 40000 without normalization (up to two times lower than WT). Heterozygous carriers of *TLR5* SNP R392X reveal a strong tendency for (up to two times) higher TLR5 activation compared to WT, which is significant after normalization of the result to dry weight. No significant changes are observed for *TLR5* F616L and *NLRP6* SNP carriers.
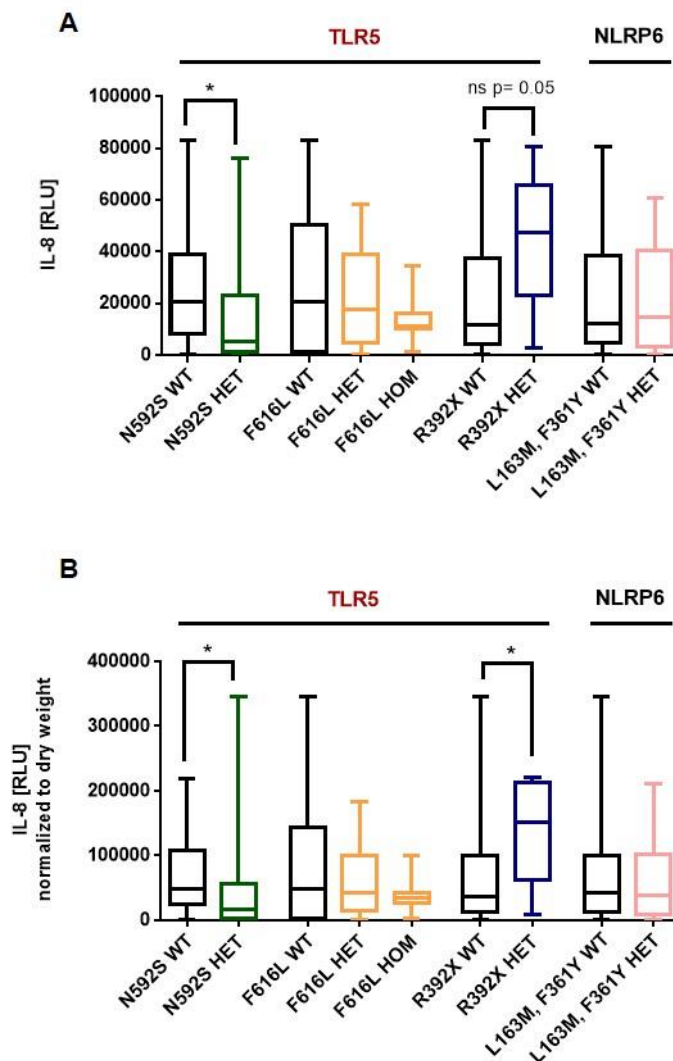
Figure 3-14 Heterozygous N592S carriers show reduced, while heterozygous R392X carriers elevated TLR5-dependant IL-8 level in stool samples.
HEK-Dual™ hTLR5 cells stably expressing TLR5 were stimulated with stool supernatant from donors for about 22 hours and luminescence measured to assess IL-8 dependent luciferase activity. Results were stratified for tested *TLR5* and *NLRP6* genotypes. Data derive from triplicates of 1 experiment and are illustrated as min-to-max box-and-whisker plots with differences tested using the Mann-Whitney U test. *p< 0.05. A) raw data. B) data normalized to dry weight.

Taken together, in this study we evaluated, for the first time, TLR5 activation potency of human stool samples with defined *TLR5* and *NLRP6* genotypes. We found that heterozygous N592S carriers show significantly reduced TLR5 dependent *TNF-α* levels in the TLR5 HEK Flp-In™ 293T cell assay, and IL-8 dependent luciferase activity in HEK-Dual™ hTLR5 cells. However, NF-κB activation in HEK-Dual™ hTLR5 cell assay, for heterozygous N592S carriers, are not affected. Heterozygous *TLR5* R392X carriers show in all tested methods a tendency or significant elevation of TLR5 activation. Of note is, that in this study we tested in total 6 heterozygous R392X donors, thus additional donors will complement these results. However, since the effect is quite strong, the significance is easily reached. TLR5 activation of stool samples from *TLR5* F616L and *NLRP6* SNP carriers are not significantly affected. All employed methods to analyze TLR5 potency of stool samples from different *TLR5* and *NLRP6* SNP carriers result in similar outcomes.

Table 3-2 Summary of TLR5 activation of stool samples from tested *TLR5* and *NLRP6* SNP carriers in TLR5 assay and HEK-Dual™ hTLR5 assay.
Results for TLR5 assay and HEK-Dual™ hTLR5 assay are collected in the following table for raw data and data normalized to dry weight. Changes for each genotype compared to WT are indicated. ↑, elevated ↓, reduced. *, significant (Mann-Whitney-U-test). Tendencies are indicated with the respective arrow (with p-value when close to significance). –, no change compared to WT. Het, heterozygous. Hom, homozygous. *NLRP6* het, *NLRP6* M163L, and F361Y heterozygous carriers.

Assay	Data	N592S het	F616L het	F616L hom	R392X het	*NLRP6* het
TLR5 assay	raw	↓*	-	-	↑	-
	Normalized to dry weight	↓*	-	-	↑	-
HEK-Dual™ hTLR5 assay (NF-κB)	raw	-	-	-	↑*	-
	Normalized to dry weight	-	-	-	↑? (p=0.07)	-
HEK-Dual™ hTLR5 assay (IL-8)	raw	↓*	-	-	↑? (p=0.05)	-
	Normalized to dry weight	↓*	-	-	↑*	-

Overall, our data reveal that heterozygous N592S carriers have significantly reduced TLR5 activation, which suggests that altered TLR5 signaling in this genotype leads to reduced flagellin expression or reduced TLR5 activation potential. On the other hand, elevated TLR5 activation is observed in R392X carriers. This result indicates that abrogated signaling of TLR5, in this case, leads to elevated flagellin expression or altered flagellin content with higher activation capacity. Further, we observed that a significant reduction in TLR5 activation of stool samples from heterozygous N592S carriers occurs earlier, while an elevation of TLR5 activation in heterozygous R392X carriers appears delayed. Thus, heterozygous N592S carriers display an effect on TLR5 activation in TLR5 assay after 3 hours stimulation, but it is not visible anymore in NF-κB activation in HEK-Dual™ hTLR5 cells after 22 hours of stimulation. Compared to these, heterozygous R392X carriers show a delayed TLR5 activation of stool samples, which is found significantly elevated by NF-κB activation in HEK-Dual™ hTLR5 assay after 22 hours stimulation. These results are further discussed in 4.2.2.

3.5.4.2 TLR4 activation by stool supernatant in HEK-Blue™ hTLR4 cells

LPS is one of the most potent activators of innate immune signaling and thus its regulation of high importance[216,217]. Therefore, we thought to further test the effect of *TLR5* and *NLRP6* SNPs on TLR4 activation in the human gut, utilizing stool samples.

Assessment of TLR4 activation by stool supernatant from homozygous *TLR5* F616L carriers compared to WT in HEK-Blue™ hTLR4 cells reveals a significant reduction in TLR4 activation, when normalized to dry weight (see Figure 3-15). No significant changes are observed for any other tested genotype regarding TLR4 activation.
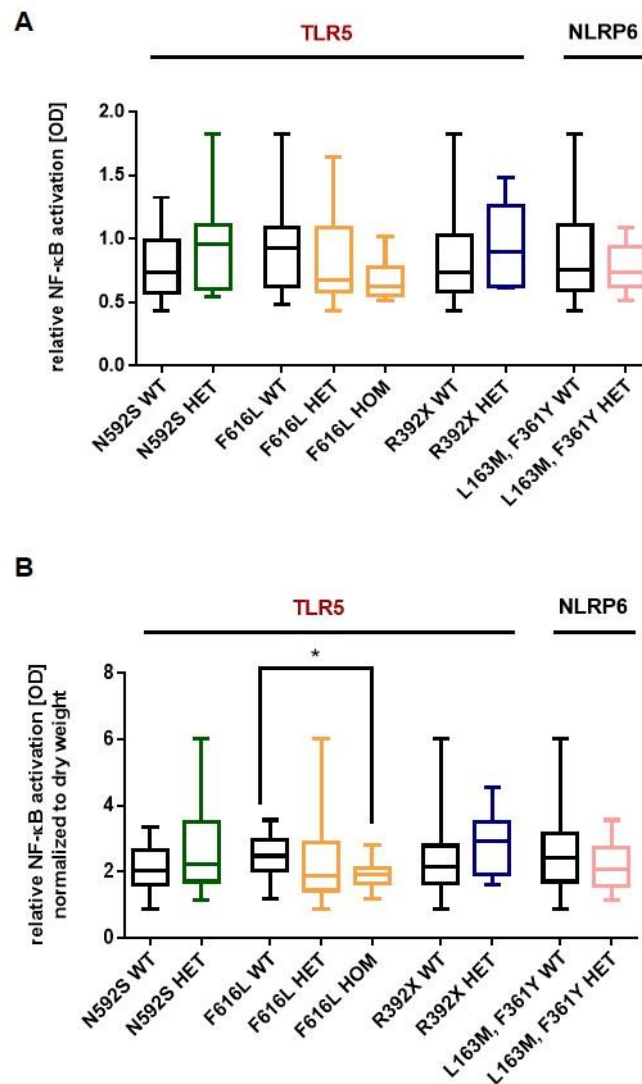
Figure 3-15 Homozygous *TLR5* F616L carriers display altered TLR4 activation in the stool assessed by HEK-Blue^{TM} hTLR4 assay.

HEK-Blue^{TM} hTLR4 cells stably expressing TLR4 were stimulated with stool supernatant from donors for about 22 hours. NF-κB dependent SEAP expression in cell supernatant was assessed by spectrophotometric analysis and normalized to internal controls. Results were stratified for tested *TLR5* and *NLRP6* genotypes. Data derive from triplicates of 1 experiment and are illustrated as min-to-max box-and-whisker plots with differences tested using the Mann-Whitney U test. *p< 0.05. A) raw data. B) Data normalized to dry weight.

This result in homozygous *TLR5* F616L carriers may indicate reduced LPS quantity or altered LPS content with reduced activation potential by i.e. altered expression or altered microbiota. To conclude on TLR4 activation, additional assays to verify our result and further analysis to elaborate LPS quantity and quality, and microbiome composition in F616L carriers have to be carried out.

3.5.5 β-defensin levels in stool supernatant

AMPs, such as β-defensins, allow to regulate the microbiota in the gut and protect the host from invading pathogens at the gut mucosal surface[218]. HBD-2, which we have investigated in stool samples of our cohort, are reported to be less detectable in the gastrointestinal tract and colon of healthy individuals[219] and induced in their expression to probiotic microbes[220], LPS[221] or to proinflammatory cytokines, such as TNF-α, IL-1β and IL-8[222]. Reduced β-Defensin levels are linked to compromised gut barrier function allowing bacteria to invade[223].

β-defensin 2 (referred to as β-defensin in the following) levels in tested *TLR5* and *NLRP6* genotypes are not significantly different from WT. According to the β-defensin kit reference (Immundiagnostik), healthy donors have a β-defensin level ranging from 8-60 ng/ml stool. Most of the values for all donors, besides some exceptions, are in line with this range.
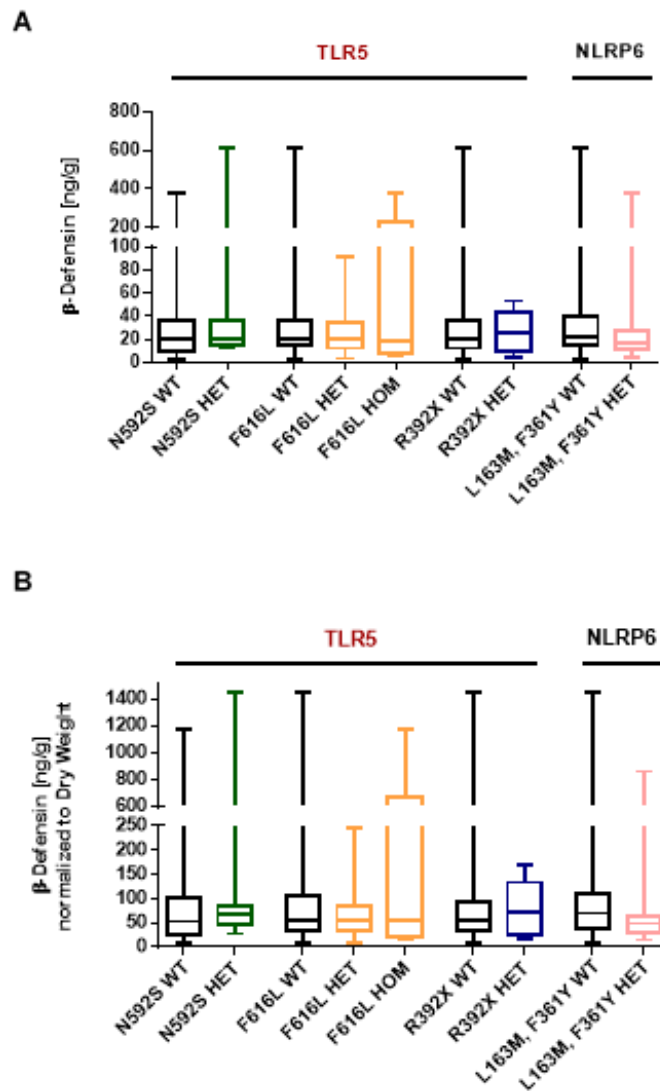
Figure 3-16 Tested *TLR5* and *NLRP6* genotypes do not show any significant changes in β-defensin level in stool samples.
ELISA of human β-defensin in stool supernatant of donors stratified for *TLR5* and *NLRP6* genotype status. Data derive from triplicates of 1 experiment and are illustrated as min-to-max box-and-whisker plots with differences tested using the Mann-Whitney U test. *p< 0.05. A) raw data. B) data normalized to dry weight.

The β-defensin ELISA seems reliable and we did not find any significant correlation of our tested genotypes and β-defensin level. Since we tested healthy donors, an alteration in the β-defensin level is not necessarily expected and does not occur in healthy donors in a *TLR5* or *NLRP6* SNP dependent manner.

3.5.6 Calprotectin levels in stool supernatant

Calprotectin is mainly present in neutrophils and measurement of calprotectin allows to determine neutrophil recruitment upon bacterial stimulation[224] or inflammatory conditions[225] in the gut[226].

Homozygous F616L carriers, compared to heterozygous or WT carriers, have significantly reduced calprotectin levels. This is also valid after normalization of the results for homozygous F616L carriers compared to WT carriers. This result suggests reduced inflammatory conditions for homozygous F616L carriers.

The commercial purpose of the applied Calprotectin ELISA is to assess the Calprotectin level and gain indications on inflammatory processes in the gut. The median of healthy individuals for calprotectin in human stool samples is 25 µg/g, below 50 µg/g calprotectin is considered as negative for indications on inflammatory processes in the gut according to the Calprotectin kit reference (Immundiagnostik). Above 100 µg/g calprotectin is considered as positive, whereas 50-100 µg/g calprotectin probably positive. Calprotectin values for WT healthy donors are close and below the threshold of 50 µg/g. Distinctly, in comparism to WT, homozygous F616L carriers and heterozygous R392X carriers show reduced calprotectin levels, whereas N592S and *NLRP6* SNP carriers are slightly higher compared to WT in their calprotectin level. We found some outliers in some of the genotypes and also WT. However, except for F616L carriers, for other tested *TLR5* and *NLRP6* SNPs, the observed low tendencies are not significant.
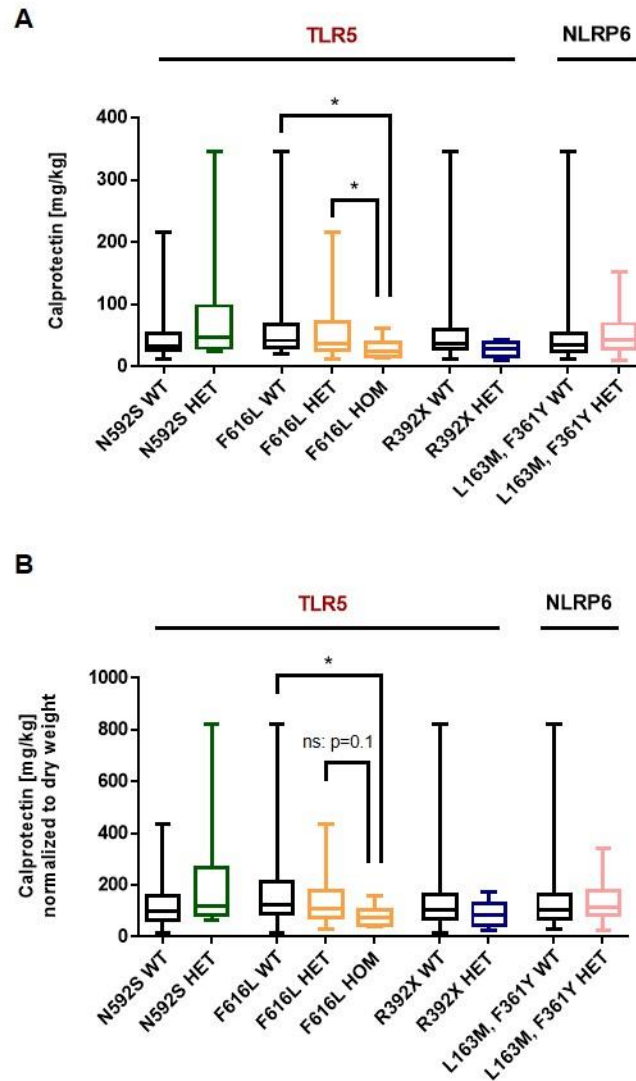
Figure 3-17 Homozygous *TLR5* F616L carriers reveal significantly reduced calprotectin levels in stool samples compared to heterozygous *TLR5* F616L carriers or WT.
ELISA of human Calprotectin in stool supernatant of donors stratified for *TLR5* and *NLRP6* genotype status. Data derive from triplicates of 1 experiment and are illustrated as min-to-max box-and-whisker plots with differences tested using the Mann-Whitney U test. *p< 0.05. A) raw data. B) Data normalized to dry weight.

Repeated freeze-thaw cycles can lead to burst of cells and release of calprotectin, leading to elevated values in the calprotectin ELISA. Thus, we considered this in our experimental design and measured calprotectin level of all samples combined after one freeze-thaw cycle.

Reduced levels in F616L carriers suggest a protective environment for inflammatory related diseases. Calprotectin levels close to significance in other genotypes may hint at normal levels in healthy donors, which probably are easily prone to inflammatory conditions in disease settings.

TLR5 and *NLRP6* SNPs impact to different extents calprotectin levels in healthy donors and calprotectin, potentially, can be a very sensitive marker.

Summary:

In the following table, results on TLR4 activation and intestinal barrier regulators are summarized.

Table 3-3 Summary of TLR4 activation, sIgA, β-defensin and calprotectin level in stool samples from tested *TLR5* and *NLRP6* SNP carriers.
Results for each assay are collected in the following table for raw data and data normalized to dry weight. Changes for each genotype compared to WT are indicated. ↑, elevated. ↓, reduced. *, significant (Mann-Whitney-U-test). Tendencies are indicated with respective arrow (with p value when close to significance). –, no change compared to WT. F616L homozygous carriers are also compared here to F616L heterozygous carriers. Het, heterozygous. Hom, homozygous. *NLRP6* het, *NLRP6* M163L and F361Y heterozygous carriers.

Assay	Data	N592S het	F616L het	F616L hom	R392X het	NLRP6 het
HEK-Blue™ hTLR4 assay	raw	-	-	↓? p=0.1	-	-
	Normalized to dry weight	-	-	↓*	-	-
sIgA	raw	-	-	-	↑? (p=0.07)	↑*
	Normalized to dry weight	-	-	-	↑*	↑*
β-Defensin	raw	-	-	-	-	-
	Normalized to dry weight	-	-	-	-	-
Calprotectin	raw	↑?	-	↓* / Het compared to Hom ↓*	↓?	↑?
	Normalized to dry weight	↑?	- / -	↓* / Het compared to Hom ↓? p=0.1	↓?	↑?

Taken together, we were able to confirm our hypothesis by the conducted study. Alterations in TLR5 and NLRP6 signaling, here in the case of SNPs, indeed leads to genotype specific changes in immune parameters and thereby further could render them prone to diseases. Remarkably, we could find significant *TLR5* and *NLRP6* SNP dependent effects in stool on immune parameters, such as TLR5 and TLR4 activation, sIgA or calprotectin levels in healthy donors. These results, in combination with an analysis of the effect of these SNPs on gut microbiota, give insight into the role of these *TLR5* and *NLRP6* SNPs in immunologic and microbial parameters, and valuable information to understand disease associations.

4 Discussion

From what has been reported for mice, NLRP6 is a central and versatile PRR in gut homeostasis. Thus, naturally occurring SNPs in this cytosolic PRR may influence its function in humans. To date, intensive investigations have been focused particularly on its role in gut defense parameters and on the murine system, whereas mechanistic insights on a molecular level and data regarding the role of NLRP6 in humans are missing. Before the compilation of this thesis work, NLRP6 and ASC together have been found to activate NF-κB[189], but its existence as inflammasome is still debated. *NLRP6* SNP L163M were found to be associated with risk for colorectal cancer[197], however, its contribution to oncogenesis has been unclear. Even though SNP F361Y is not significantly associated with a higher risk for CRC[197], both SNPs are usually found together in humans and therefore may contribute to oncogenic signaling pathways of M163L. Based on these findings, one aim of this study was to (i) elucidate the effect of human NLRP6 SNPs on NF-κB signaling and (ii) a possible interaction with ASC *in vitro* in cellular systems. Additionally, using cells from SNP carriers, (iii) a physiological role, namely a functional effect of individual alleles on immune parameters in blood cells was analyzed. Finally, by analyzing stool samples from SNP carriers, (iv) an effect on gut immune parameters was assessed. In the latter question, SNPs for *TLR5* were included since their effect on gut immune parameters and the microbiota was unknown but a functional effect had been documented[147].

In the following, I will, therefore, discuss the results obtained for these 4 key avenues of research. I will start with (i) how the phenylalanine to tyrosine change in F361Y may contribute to elevated NF-κB signaling, and how this SNP may synergize with M163L, which was found in almost exclusive linkage with F361Y in our study. (ii) I will discuss a possible connection between NF-κB activation and stronger interaction of NLRP6 SNP variant proteins with ASC. (iii) I will point out reasons, why probably a functional role in whole blood could not be confirmed in our study and how this can be achieved in future studies. (iv) how the data obtained for intestinal sIgA level, flagellin content, LPS content, β-defensin, and calprotectin level relate to *TLR5* and *NLRP6* SNP carriage and how this may relate to the observed genetic association with colorectal cancer will be discussed. In the end, I will conclude on the limitations of this study and summarize suggestions for future research directions and experiments, which may advance our knowledge in this area and initiate a way for therapeutic implications.

4.1 Functional consequences of NLRP6 F361Y in different human *in vitro* systems

4.1.1 NLRP6 SNP F361Y reveals induced NF-κB activation and promotes synergistic effect of M163L *in vitro*

To gain a first insight into the role of both *NLRP6* SNPs, we generated expression constructs corresponding to the relevant amino acid substitutions and tested their capacity to activate NF-κB *in vitro* in HEK cells. Intriguingly, tyrosine at position 361 in NLRP6 SNP F361Y revealed a small, but a significant trend towards nearly two times higher NF-κB activation together with ASC. Tyrosine at positions 357 and 359 also enhanced slightly but significantly NF-κB at different tested amounts of *NLRP6*. As several experimental parameters may contribute to the observed experimental variability as discussed in the results and we employed here HEK cells for *in vitro* analysis to gain a first idea, additional confirmation is advisable.

Tyrosine in proteins allow for sterically conformational changes in proteins (either directly or by acting as recipients for phosphorylation events) and thereby could promote interaction with ASC and induce NF-κB-signaling. Structural studies of two NLR members, NOD2 and NLRC4 have shown that these receptors are found in an autoinhibited state imposed by their C-terminal LRR domain[227,228]. Thereby, the LRR domain in the receptor is thought to bind to the NBD domain and remain it in an autoinhibited state. Upon ligand sensing by the LRR domain, it is thought to release the NBD domain and allows conformational changes of the NBD domain and activation. Probably F361Y, which is located in the NBD domain, can contribute to changes in this conformation by altered target sequence and activation of the receptor. For example, several individual mutations in *NOD2* have been reported to alter its activation status[228]. A way to test whether the amino acid change is functional due to a different sensitivity to autoinhibition, NLRP6 constructs without an LRR domain harboring either F361Y SNP or WT could be tested for NF-κB activation. One would expect similar activation, if F361Y SNP is no longer needed to alter the autoinhibition. To test conformational alterations for F361 vs. Y361 in NLRP6 proteins one can examine the structural conformation by i.e. nuclear magnetic resonance spectroscopy and x-ray crystallography. Alternatively, a BRET-based assay, as recently employed for NLRP3[229], could be used.

On the other hand, studies in NLRP3 and other well-known inflammasomes have shown that phosphorylation steps are crucial and necessary for the interaction of NLR and ASC and inflammasome formation[230-232]. In particular, phosphorylation in the NBD in NLRP3 has been shown to be associated with autoactivation without a second signal in autoinflammatory diseases like CAPS[233]. An altered and elevated

NF-κB activation during oncogenic processes may be detrimental or contribute to a worsened outcome in oncogenesis, either directly by inducing pro-survival factors or by promoting cytokine production that can favor progression e.g. via IL-6 and STAT3 signaling[234].

4.1.2 NLRP6 mutant M_Y shows elevated interaction with ASC *in vitro* in IP

To test if higher NF-κB activation by NLRP6 F361Y is induced by higher interaction of this construct with ASC, we conducted interaction assays by LUMIER and Co-IP and determined the intensity of interaction. LUMIER did not show any interaction of NLRP6 and ASC, whereas an interaction was found for MyD88 and MAL with this method (positive controls). However, probably only very strong intermolecular interactions can be evaluated well by LUMIER. Analysis of the interaction by Co-IP, an alternative method, in HEK cells revealed a tendency for stronger interaction of NLRP6 M_YYY in HEK cells and clearly stronger interaction of NLRP6 L_YYY and M_YYY in HEK Flp-In™ TRex™ 293T cells, stably expressing respective NLRP6 variant, which would be consistent with the elevated NF-κB activation seen in DLA assays. As discussed in section 3.3, results from HEK FLP-IN™ T-REX™ 293 cells with inducible expression of NLRP6 variants are more reliable when looking at the ratio of ASC immunoprecipitated/expressed as the similar levels of expression and immunoprecipitation of NLRP6 are essential and given in these HEK FLP-IN™ T-REX™ 293 cells. Further repeats in HEK FLP-IN™ T-REX™ 293 cells stably expressing NLRP6 would allow confirming these results and evaluate statistical significance.

However, due to the high linkage of both individual SNPs, an NLRP6 construct carrying both SNPs would be most relevant physiologically. The corresponding NLRP6 clearly showed stronger interaction with ASC and in the previous experiment a higher induced NF-κB dependent activation *in vitro*. Thus, a linked presence of both individual SNPs would mean a higher interaction of NLRP6 with ASC, resulting in increased NF-κB activation. Thereby, an induced proinflammatory environment by i.e. secretion of proinflammatory cytokines can be promoted, which may explain a higher risk found for M163L SNP carrier for CRC in the CRC association study by Huhn et al.[197].

During my thesis work, Elinav et al. have also shown interaction of NLRP6 and ASC by Co-IP. FLAG-NLRP6, HA-ASC, and MYC-Caspase-1 were overexpressed in HEK293T cells and pulled down using anti-HA Sepharose beads. HA-ASC and MYC-Caspase-1 were found in the immunoblot after pulldown of FLAG-NLRP6.[191]

In line with this, our results confirm interaction of NLRP6 and ASC and further reveal the effect of individual and combined SNP on (strength of) ASC interaction.

Further, after completion of my thesis work, Caspase-8 was also reported to be part of this interaction in the case of inflammasome formation by Hara et al[194]. As both SNPs are not found in the pyrin domain, which is known to interact with ASC, and thus not directly in interaction with ASC, their positions might indirectly promote the interaction of NLRP6 with ASC. As aforementioned, lower autoinhibition favored by the NLRP6 SNPs may stabilize a conformation of NLRP6 that exposes the PYD domains more, leading to better ASC recruitment. Generated HEK Flp-In™ TRex™ 293T cells stably expressing NLRP6 WT or variant can be employed for several other experiments to gain molecular insights on this part and possibly identify additional partners that promote or stabilize this interaction.

Further, interaction with other reported interaction partners, such as Dhx15, with different NLRP6 constructs should be tested in HEK or, preferably, in HEK FLP-IN™ T-REX™ 293 cells stably expressing these NLRP6 variants, to elucidate the role of the SNPs. Previously, *NLRP6* was found to play a role in intestinal antiviral immunity[188]. Here, NLRP6 was shown to bind viral RNA by RNA helicase Dhx15 and interact with mitochondrial antiviral signaling protein (MAVS), leading to type I/II interferons (IFNs) and interferon-stimulated genes (ISG). Interaction of NLRP6 with DHX15 was analyzed, whereby each domain itself (Pyrin, Nacht or LRR) failed to interact with DHX15, but NLRP6 as a complete construct or only a fragment from amino acid 170-715 were able to interact with DHX15 found in Co-IP assay overexpressed in HEK cells.[188] As M163L is not part of this fragment, but F361Y is, it may be interesting to test if these SNPs influence interaction with DHX15 or IFN-signaling and whether the presence of F361Y promotes M163L induced signaling. Further, the interaction of NLRP6 SNPs with MAVS could be evaluated. If NLRP6 SNPs have an effect, they may alter viral clearance. These experiments would allow to gain important insights into the effect of *NLRP6* SNPs on antiviral immunity.

Recently, a paper was published showing that LTA, a major component of the cell wall of gram-positive bacteria, acts as a cytosolic MAMP and directly binds to NLRP6 to activate a non-canonical inflammasome.[194] Therefore, the binding capacity of NLRP6 SNPs and LTA and the influence of NLRP6 SNPs on signaling would also be an interesting subject to study. As these additional insights only became available at the end of this thesis, the effect of NLRP6 SNPs on LTA recognition may be an interesting topic for future study.

4.1.3 *NLRP6* SNPs do not affect TLR4, 5 and 7/8-mediated gene transcription in whole blood

Induced NF-κB activation by NLRP6 SNPs would be expected to lead to elevated cytokine expression after whole blood stimulation. However, our results rather showed *reduced* cytokine expression in homozygous carriers after whole blood stimulation, but this trend was not significant. Two factors may explain this apparent discrepancy, which will be discussed in turn:

Kinetics of assay:

Based on a survey of the literature, it appears possible that at our time of sample harvest and analysis, saturation on the level of mRNA transcription is already reached and cytokine expression may go down. A study by Boeuf et al.[235], in which PBMCs were stimulated *in vitro* with LPS showed that already after 2 hours of stimulation a decline in cytokine mRNA expression for *IL-1β*, *IL-18* and *TNF-α* occurred. The observation that heterozygous *NLRP6* SNP carriers rather seem to have a tendency for elevated cytokine expression compared to WT (compare Figure 3-10) may thus be due to the fact that in samples from homozygous carriers saturation level had already been reached at this timepoint while heterozygous carriers did not. Additional donors and other timepoints assessed could reveal the impact of homozygous *NLRP6* SNP carriers more clearly.

Choice of readout:

mRNA levels, especially for cytokines, are rapidly regulated and may thus be highly dependent on kinetic differences. Quantification of secreted protein levels of these cytokines as an endpoint, e.g. by ELISA, rather than mRNA, could have thus served as a more advantageous readout. Further, NLRP6 so far has been often associated *in vivo* with influence on IL-18[187,191], rather than IL-1β[189]. Therefore, testing *IL-18* levels could add value to the here described findings.

Choice of agonist:

In our studies, we used flagellin, LPS, and R848 as agonists to investigate an effect on NF-κB signaling. Recently, a paper by Hara et al. was published showing that LTA as a cytosolic MAMP directly binds to NLRP6 and activates signaling[194]. Although the effect on NF-κB was not investigated, a reasonable explanation for our results may be that our system is not fully *NLRP6* dependent and thus did not reflect *NLRP6* SNPs dependent effect on immune cells. The finding of Hara et al. suggests that probably our assumption, NLRP6 to be downstream of TLR5 is not right and further the employed ligands not suitable.

On the other hand, inflammasomes are known to be triggered by a first signal, i.e. flagellin for TLR5 activation or LPS for TLR4 activation, so that it seemed plausible to investigate the effect of NLRP6 SNPs after employing a signal I-type stimulus described for the NLRP3 inflammasome. This setup was chosen based on data showing that NLRP6 modulates TLR-mediated NF-κB activation and subsequent cytokine responses[189,191]. Using LTA as an NLRP6-specific activator for the second signal was not known then but may be useful for future analysis. Alternative triggers in such subsequent analyses could be metabolites such as the bile acid conjugate taurine, carbohydrates and long-chain fatty acids that were proposed to activate NLRP6 during the course of this study[191]. To test this, transfection with LTA or metabolite incubation of isolated macrophages or human Thp1 cells expressing NLRP6 variants might be used. These experiments will give important information on the functional effect of individual SNPs on immune parameters and may underline their functional status in a healthy state and possible hints on consequences in disease settings.

4.2 *TLR5* and *NLRP6* SNPs impact gut immune parameters

4.2.1 Association of *TLR5* and *NLRP6* SNPs with intestinal sIgA level

Next, we examined the effect of *TLR5* and *NLRP6* SNPs on gut immune parameters, starting by determining the intestinal sIgA level in stool samples by ELISA. We found the total intestinal sIgA level for heterozygous R392X carriers to be elevated, which was significant when normalized to dry weight. Strikingly, the total sIgA level for heterozygous *NLRP6* carriers was significantly elevated before and after normalization.

Cullender et al. found *Tlr5* KO mice contain reduced flagellin-specific sIgA, while total sIgA level was increased for compensation[145]. This is in line with our observed trend for elevated total intestinal sIgA level for R392X carriers and therefore may hint on reduced flagellin-specific sIgA for heterozygous R392X carriers upon abrogated signaling respectively. Elevated sIgA level in heterozygous R392X donors indicating highly inflammatory conditions in the human gut may further correlate with observed inflammatory conditions, i.e. increased inflammatory cytokines in *Tlr5* KO mice model by Vijaykumar et al.[140].

Previously, we described NLRP6 SNPs M163L and F361Y to induce a higher activation of NF-κB in HEK cells together with ASC, but no phenotype was found in whole blood. Intriguingly, we observed an elevated sIgA level in heterozygous *NLRP6* SNP carriers, which may correlate to higher NF-κB activation in the human gut.

Further, Elinav et al. reported NLRP6 to determine the microbial composition[191,192], however, Mamantopoulos et al. argued that this finding is based on the experimental setting and not on genotype status[193,204]. Thus, in line with Elinav et al., *NLRP6* SNP carriers may display an altered microbiome and respectively modified ligands, which may be a cause or consequence of induced sIgA level in *NLRP6* SNP carriers. Whether this is the case, and how or by which ligands NLRP6 (SNPs) are activated, have to be further investigated. Supporting our findings, *NLRP6* has been shown to be involved in the regulation of many intestinal parameters, i.e. mucus[195] and antimicrobial peptide secretion[191] in mice and further, *Nlrp6* inflammasome deficient mice have been linked to elevated serum IgA level[191]. Our results provide the first evidence for a physiologic role of these NLRP6 SNPs in the human gut and reveal an important role of NLRP6 in maintaining intestinal microbiota in humans by sIgA secretion.

Heterozygous N592S carriers have no significant alterations on sIgA level, while we found significantly reduced TLR5 activation in HEK cells upon stimulation by stool samples of these SNP carriers. Therefore, the total sIgA level remains unaffected for these SNP carriers and WT. However, they may contain different levels of flagellin or LPS specific sIgA, i.e. elevated flagellin specific or species-specific sIgA reducing TLR5 activation for these SNP carriers, while other sIgA are elevated or/and an altered microbiome with reduced TLR5 activation, indicating reduced microbes with flagellin activating potential. *TLR5* F616L carriers have also no significant effect on the sIgA level, while probably TLR4 activation is probably reduced for homozygous F616L carriers.

To evaluate, beside the total level, also alterations in specific sIgA levels, which can result from changes in abundance of total sIgA, but also include changes in balance of strain-specific IgA, i.e. LPS or flagellin – specific IgA or certain i.e. flagellin or LPS species-specific IgA, targeted ELISAs can be employed and would be a logical next step. For example, to determine species-specific sIgA ELISA, plates could be coated with known purified flagellin or even entire gut bacteria, and incubated with extracted stool supernatant (see section 2.4.7 for extraction). Titration of a common human gut-related flagellin, i.e. *Roseburia intestinalis* may be used as a standard and allow to quantify roughly the amount of flagellin strain-specific sIgA. The same method can be applied with LPS for LPS strain-specific sIgA. Should this yield any interesting differences, it would be interesting to determine whether coating of bacterial phyla by sIgA by FACS differ for tested genotypes.

4.2.2 Association of *TLR5* and *NLRP6* SNPs with intestinal MAMP levels

We measured the impact of *TLR5* and *NLRP6* SNPs on TLR5 activation by applying two different methods, a TLR5 assay and a HEK-Dual^{TM} hTLR5 assay.

In these assays, R392X carriers show either a trend or significantly elevated TLR5 activation, indicating abrogated signaling of TLR5 leads to elevated flagellin expression or altered flagellin content with higher activation capacity. This is in line with elevated flagellin expression found upon the abrogation of TLR5 signaling in mice[145]. Further, it correlates with the observation that R392X carriers are highly susceptible to infectious diseases[148,154-156]. The variances in significance for elevated TLR5 activation in aforementioned assays may result from a limited number of tested donors (n=6) and therefore additional heterozygous donors, and further homozygous donors, may confirm and add additional value to these results.

On the other hand, the conducted assays revealed that heterozygous N592S carriers have significantly reduced TLR5 activation, which suggests that the altered TLR5 signaling leads to reduced flagellin expression or reduced TLR5 activation potential, i.e. by altered flagellin expression or altered microbiome. These results are based on TLR5 assay and IL-8 dependent luciferase activity in HEK-Dual^{TM} hTLR5 assay, while NF-κB activation in HEK-Dual^{TM} hTLR5 assay did not show any impact on TLR5 activation by these donors. As in the HEK-Dual^{TM} hTLR5 assay, a stimulation by stool supernatant is carried out about 22 hours, before measuring NF-κB activation dependent SEAP and IL-8 dependent luciferase activity, the signal probably accumulates and thus may be saturated at the time of measurement for NF-κB induced SEAP, while not for IL-8 induced luciferase for these donors. Further, beside kinetic differences, results depend on the sensitivity of the reporters utilized in the assays. The sensitivity of luciferase reporter assays are described to be higher than SEAP based reporter assays (https://www.promega.de/resources/guides/cell-biology/bioluminescent-reporters/).

Another explanation may be that a significant reduction in TLR5 activation of stool samples from heterozygous N592S carriers is stronger and therefore occurs earlier. This may be reflected in the TLR5 assay after 3 hours of stimulation time, while for NF-κB activation in the HEK-Dual^{TM} hTLR5 assay after 22 hours of stimulation, it is probably not apparent anymore. On the other hand, TLR5 activation of stool samples from heterozygous R392X carriers is probably weaker and delayed in TLR5 activation and is found significantly elevated NF-κB activation in HEK-Dual^{TM} hTLR5 assay after 22 hours of stimulation. Additional stimulation time in HEK-Dual^{TM} hTLR5 assay may clarify this assumption. It could mean that TLR5 activation in heterozygous N592S carriers is stronger and therefore suggest flagellin with higher TLR5 activation potency compared to *TLR5* R392X carriers.

Intriguingly, for N592S carriers, which were linked to worse survival in CRC[147], this is the first evidence, indicating a physiologic role of N592S carriers in the human gut.

Another study, however from a population of a different ethnical background, reported a link on N592S on worsened UC and found significantly reduced *TNF-α* and *IFN-γ* compared to WT patients in blood plasma samples[157], which fits our results and additionally indicates a systemic effect of this SNP. Whole blood stimulation with different ligands and assessment of proinflammatory cytokines may complement the results.

To further understand our results on TLR5 activation, i.e. of reduced TLR5 activation in N592S carriers, additional analysis is required. One has to elucidate, whether the quantity and which kind of flagellin expression is reduced or whether flagellin expression is changed by altered expression or an altered microbiome, which are different in their TLR5 activating potential. Different approaches are possible to elucidate these questions. To elaborate whether the quantity of flagellin is different, one can determine flagellin content in stool samples by qPCR with flagellin species-specific primers to measure the quantity of particular gut-related species. By PCR with random primers for flagellin covering conserved regions, without species-specific primer total flagellin amount can be assessed. Shotgun sequencing of RNA isolated from stool samples in a metatranscriptome analysis would allow for assessing flagellin transcription and flagellin related pathways, but would be difficult to extrapolate into information on protein abundance Additional methods are employing microarray for species-specific flagellin, 16S Gene sequence analysis to determine microbial species and their quantity, which is in process by our collaboration partners. For evaluation of these parameters, large cohorts, where samples are available for genotyping, would be an advantage, to stratify for genotype and utilize for retrospective analysis of these parameters.

Furthermore, we determined the impact of *TLR5* and *NLRP6* SNPs on TLR4 activation. We found significantly reduced TLR4 activation for homozygous F616L carriers compared to WT, when data were normalized to dry weight. This indicates a reduced LPS expression or reduced TLR4 activation potential by LPS, i.e. by altered LPS expression or altered microbiome. Our results for TLR4 activation in tested genotypes are only based on HEK-Blue™ hTLR4 assay. Therefore, our data for TLR4 activation remain to be verified and deeper investigated by additional assays with further read outs for further conclusions.

4.2.3 Association of *TLR5* and *NLRP6* SNPs with intestinal barrier regulators.

In our study, β-defensin 2 levels in tested *TLR5* and *NLRP6* WT or SNP carriers are not significantly different and lie in an expected range from 8-60 ng/ml stool for healthy donors except some outliers.

β-defensin-2 levels are reported to be induced upon stimulation by probiotic bacteria[220], LPS[221] or proinflammatory cytokines, such as TNF-α, IL-1β and IL-8[222]. The expression of many TLRs in the gut, in general, is known to be low[24] and therefore, in a healthy gut, the level of proinflammatory cytokines accordingly moderate. Thus, TLR5 or NLRP6 dependent differences do not manifest themselves in a healthy state, whereas under disease setting and induction of proinflammatory cytokines or stimulation by LPS, genotypic differences may occur and be evident. Our results show higher occurrence and variances in outliers, therefore this parameter may be more affected by i.e. environmental factors than other tested parameters and thus a larger cohort advisable. Interindividual differences in the composition of the gut microbiota, medical history, diet and the intake of probiotics could affect their hBD-2 level and explain occuring outlayers. However, the role of β-defensin in different disease settings and its suitability as a biomarker is still controversial and not clear in other studies. For example, even in disease settings as in IBD[236] or cystic fibrosis[237] in children, no changes in β-defensin were found and suggested not to be suitable as a biomarker for these diseases.

For calprotectin levels, intriguingly, we found homozygous F616L carriers to have significantly reduced calprotectin levels. Other tested genotypes did not show any significant changes compared to WT carriers. Reduced levels in F616L carriers suggest a protective environment for inflammatory related diseases and may explain a better survival of these SNP carriers in CRC[147].

We observed similar results for tested parameters as i.e. sIgA level and TLR5 activation for *TLR5* R392X carriers in human and *Tlr5* KO mice. Different to the *Tlr5* KO mice model, where inflammatory conditions were found upon flagellin invading mucus layers, here we find for heterozygous R392X carriers no significant changes in Calprotectin levels. In line with our result, PBMCs of heterozygous R392X carriers compared to homozygous R392X carriers are associated with reduced production in proinflammatory cytokines upon flagellin stimulation[150], which may explain our result. Additional analysis of homozygous R392X carriers, which were not available in our cohort, may contribute to additional insight.

Interestingly, Calprotectin levels indicating inflammatory conditions, which can contribute to CRC, show low tendencies which are in alliance with associations found in *TLR5* and *NLRP6* SNPs. For example, a tendency for elevated Calprotectin levels compared to WT in *TLR5* N592S carriers and *NLRP6* SNP carriers are in line

with associated worse survival in CRC or higher risk for CRC, whereas *TLR5* F616L carriers are associated with better survival in CRC and show significantly reduced Calprotectin level. Thus, Calprotectin could be a suitable indicator of inflammatory conditions and associated diseases. Other studies have suggested Calprotectin as a reliable indicator[238], as well.

4.2.4 Summary, limitations and future work

Summary:

In this study we wanted to gain insights on NLRP6 on a molecular level by studying its interaction with ASC, the effect on NF-κB activation and its role in inducing or regulating *TLR 4, 5, 7/8* gene transcription in whole blood. In the second part, we aimed to understand, if CRC associated *TLR5* and *NLRP6* SNPs have an impact on gut immune parameters in healthy donors, which thereby may render them susceptible to diseases.

According to our data in this study, we suggest that the occurrence of both NLRP6 SNPs, M163L and F361Y leads to a higher interaction with ASC, thereby inducing NF-κB activation by F361Y in HEK cells, *in vitro. Ex vivo* study of the role of these SNPs in inducing or regulating *TLR*-dependent gene transcription in whole blood did not show a significant effect. Different from these results, we expected homozygous *NLRP6* SNP carriers to induce higher cytokine levels. However, we propose that the system in which we tested the effect of *NLRP6* SNPs in whole blood is not appropriate to elucidate its effect. The experimental design might have to be adjusted to determine truly *NLRP6*-specific effects. Further, this effect may be more prominently seen in macrophages and neutrophils (phagocytic cells carrying inflammasome components). As our insight on *NLRP6* SNPs is limited to the *in vitro* system, an ex vivo approach is necessary to verify and elucidate a physiologic role of NLRP6 SNPs. Mice with an *Nlrp6* F361Y and L163M double knock-in may be another, if time and cost-intense, way to gain insights into the physiological impact of these variants.

In the second part of our study, we could show that indeed colorectal cancer-associated SNPs affecting intestinal PRRs such as TLR5 and NLRP6 SNPs have an impact on several gut immune parameters. Stool samples of donors from heterozygous *TLR5* N592S carriers revealed significantly reduced TLR5 activation, while increased TLR5 activation was found for the stool content of heterozygous *TLR5* R392X carriers indicating altered flagellin composition or level which are able to activate TLR5. Further, TLR4 activation for stool content of homozygous F616L carriers was significantly reduced when normalized to dry weight, however, this result has to be verified in further assays. Whereas *TLR5* and *NLRP6* SNPs had no significant effect on the β-defensin 2 levels, they influenced calprotectin and sIgA levels. Calprotectin was significantly reduced for homozygous carriers of F616L and *NLRP6* M163L and F361Y SNP carrier or also heterozygous *R392X* carriers after normalization to dry weight had significantly induced sIgA levels. Thus, each of the tested *TLR5* and *NLRP6* SNPs displays individual immune signatures.

By altering gut immune parameters and probably microbial composition, these PRR SNPs may render these carriers prone to diseases. A deeper analysis of the pathway is necessary to understand the intestinal immunologic and microbial process and find suitable targets for interventions. Therapeutic interventions may allow to target in general either altered immune parameters or further downstream microbial composition by so far known regulators such as metabolites or IL-18, found in mice.

Study limitations:

Our study is the first attempt to elucidate the role of *TLR5* and *NLRP6* SNPs on gut immune parameters in healthy donors. For this study, we enrolled around 250 participants, who donated saliva and whole blood. However, even though we considered in our study design a deposit of stool samples without direct personal contact, only 51 donors from our established cohort participated in stool donation. Nevertheless, within the limited time frame of my doctoral thesis, we were able to establish methods to assess the aforementioned immunologic parameters and carry out an analysis of these. Samples were also prepared for metagenomics analysis, which is currently being conducted by our collaboration partners. This will enable an advanced understanding of *TLR5* and *NLRP6* SNPs in microbial parameters on the host and may explain immunologic parameters. Even though our results are promising, they are based on a one-time stool sampling and hence require further verification. We also have to take into account, that the analysis is based on a limited number of donors out of 51 in total when categorized to each genotype. For instance, we did not have any homozygous R392X, N592S, and *NLRP6* carriers, and the total number of heterozygous R392X carriers out of fifty-one donors were six. A larger number of participants are required to include all genotypes and allow more reliable analysis, especially for microbial analysis, beyond the influence of environmental factors such as diet and allergy. However, larger cohorts for stool studies are hardly accessible. Our attempt to genotype gDNA from stool samples may allow to enlarge the cohort in future, by a collection of stool samples from numerous donors anonymously and determine their genotype status.

Admittedly, we can here only report correlations and validation of key findings in an *in vivo* model amenable to purposeful intervention may be required to establish causalities. However, such an analysis, for practical reasons, would again be limited to using murine *in vivo* models. Ideally, these studies should therefore rather be repeated in another cohort and/or more individuals analyzed. Despite these limitations in our study, we were able to show significant associations of *TLR5* and *NLRP6* SNPs and gut immune parameters.

These results encourage to expand the analysis in larger cohorts and further include additional important PRRs, i.e. other PRRs known to be associated with CRC, for example from the association study by Huhn et al.[197]. Our collected data by questionnaires and comprehensive samples (saliva, blood, stool) in established biobank allow analysis for multiple parameters, which can target a broad range of associations of any parameters (i.e. genetical, environmental) in the stool. Further, several parameters of one time point for a donor can be assessed and connected for new conclusions.

Future work:

In affiliation to our previously performed experiments, subsequent targets on mice and humans are obvious for future experiments. On the one hand, completing the knowledge in mice, *Nlrp6* WT or generated heterozygous or homozygous SNP mice, can be tested for, i.e. TLR5 and TLR4 activation of feces as well as sIgA, calprotectin and defensin level in feces. It will give additional molecular insights on NLRP6 in mice and further include homozygous *Nlrp6* carriers, which were not represented in our study in humans. Further, based on the described binding of LTA by NLRP6[194], an *in vivo* viral challenge of the aforementioned mice could be conducted and *Ifn* measured. This would allow to assess the impact of NLRP6 SNPs physiologically, may disclose NLRP6 SNP associations with the viral pathway and extend knowledge for therapeutic approaches in human.

Seeking insight in disease association in human, subsequent step would be to focus on *TLR5* or *NLRP6* disease-associated blood and stool samples, to evaluate the impact of *TLR5* and *NLRP6* genotype on previously tested immunologic and microbial parameters in a disease setting. Based on known *TLR5* or *NLRP6* associations with diseases, patient groups subjected could be patients affiliated with CRC, adiposity, metabolic syndrome or colitis. Comparison of these immunologic and microbial profiles for each of the genotypes will improve our knowledge on how the immunologic and microbial status for each genotype is impacted in a disease setting and possible therapeutic targets to alter disease development or progress. Assessing different stages in disease further may give an understanding of immune and microbial status in disease progress. Complementary, sampling patients before, during and after therapeutic approaches that improve disease setting, i.e. in dietary approaches may further add value to the previous question.

Besides these main targets, to gain insight on *NLRP6* SNPs on a molecular level, one can further address known roles of NLRP6 and assess the impact of NLRP6 SNPs here. These areas can include the following questions:

- *TLR5* and *NLRP6* are known to contribute in mucus secretion. Therefore, one may examine whether and how *TLR5* or *NLRP6* SNPs or their combination affect mucus secretion. In parallel to Johannson et al.[195], colonic explants from double or single *Nlrp6* SNP knock-in mice, could be stimulated with TLR ligands and mucus quantified.

- Further, *NLRP6* was shown to regulate *Akkermansia muciniphila*[239], which is known to be a pathobiont associated with colitis and impact mucus degradation. The effect of *NLRP6* SNPs on *Akkermansia muciniphila* may be determined by qPCR testing the 16S rDNA.

- Metabolites are suggested to activate NLRP6 thereby determining IL-18 secretion and microbial balance[191]. Consequences of NLRP6 harboring SNP activation by metabolites, such as prominent metabolite members, taurine and spermine may be elucidated.

- Do NLRP6 SNPs affect IL-18 production, and if as discussed NLRP6 dependent determination of microbial composition is true and not influenced by the environment, alter microbial composition? How do these SNPs further affect antimicrobial peptide secretion?

- If altered composition is found in NLRP6 SNPs presence, can it be modulated by IL-18 administration, metabolite change or microbial alterations?

- Is there a relation of these SNPs with BAFF and APRIL level, which influence B cells and IgA production?

- What is the expression level in the colon in humans of NLRP6 WT or SNPs and is the level altered in CRC?

Thus, many questions remain still elusive and can be targeted in future research.

4.3 General conclusions

To our knowledge, this thesis is the first study worldwide, which subjects *NLRP6* SNPs, M163L and F361Y. *NLRP6* SNP M163L was previously reported to be associated with two times higher risk for colorectal cancer[197] and SNP F361Y was found in our study to be often linked to M163L. We could show these SNPs in comparison to WT interact higher with ASC and thereby result in a higher NF-κB activation by F361Y *in vitro*. Thus, the elevated signaling cascade may promote a proinflammatory environment and therefore provide an explanation for the association of these SNPs with CRC.

We further could determine *TLR5* and *NLRP6* specific effects on immune parameters in healthy donors, which allows us to characterize the immune status for each PRR and compare it with these PRR carriers in a disease setting. This will give us information on changes after disease setting and allow us to interfere with therapeutic approaches.

The gut microbiota becomes increasingly important and studies in this field are increasing. The gut microbial composition is known to have a profound effect on several dimensions on humans and turns out to be a relevant factor in numerous diseases, of gut-related or unrelated nature. Mice studies allow us to understand the features of any investigated molecule, however, the intestine in mice is distinct to humans by its physiology and microbial inhabitants[65]. Thus, investigations in humans are necessary to find suitable and specific approaches for humans. The use of a human stool sample, which is non-invasive, enables a fascinating tool to proceed with further investigations and explore further parameters.

The American Cancer Society has reported that colorectal cancer in the United States is the third leading cause of cancer-related deaths in men and in women (https://www.cancer.org/cancer/colon-rectal-cancer/about/key-statistics.html). CRC diagnosed at an early stage can often be cured, whereas at a late stage has no chance for cure. Therefore, deep investigations in this field and new therapeutic strategies and approaches are necessary to detect CRC early and to cure CRC. Our approach allows a personalized treatment by determining in an easy, less expensive and fast way the genotype of the donor, when genotype-dependent difference promotes CRC progression and apply a tailored treatment. We have established a cohort in a highly time-consuming procedure, which allows in future an easy and rapid analysis on a broad spectrum of gut parameters in the stool.

5 Appendix

5.1 Supplemental Data

5.1.1 Expression of NLRP6 expression clones

To verify the expression of the generated expression clones by Gateway cloning, HEK cells were transfected with 100 ng of the expression clone and lysed 48 hours later. The lysate was immunoblotted for differently tagged NLRP6 using a respective antibody against the tag.

Except NLRP6 L_**F**F**KF**-Strep-HA clone 1 (see Figure 5-1 A, lane 3) and NLRP6 M_FFFKF-n-term ProA clone 1 (see Figure 5-1 D, lane 2), all expression clones are expressed. Among different clones, best expressed clones were selected to use in further analysis. However, the antibody against Renilla was very messy and a negative control is advisable to confirm the results, which was not conducted during this thesis.
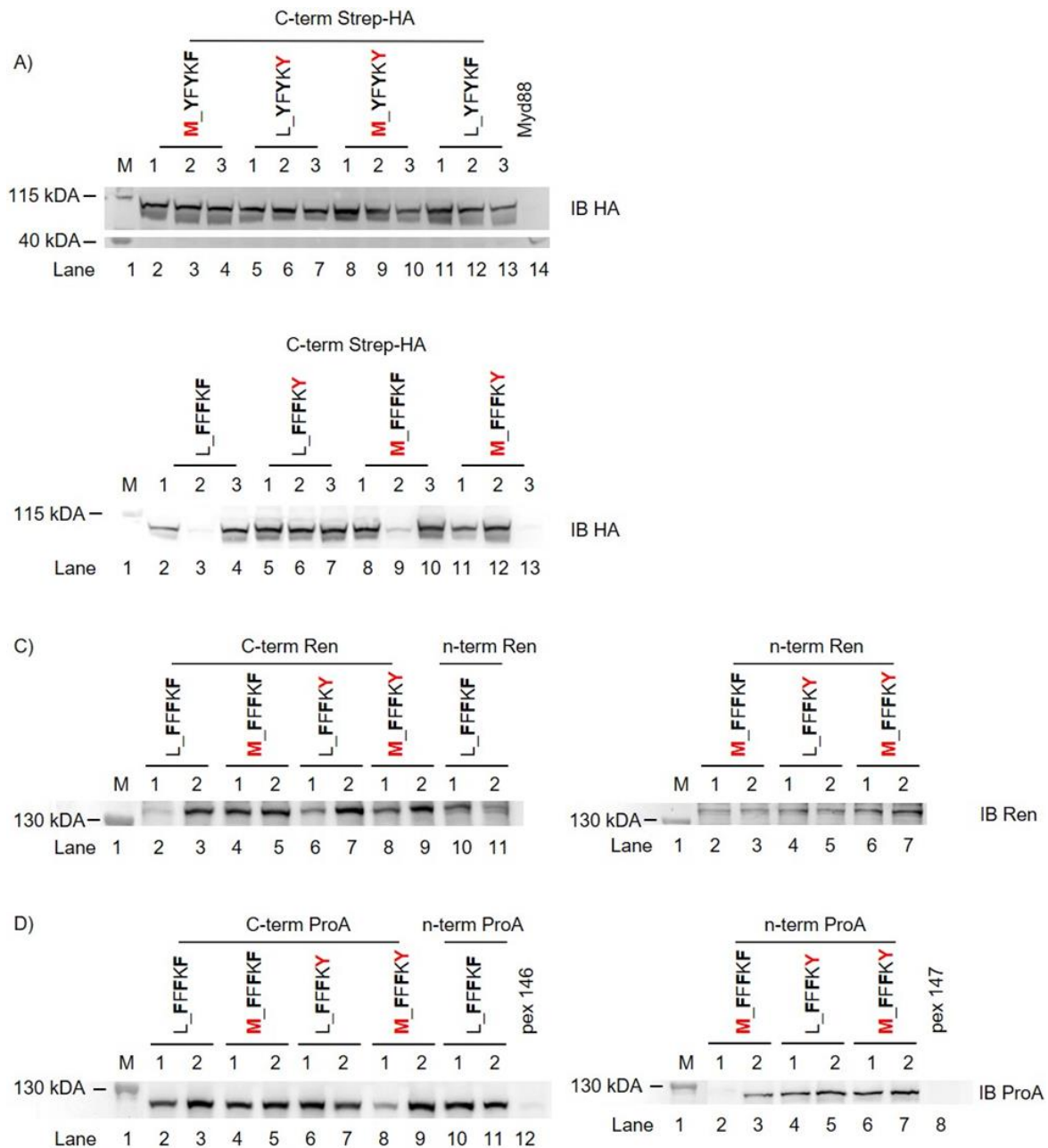
Figure 5-1 Verification of expression of generated differently tagged NLRP6 expression clones.

Immunoblot analysis for A) B) c-terminal Strep-HA tagged NLRP6 expression clone and Strep-HA tagged Myd88 as a positive control. C) generated c- and n-terminal Renilla tagged NLRP6 expression vectors. D) generated c- and n- terminal ProA tagged NLRP6 expression vectors and backbones as controls. Used antibody and expected molecular weight of expressed protein: A) B) α-HA: NLRP6-Strep-HA (104 kDA), C) α-Renilla: NLRP6-Renilla (134 kDA), D) α—ProA: NLRP6-ProA (114 kDA).

5.1.2 Expression analysis of generated HEK FLP-IN^{TM} T-REX^{TM} 293 cells stably expressing NLRP6

To compare the expression level of different Strep-HA tagged *NLRP6* constructs stably transfected in HEK Flp-In^{TM} T-REx^{TM} 293 cells, these cells were treated with Doxycycline with a final concentration of 1 µg/ml or selection medium (control) overnight. The next day, cells were lysed and equal amounts of protein immunoblotted for HA (NLRP6) or Tubulin (as a loading control).

All generated HEK FLP-IN^{TM} T-REX^{TM} 293 cell lines show comparable expression of respective NLRP6 after induction with DOX. Generated both sets of HEK FLP-IN^{TM} T-REX^{TM} 293 cells stably expressing NLRP6 can be employed in further experiments and are successful.
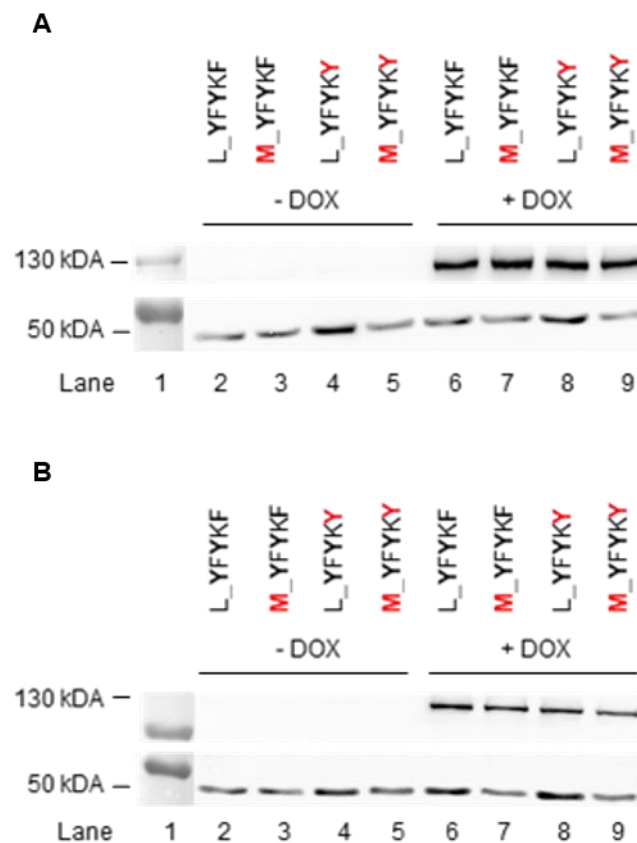
Figure 5-2 Verified expression of *NLRP6* constructs, stably transfected in HEK FLP-IN^{TM} T-REX^{TM} 293 cells, upon Doxycycline induction.
HEK FLP-IN^{TM} T-REX^{TM} 293 cells expressing different c-terminally Strep-HA tagged *NLRP6* constructs were generated and their expression verified by treatment of cells with 1 µg/ml Doxycycline overnight and immunoblot of 10 064 µg protein for HA or Tubulin (loading control). A), B) Two sets of HEK FLP-IN^{TM} T-REX^{TM} 293 cells stably expressing *NLRP6* were generated and tested.

5.1.3 Analysis of suitable *NLRP6* and *ASC* amounts for comparison by DLA

In order to find the best window to compare the activation of NF-κB by the different *NLRP6* constructs, we titrated the amount of *NLRP6* from 25 – 200 ng. We tested its effect, co-expressed with either, as in our former experiment, 10 ng or as used in the publication by Grenier, 30 ng *ASC*. In this case, we used NLRP6 M_Y construct and selected another mutant, NLRP6 M_F for comparison.

As shown in Figure 5-3, we found both constructs to activate NF-κB, but in the case of *NLRP6* M_Y saturation is reached faster already at the lowest tested amount of 25 ng whereas *NLRP6* M_F show NF-κB activation in a dose-dependent manner and reach saturation at 50 ng with 10 ng *ASC* or at 100 ng with 30 ng *ASC*. Intriguingly, levels of NF-κB activation are elevated for *NLRP6* M_Y with 30 ng *ASC* and saturation of NF-κB activation is reached at a higher amount of *NLRP6* M_F with 30 ng *ASC*, implicating the combinatory effect of *NLRP6* and *ASC* to activate NF-κB. Interestingly, when not saturated, NLRP6 SNP construct M_YYY show nearly two-fold higher NF-κB activation than a comparable amount of M_FFF. Thus, further titration with lower amounts than 25 ng *NLRP6* is required to find the optimal plasmid amounts to compare by DLA (see Figure 3-4).
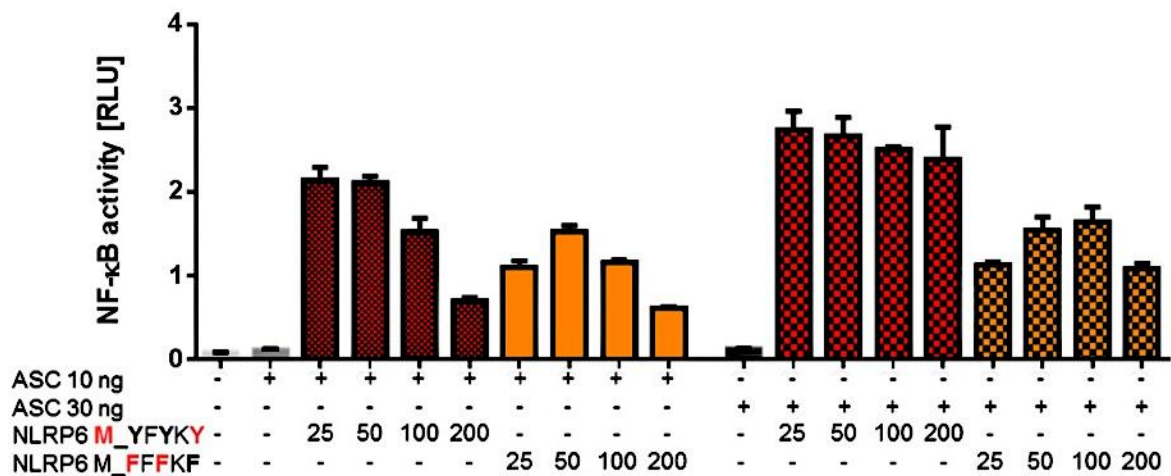
Figure 5-3 NF-κB activation is enhanced by NLRP6 in an ASC-dependent manner.
HEK cells were transfected with indicated amounts of *NLRP6* construct with 10 or 30 ng *ASC*, 100 ng *NF-κB reporter plasmid*, 10 ng *Renilla,* and 100 ng *eGFP*. After 2 days NF- κB dependent activation was assessed by DLA. Data show the mean of values with SD representative of technical triplicates from one experiment.

5.1.4 Dry Weight determination and the association of dry weight with tested *TLR5* and *NLRP6* genotypes

Different stool amounts were deposited from participants of the study. We homogenized each stool sample for equal distribution and stored multiple aliquots at – 80 ° C for any further analysis. Each sample is distinct from its hydration level. Therefore, we first thought to determine the dry weight of one sample of each tested donor, as this will affect any further parameters measured. We optimized conditions at which dry weight will be measured: In brief, 100 – 600 mg of stool sample was strived in a petri dish and incubated without lid in a dehydrator (Bielmeyer BHG601) for 12 hours at stage 3 (equals 20 ˚ C above room temperature) overnight. The next day, the dry weight was measured and H_2O content of each sample determined. Dry weight for 100 mg fresh weight stool sample of each donor was calculated and plotted (see Figure 5-4).

The dry weight from each stool sample of our cohort is widely distributed (up to around 3 x dry weight difference) and ranging from around 45 – 80 % H_2O content in the fresh stool. The mean value of 100 mg fresh weight in our cohort equals to 37,26 mg +/- 8,575 dry weight. This is in line with the general agreement that stool consists of 75 % H_2O and 25 % solid matter.
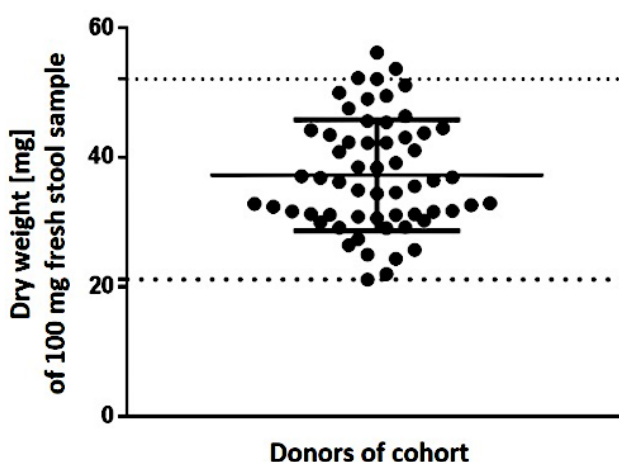
Figure 5-4 The dry weight of stool samples varies in our cohort.
100 – 600 mg of stool sample from each donor was well distributed on a 2 cm Petri dish and incubated without lid in a dehydrator at stage 3 (equals 20 ˚ C above room temperature) for 12 hours. Dry weight was determined by weighing a stool sample after dehydration and calculating its percentage of initially used stool amount. The respective calculated dry weight for 100 mg fresh weight was plotted. Data are representative of one experiment and show the mean of all values with SD.

According to D`Agostino & Pearson Omnibus normality test and Shapiro-Wilk Normality test, dry weight values fall under Gaussian distribution, but not according to the KS normality test (significance value: 0.0415). Therefore, the dry weight of stool samples should be definitely taken into consideration. However, in many studies, when feces as a study object is used, dry weight as a parameter is

neglected. To consider the dry weight of each sample in our study, measured parameters in stool are shown without and after normalization to dry weight. Obviously, the dry weight of stool sample from each donor can vary each time sampled, i.e. respective to their fluid intake, health conditions, etc. As we measure all parameters from one sample collected of each donor and aliquots are frozen after homogenization, dry weight remains consistent for a particular sample of the donor.

To check that the dry weight of stool samples does not correlate with any stratification of genotypes, we plotted all corresponding values (Figure 5-4). When stratifying for N592S and F616L WT, heterozygous or homozygous carriers, donors carrying *TLR5* R392X SNP were excluded. As expected, the dry weight of stool samples reveals random distribution among different tested genotypes.
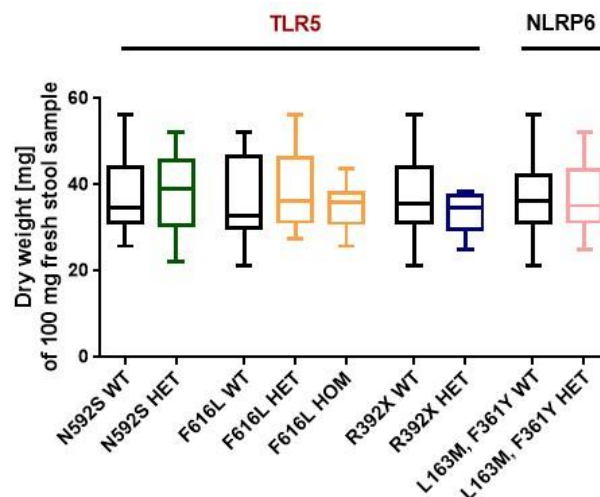
Figure 5-5 Dry weight of stool samples do not correlate significantly with stratified *TLR5* or *NLRP6* genotype.

100 – 600 mg of stool sample from each donor was well distributed on a 2 cm Petri dish and incubated without lid in a dehydrator at stage 3 (equals 20 ° C above room temperature) for 12 hours. Dry weight was determined by weighing a stool sample after dehydration and calculating its percentage of initially used stool amount. The respective calculated percentage of dry weight for 100 mg fresh weight was plotted stratified to tested genotype. Data derive from 1 experiment and are illustrated as min-to-max box-and-whisker plots with differences. Data are representative of one experiment.

5.1.5 TLR5 assay establishment

We first wanted to assess the stimulation potential of known concentrations of the commercially available *S. typhimurium* flagellin, which can serve as a positive control in our assay. For this purpose, we wanted to measure by qPCR flagellin induced *TNF-α* levels based on mRNA as readout and further assess, if increasing concentrations of flagellin in return do also impact on the expression level of *TLR5* based on mRNA.

TLR5 expression was induced by Doxycycline in HEK Flp-In™ T-REx™ 293 cells stably expressing TLR5 or treated with the medium as a control for internal TLR5 expression level. The next day, cells were stimulated with the indicated concentrations of *S. typhimurium* flagellin in Figure 5-6 for 3 hours and *TNF* α and *TLR5* assessed by RT-qPCR.

TNF α is induced in a flagellin concentration-dependent manner proportionally, whereas *TLR5* is increased in a non-proportional way only very modestly with increasing concentration of flagellin and therefore is neglectable. *S. typhimurium* flagellin concentration at 50 ng/ml can be used as a clear positive control for the assays.
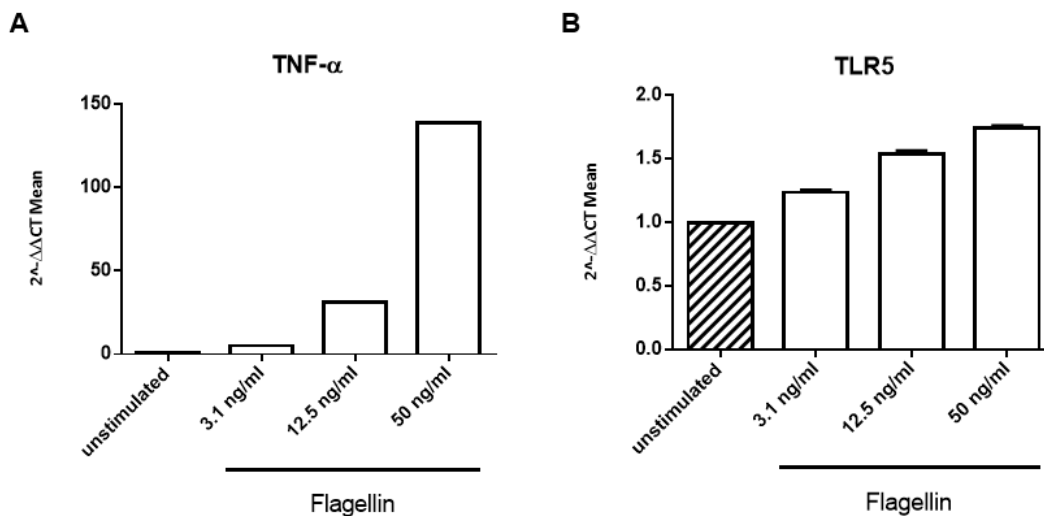
Figure 5-6 *TNF-α* is induced by flagellin in TLR5 dependent manner and thereby hardly affects *TLR5* expression.
TLR5 expression of HEK FLP-IN™ T-REX™ 293 cells stably expressing TLR5 were induced with Doxycycline and afterwards stimulated with the indicated concentration of *S. typhimurium* flagellin for 3 hours. Cells were harvested and qPCR for *TNF-α* and *TLR5* together with *TBP* were measured. Data is representative of 1 experiment in triplicates with SD. A) The *TNF-α* expression upon flagellin stimulation. B) *TLR5* expression upon flagellin stimulation.

Next, we tested the stimulation potential of stool samples by different dilutions in HEK FLP-IN™ T-REX™ 293 cells stably expressing TLR5. Therefore, the stool supernatant was prepared as in section 2.4.7.

TLR5 expression in HEK FLP-IN^{TM} T-REX^{TM} 293 cells stably expressing TLR5 was induced by Doxycycline and stimulated for 3 hours with 50 µl of different dilutions of stool supernatant from two different donors.

The positive control, 50 ng/ml flagellin from *S. typhimurium* worked well, even though it gave fewer *TNF-α* than before. Stool supernatant pure or 1:2 diluted give the best window to compare stool from different donors regarding TLR5 activation according to this experiment, as dilution 1:50 is nearly non-inductive anymore.
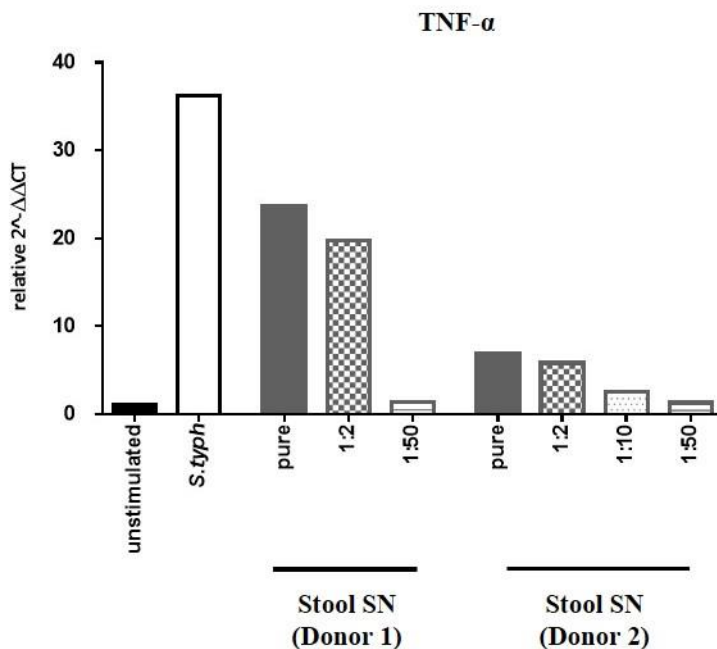
Figure 5-7 Undiluted stool supernatants are suitable to compare their TLR5 activation HEK FLP-IN^{TM} T-REX^{TM} 293 cells stably expressing TLR5.
HEK FLP-IN^{TM} T-REX^{TM} 293 cells stably expressing TLR5 were either induced with Doxycycline or not induced as a control for endogenous TLR5 and stimulated for 3 hours with undiluted or indicated different dilutions of stool supernatants extracted from stool samples of two distinct donors. *TNF-α* was measured by RT-qPCR and to show induction of TLR5 activation by each sample, relative 2^$^{-ΔΔCT}$ of Doxycycline induced sample were subtracted from relative 2^$^{-ΔΔCT}$ of Doxycycline non-induced sample. Data is representative of 1 experiment. SN, supernatant.

To further find a suitable volume of stool supernatant to use for stimulation, where *TNF-α* is in a linear range and samples best comparable, we tested indicated volumes of stool supernatant for stimulation from two different donors, where different stimulation potential was observed from previous tests. Further, as the dry weight of both samples was known, volumes adjusted to the dry weight of samples were also tested. The experiment was conducted as before, this time by Yesim Tuzcu.

Unfortunately, the positive control did not work. As the values are similar to the unstimulated ones, most likely *S. typhimurium* was not added for stimulation. As expected from previous experiments (not shown), a stool sample of donor stud175 activates TLR5, whereas stool sample of donor stud185, does not seem to activate TLR5 at all, or to a very low extent at 400 µl of supernatant (see Figure 5-8). *TNF-α* readout of stool from donor stud175 is proportional to volume until 120 µl and is not linear anymore at the tested volume of 200 µl. Therefore, 100 µl was selected as a volume for stool supernatant for stimulation under established conditions.
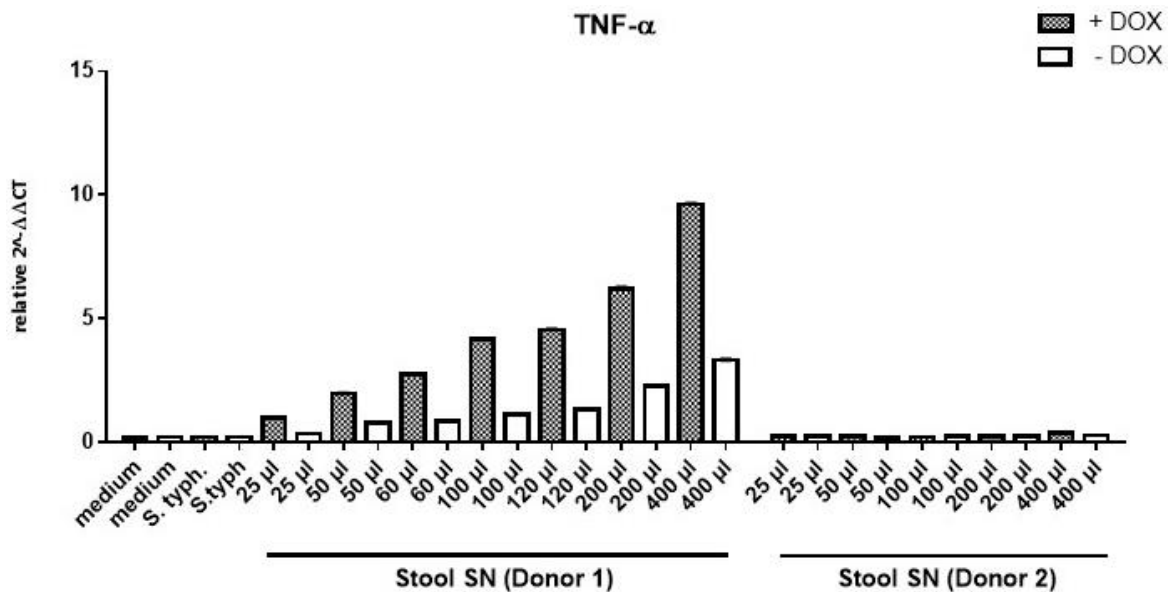
Figure 5-8 Establishment of TLR5 stool assay by different volumes of stool supernatant used for stimulation of HEK FLP-IN^TM T-REX^TM 293 cells stably expressing TLR5 and show 100 µl of stool supernatant to be in linear range and suitable.
TLR5 expressing HEK FLP-IN^TM T-REX^TM 293 cells were either induced with Doxycycline or not induced as a control for endogenous TLR5 and stimulated for 3 hours with indicated different volume of stool supernatant extracted from two distinct stool samples. *TNF-α* was measured by RT-qPCR and data shown as relative $2^{-\Delta\Delta CT}$. Data is representative of 1 experiment. + DOX, with Doxycycline; - DOX, without Doxycycline.

5.1.6 Interaction of different NLRP6 SNP constructs and ASC *in vitro* by LUMIER

Since direct interaction of NLRP6 and ASC has been suggested but not shown (at the time of our investigation), we further wanted to look for the interaction of NLRP6 and ASC and evaluate, whether the seen increase in NF-κB activation might be due to higher interaction of respective NLRP6 constructs with ASC. For this purpose, we first thought to test interaction employing LUMIER assay.

In a LUMIER Assay, basically two proteins of interest, here, one tagged with Protein A (ProA) and the other with Renilla, are expressed in HEK293T cells and lysed. With the help of IgG coated magnetic beads, which binds to ProA, ProA tagged proteins are pulled down, thereby if any interaction is present, also the Renilla-tagged Protein will be pulled down. As in the case of DLA, the luciferase activity of Renilla can be detected by adding luciferin. In a part of the total lysate the overall luciferase activity is measured, to see the expression of the Renilla-tagged protein, and then after adding the lysate to IgG coated magnetic beads and washing, the Renilla activity is measured to assess the remaining Renilla-tagged proteins after pull down, in case of interaction.

NLRP6 and ASC are thought to interact via their N-terminal Pyrin domains. Therefore, NLRP6 and ASC with c-terminal tags were employed in the assay, to avoid hindrance in interaction. As we want to compare the different NLRP6 constructs, for their possible interaction and interaction differences, further it is critical to normalize to their expression level, which is possible by using Renilla tagged NLRP6 constructs, and therefore ProA tagged ASC constructs. As a positive control, we used MAL-ProA and MYD88-Ren or the mutated hyperactive version, L265P. As a negative control, the interaction of a Pro-A backbone (pex140) is tested with Renilla tagged NLRP6. Separately, a triplicate of HEK293T cells were transfected with eGFP in each set of experiment, to confirm the success of transfection in general.

To understand the data, first, we look for the binding of protein, compared to its expression. To evaluate real interactions, interaction of two possible interaction partners, are compared to unspecific interaction (negative control) of the tested partner in this case tagged with Renilla, to the backbone of the other partner, on which is pulled down, in this case, ProA, which would indicate unspecific interaction to the backbone or to the magnetic beads used. Only when bound/expressed normalized to 1 negative control has a value over 3, this is accounted as a true interaction. Comparing the interaction of MYD88 and MAL, as well as different NLRP6 constructs and ASC, only MYD88 and MAL fulfill this criterion and show interaction (see Figure 5-9).
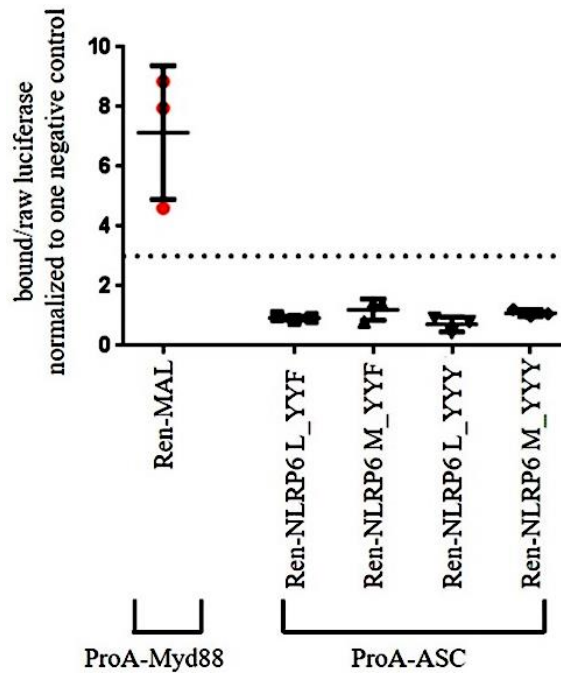
Figure 5-9 LUMIER shows no interaction between NLRP6 constructs and ASC in HEK cells.
LUMIER assay was conducted with c-terminal ProA tagged ASC and a c-terminal Renilla tagged NLRP6 constructs in HEK cells and immunoprecipitated utilizing magnetic Dynabeads® M-280 Sheep Anti-Mouse IgG slurry. Luciferase activity was assessed in 10 % of lysate for initial NLRP6 expression and determined for bound NLRP6 in residual lysate after Protein A purification. Negative control implies interaction measured in ProA tagged backbone with respective Renilla tagged construct. Interaction criteria are fulfilled when the interaction level of two partners is three times higher than the negative control, indicated as a threshold. Data represent ratios of bound versus raw luciferase for each transfection upon the subtraction of negative control from one experiment. Data show triplicates from one experiment.

To improve the assay, LUMIER assay was repeated with different amount of plasmid (20 ng and 100 ng) used, focusing only on the interaction of NLRP6 WT with ASC, and as a further control this time pulled down on ProA tagged NLRP6 with ASC-Ren tagged (data not shown). The positive control showed even a higher interaction of around 25 (comparable to results of other lab members) with 20 ng plasmid used, rather than similar to the previous experiment around 7 with 100 ng plasmid. Nevertheless, there was no interaction found between NLRP6 WT and ASC, but the assay showed that for Renilla tagged NLRP6 the unspecific binding to IgG magnetic beads was around 10-fold higher than Renilla tagged ASC.

Further experiments, by altering conditions, employing HA beads and using different buffers, i.e. normally used in LUMIER or IP, failed also to verify known interaction of the prominent inflammasome member, NLRP3, and ASC in my hands.

Discussion

Positive control MYD88 and MAL reveal an interaction but no interaction is found between NLRP6 and ASC, in LUMIER. Trying to pull down with different beads and using respectively tagged NLRP6 constructs, or changing additional parameter, i.e. buffer, still did not show any interaction in further experiments. It can be that LUMIER interaction, in particular, is suitable to reveal the strong interaction of two interaction partners like MYD88 and MAL, but not weaker interactions. However, also within our laboratory interaction of i.e. NLRP3 and ASC, which are known to interact, were not consistently found and also resulted if positive, in a weak positive interaction by number. To further test NLRP6 and ASC interaction, other methods, i.e. IP were employed (see section 3.3).

5.2 Generated NLRP6 expression plasmids:

Table 5-1 Generated differently tagged *NLRP6* expression constructs.
NLRP6 differently tagged expression vectors were generated by LR reaction.

Template	Amino acid at 163_361	Backbone	tag	Tag size nucleotide	Resulting construct	Feature of resulting construct	Used for in thesis
pex484	L_**YFYKF**	Pex145	c-term Strep-HA	141	pTS9	L_**YFYKF**-**c-term Strep HA**	DLA IP
pTS4	M_**YFYKF**	Pex145	c-term Strep-HA	141	pTS13	M_**YFYKF**-**c-term Strep HA**	DLA IP
pTS1	L_**YFYKY**	Pex145	c-term Strep-HA	141	pTS10	L_**YFYKY**-**c-term Strep HA**	DLA IP
pTS6	M_**YFYKY**	Pex145	c-term Strep-HA	141	pTS14	M_**YFYKY**-**c-term Strep HA**	DLA IP
pTS2	L_**FFFKF**	Pex145	c-term Strep-HA	141	pTS11	L_**FFFKF**-**c-term Strep HA**	DLA
pTS3	L_**FFFKY**	Pex145	c-term Strep-HA	141	pTS12	L_**FFFKY**-**c-term Strep HA**	-
pTS7	M_**FFFKF**	Pex145	c-term Strep-HA	141	pTS15	M_**FFFKF**-**c-term Strep HA**	DLA
pTS8	M_**FFFKY**	Pex145	c-term Strep-HA	141	pTS16	M_**FFFKY**-**c-term Strep HA**	-
pex484	L_**YFYKF**	Pex117	c-term Renilla	930	pTS25	L_**YFYKF**-**c-term Renilla**	LUMIER
pTS4	M_**YFYKF**	Pex117	c-term Renilla	930	pTS26	M_**YFYKF**-**c-term Renilla**	LUMIER
pTS1	L_**YFYKY**	Pex117	c-term Renilla	930	pTS27	L_**YFYKY**-**c-term Renilla**	LUMIER
pTS6	M_**YFYKY**	Pex117	c-term Renilla	930	pTS28	M_**YFYKY**-**c-term Renilla**	LUMIER
pex484	L_**YFYKF**	Pex118	n-term Renilla	933	pTS29	L_**YFYKF**-**n-term Renilla**	LUMIER (not shown)
pTS4	M_**YFYKF**	Pex118	n-term Renilla	933	pTS30	M_**YFYKF**-**n-term Renilla**	LUMIER (not shown)
pTS1	L_**YFYKY**	Pex118	n-term Renilla	933	pTS31	L_**YFYKY**-**n-term Renilla**	LUMIER (not shown)
pTS6	M_**YFYKY**	Pex118	n-term Renilla	933	pTS32	M_**YFYKY**-**n-term Renilla**	LUMIER (not shown)

Template	Amino acid at 163_361	Backbone	tag	Tag size nucleotide	Resulting construct	Feature of resulting construct	Used for in thesis
pex484	L_**YFYKF**	Pex146	c-term ProA	411	pTS33	L_**YFYKF-c-term ProA**	LUMIER (not shown)
pTS4	M_**YFYKF**	Pex146	c-term ProA	411	pTS34	M_**YFYKF-c-term ProA**	LUMIER (not shown)
pTS1	L_**YFYKY**	Pex146	c-term ProA	411	pTS35	L_**YFYKY-c-term ProA**	LUMIER (not shown)
pTS6	M_**YFYKY**	Pex146	c-term ProA	411	pTS36	M_**YFYKY-c-term ProA**	LUMIER (not shown)
pex484	L_**YFYKF**	Pex147	n-term ProA	411	pTS37	L_**YFYKF-n-term ProA**	LUMIER (not shown)
pTS4	M_**YFYKF**	Pex147	n-term ProA	411	pTS38	M_**YFYKF-n-term ProA**	LUMIER (not shown)
pTS1	L_**YFYKY**	Pex147	n-term ProA	411	pTS39	L_**YFYKY-n-term ProA**	LUMIER (not shown)
pTS6	M_**YFYKY**	Pex147	n-term ProA	411	pTS40	M_**YFYKY-n-term ProA**	LUMIER (not shown)

5.3 Recipes of buffer and media

Table 5-2 Buffer and media

Buffer	Recipe	Methods used in
PBS	8 g NaCl, 0.2 g KCl, 1.44 g Na_2HPO_4, add dH_2O to a final volume 1 L, adjust to pH 7.4	SDS-PAGE, Western Blot
RIPA	50 mM HEPES, 150 mM NaCl, 0.1% NP-40, 20 mM ß-glycerophosphate, 2 mM DTT, adjust to PH 6.9, freshly supplemented with Roche inhibitor tablets Complete Mini Protease Inhibitor and PhosSTOP	Protein Lysis
SDS running buffer	Tris 25 mM, glycine 250 mM, SDS 0.1%	SDS-PAGE
TBS	50 mM Tris HCl, pH 7.4 and 150 mM NaCl	Western Blot
TBS-Tween 0.1% (immunoblot washing buffer)	TBS, 0.1% Tween-20	Western Blot
HBS	2x HBS stock: 50 mM HEPES pH 7.05, 10 mM KCl, 12 mM dextrose, 280 mM NaCl, 1.5 mM Na_2HPO_4, aliquot and store at -80° C	DLA (calcium phosphate transfection)
Lysis buffer	TRIS 8 1 M, 5 M NaCl, 0,5% NP40, 0.5 M EDTA, 0.5 M EGTA, 1 M DTT, 10 % Glycerol, add dH_2O to a final volume of 50 ml. Freshly supplemented with Roche inhibitor tablets Complete Mini Protease Inhibitor and PhosSTOP	Co-IP Protein Lysis
Lysis buffer	20 mM Tris pH 7.5, 1% Triton-X100, 250 mM NaCl, 10 mM EDTA, 10 mM DTT, protease and phosphatase inhibitors from Roche, 0.0125 U/µl Benzonase (Sigma-Aldrich). Buffer was supplemented with 10 % v/v of PBS-washed Dynabeads® M-280 Sheep Anti-Mouse IgG (Thermo Fisher).	LUMIER
Renilla assay buffer	220 mM potassium phosphate buffer (1 M K2HPO4, 1 M KH2PO4, pH 5.1), 2.2 mM EDTA, 1.1 M NaCl, 0.44 mg/ml BSA	LUMIER TLR5 Dual Reporter Assay
STOP solution	2N H_2SO_4	ELISA
RIDASCREEN extraction buffer (10x)	phosphate-buffered NaCl solution; contains 0.1 % Tween and 0,1% NaN_3 (purchased from Ridascreen)	Stool Lysis Buffer
LB medium	1% w/v bacto tryptone, 0.5 % w/v yeast extract, 0.5% w/v NaCl, pH 7.5	Transformation of *E.coli*
S.O.C medium	2% w/v bacto tryptone, 0.5 % w/v yeast extract, 2.5 mM KCl, 10 mM NaCl, 20 mM glucose	Transformation of *E.coli*

5.4 Oligonucleotides

Table 5-3 Mutagenesis primer

Primer Name	Amino Acid mutation	Nucleotide Sequence	Mutagenesis in NLRP6
AWm523	L163M	cggaggaggcgatggggcccgcg	c487a FWD
AWm524	L163M	cgcgggccccatcgcctcctccg	c487a REV
AWm525	F361Y	gaagaagtatttctacaagtacttccgggatgagagga	t1082a FWD
AWm526	F361Y	tcctctcatcccggaagtacttgtagaaatacttcttc	t1082a REV
AWm527	Y357F, Y359F	cgacaaggacaagaagaagttcttcttcaagttcttccgggatgaga	a1070t, t1071c), a1076t
AWm528	Y357F, Y359F	tctcatcccggaagaacttgaagaagaacttcttcttgtccttgtcg	a1070t, t1071c), a1076t
AWm531	Y357F, Y359F, (F361Y)	cgacaaggacaagaagaagttcttcttcaagtacttccgggatgaga	a1070t, t1071c), a1076t
AWm532	Y357F, Y359F, (F361Y)	tctcatcccggaagtacttgaagaagaacttcttcttgtccttgtcg	a1070t, t1071c), a1076t

Table 5-4 Sequencing Primers

Name	Sequence	Annealing to (bp)	of	Direction
AWs148	ACCAGGGCCAGGTGGACTTC	778-798	human NLRP6	F
AWs149_	CGGGCGTGCTGGAGACAGAG	1575-1594	human NLRP6	F
AWs150	CCGCACTGACGGAGCTGGG	2395-2413	human NLRP6	F

5.5 Plasmid constructs

Table 5-5 Plasmids generated or employed in this study

plasmid number	Backbone	Insert	Features	Bacterial Resistance
NF-κB reporter	n/a	Firefly luciferase	Firefly luciferase reporter gene under the control of NF-κB p65 consensus promotor sequence, purchased from Stratagene	Ampicillin
pEX008	pC1-EGFP	EGFP	n/a	Ampicillin
pEX140	pT-REx-DEST30-ntProteinA	ProteinA	Protein A inserted by LR in pT-REx-DEST30-ntProteinA	Ampicillin
pEX145	pTO-C-SH	Strep-hemagglutinin tag c-term Gateway	Strep- hemagglutinin tag c-term, Gateway destination vector	Ampicillin
pEX193	EGFP-C		EGFP tag c-term, Gateway destination vector	Ampicillin
pEX351	pRL-TK	Renilla luciferase	n/a	Ampicillin
pEX484	pDONR™ Vector	human NLRP6, complete CDS	ORFEXPRESS™ Gateway Plus Shuttle Clone, NO STOP, NLRP6 with both SNPs	Kanamycin
pMS24	pT-REx-DEST30-ctProteinA	ASC	ASC, c-term ProA	Ampicillin
pOW018	pCDNA3, n-term Renilla	Myd88	pCDNA3 derived Gateway destination vector with n-term Renilla tagged Myd88	Ampicillin
pOW030	pTO-N-SH	Myd88	Myd88 Strep-HA	Ampicillin
pOW114	pT-REx-DEST30-ntProteinA	Mal Iso A, n-term ProA	pT-REx-DEST30-derived Gateway destination vector expressing human Mal Isoform A with N-term ProA tag	Ampicillin
pTP062	pEX193	ASC	ASC, EGFP c-term, Gateway	Ampicillin
pTP063	pEX193	ASC	ASC, untagged, Gateway	Ampicillin

plasmid number	Backbone	Insert	Features	Bacterial Resistance
pTS1	pDONR™ Vector	human NLRP6, complete CDS, **L(163)_YYY(361)**	ORFexpress Gateway Shuttle Clone, NO stop, mutation generated in pex484	Kanamycin
pTS2	pDONR™ Vector	human NLRP6, complete CDS, **L(163)_FFF(361)**	ORFexpress Gateway Shuttle Clone, NO stop, mutation generated in pex484	Kanamycin
pTS3	pDONR™ Vector	human NLRP6, complete CDS, **L(163)_FFY(361)**	ORFexpress Gateway Shuttle Clone, NO stop, mutation generated in pex484	Kanamycin
pTS4	pDONR™ Vector	human NLRP6, complete CDS, **M(163)_YYF(361)**	ORFexpress Gateway Shuttle Clone, NO stop, mutation generated in pex484	Kanamycin
pTS5	pDONR™ Vector	human NLRP6, complete CDS, **M(163)_YYY(361)**	ORFexpress Gateway Shuttle Clone, NO stop, mutation generated in pex484	Kanamycin
pTS6	pDONR™ Vector	human NLRP6, complete CDS, **M(163)_FFF(361)**	ORFexpress Gateway Shuttle Clone, NO stop, mutation generated in pex484	Kanamycin
pTS7	pDONR™ Vector	human NLRP6, complete CDS, **M(163)_FFY(361**)	ORFexpress Gateway Shuttle Clone, NO stop, mutation generated in pex484	Kanamycin
pTS8	pDONR™ Vector	human NLRP6, complete CDS, **L(163)_YYY(361)**	ORFexpress Gateway Shuttle Clone, NO stop, mutation generated in pex484	Kanamycin

5.6 Materials Stool study

Table 5-6 Materials employed in our stool study

Nerbe Plus	Kryogefäß PP 2ml konisch	05-642-0100	Stool aliquots
Nerbe Plus	Schraubdeckel PP	05-662-0100	Stool aliquots
dianova	PowerLyzer PowerSoil Bead Solution	12855-50-BS	Microbial analysis
dianova	Power Soil Power Bead Tubes	12888-100-PBT	Microbial analysis
roth	Probenlöffel 10ml steril 100 St.	CPT4.1	Stool sample preperation
Nerbe Plus	Rührspatel	12-521-0000	Stool aliquot and glycerol stocks
Thermo Fisher Scientific	Commode Specimen collection Systeme (Stuhlauffangbehälter)	1078-4572	Stool collection by donors
Greiner Bio-one	Petri dish 2 cm	664160	Stool dry weight determination
immundiagnostik	sekretorisches Immunglobulin A (sigA) ELISA	K8870	Stool sIgA ELISA
greiner	Microplatten 96 well high binding F-Form half area	675061	DLA, LUMIER, TLR5 HEK Dual assay, TLR4 HEK-Blue assay
greiner	ELISA-Platten half-area		ELISA
immundiagnostik	Calprotectin ELISA	K6927	Calprotectin ELISA
immundiagnostik	beta Defensin ELISA	K6500	beta Defensin ELISA
BIORAD	purified human secretory IgA	PHP133	sIgA ELISA
r-biopharm AG	Ridascreen siGA ELISA	G09035	sIgA ELISA

6 References

1   Ausubel, F. M. Are innate immune signaling pathways in plants and animals conserved? *Nat Immunol* **6**, 973-979, doi:10.1038/ni1253 (2005).

2   Chaplin, D. D. Overview of the immune response. *J Allergy Clin Immunol* **125**, S3-23, doi:10.1016/j.jaci.2009.12.980 (2010).

3   Murphy, K., Janeway, C. A., Jr., Travers, P. & Walport, M. *Janeway`s Immunobiology*. Vol. 8 468 (Garland Science, Taylor & Francis Group, 2012).

4   Janeway, C. A., Jr. & Medzhitov, R. Innate immune recognition. *Annu Rev Immunol* **20**, 197-216, doi:10.1146/annurev.immunol.20.083001.084359 (2002).

5   Brubaker, S. W., Bonham, K. S., Zanoni, I. & Kagan, J. C. Innate immune pattern recognition: a cell biological perspective. *Annu Rev Immunol* **33**, 257-290, doi:10.1146/annurev-immunol-032414-112240 (2015).

6   Medzhitov, R. Toll-like receptors and innate immunity. *Nat Rev Immunol* **1**, 135-145, doi:10.1038/35100529 (2001).

7   Barbé, F., Douglas, T. & Saleh, M. Advances in Nod-like receptors (NLR) biology. *Cytokine & Growth Factor Reviews* **25**, 681-697, doi:https://doi.org/10.1016/j.cytogfr.2014.07.001 (2014).

8   Liston, A. & Masters, S. L. Homeostasis-altering molecular processes as mechanisms of inflammasome activation. *Nat Rev Immunol* **17**, 208-214, doi:10.1038/nri.2016.151 (2017).

9   Takeuchi, O. & Akira, S. Pattern recognition receptors and inflammation. *Cell* **140**, 805-820, doi:10.1016/j.cell.2010.01.022 (2010).

10   Sun, L., Wu, J., Du, F., Chen, X. & Chen, Z. J. Cyclic GMP-AMP synthase is a cytosolic DNA sensor that activates the type I interferon pathway. *Science* **339**, 786-791, doi:10.1126/science.1232458 (2013).

11   Zinkernagel, R. M. & Doherty, P. C. The discovery of MHC restriction. *Immunol Today* **18**, 14-17, doi:10.1016/s0167-5699(97)80008-4 (1997).

12   Tokuhara, D. *et al.* A comprehensive understanding of the gut mucosal immune system in allergic inflammation. *Allergol Int* **68**, 17-25, doi:10.1016/j.alit.2018.09.004 (2019).

13   McGhee, J. R. *et al.* The mucosal immune system: from fundamental concepts to vaccine development. *Vaccine* **10**, 75-88, doi:10.1016/0264-410x(92)90021-b (1992).

14   Mowat, A. M. & Agace, W. W. Regional specialization within the intestinal immune system. *Nat Rev Immunol* **14**, 667-685, doi:10.1038/nri3738 (2014).

15   Chairatana, P. & Nolan, E. M. Defensins, lectins, mucins, and secretory immunoglobulin A: microbe-binding biomolecules that contribute to mucosal immunity in the human gut. *Crit Rev Biochem Mol Biol* **52**, 45-56, doi:10.1080/10409238.2016.1243654 (2017).

16   Cheng, H. & Leblond, C. P. Origin, differentiation and renewal of the four main epithelial cell types in the mouse small intestine. V. Unitarian Theory of the origin of the four epithelial cell types. *Am J Anat* **141**, 537-561, doi:10.1002/aja.1001410407 (1974).

17   Snoeck, V., Goddeeris, B. & Cox, E. The role of enterocytes in the intestinal barrier function and antigen uptake. *Microbes Infect* **7**, 997-1004, doi:10.1016/j.micinf.2005.04.003 (2005).

18   Furness, J. B., Rivera, L. R., Cho, H. J., Bravo, D. M. & Callaghan, B. The gut as a sensory organ. *Nat Rev Gastroenterol Hepatol* **10**, 729-740, doi:10.1038/nrgastro.2013.180 (2013).

19   Specian, R. D. & Oliver, M. G. Functional biology of intestinal goblet cells. *Am J Physiol* **260**, C183-193, doi:10.1152/ajpcell.1991.260.2.C183 (1991).

20   Cornes, J. S. Number, size, and distribution of Peyer's patches in the human small intestine: Part I The development of Peyer's patches. *Gut* **6**, 225-229, doi:10.1136/gut.6.3.225 (1965).

21   Owen, R. L., Piazza, A. J. & Ermak, T. H. Ultrastructural and cytoarchitectural features of lymphoreticular organs in the colon and rectum of adult BALB/c mice. *Am J Anat* **190**, 10-18, doi:10.1002/aja.1001900103 (1991).

22   Perry, G. A. & Sharp, J. G. Characterization of proximal colonic lymphoid tissue in the mouse. *Anat Rec* **220**, 305-312, doi:10.1002/ar.1092200313 (1988).

23   Masahata, K. *et al.* Generation of colonic IgA-secreting cells in the caecal patch. *Nat Commun* **5**, 3704, doi:10.1038/ncomms4704 (2014).

24   Abreu, M. T. Toll-like receptor signalling in the intestinal epithelium: how bacterial recognition shapes intestinal function. *Nat Rev Immunol* **10**, 131-144, doi:10.1038/nri2707 (2010).

25   Aguilera Montilla, N. P. B., M.; Lopez Santalla, M.; Martin Villa, J.M. Mucosal immune system: A brief review. *Immunologia* **23**, 207-216 (2004).

26   Mowat, A. M. Anatomical basis of tolerance and immunity to intestinal antigens. *Nat Rev Immunol* **3**, 331-341, doi:10.1038/nri1057 (2003).

27   Cerutti, A. The regulation of IgA class switching. *Nat Rev Immunol* **8**, 421-434, doi:10.1038/nri2322 (2008).

28   Mantis, N. J. & Forbes, S. J. Secretory IgA: arresting microbial pathogens at epithelial borders. *Immunol Invest* **39**, 383-406, doi:10.3109/08820131003622635 (2010).

29   Pabst, O. New concepts in the generation and functions of IgA. *Nat Rev Immunol* **12**, 821-832, doi:10.1038/nri3322 (2012).

30   Conley, M. E. & Delacroix, D. L. Intravascular and mucosal immunoglobulin A: two separate but related systems of immune defense? *Ann Intern Med* **106**, 892-899, doi:10.7326/0003-4819-106-6-892 (1987).

31   Kett, K., Brandtzaeg, P., Radl, J. & Haaijman, J. J. Different subclass distribution of IgA-producing cells in human lymphoid organs and various secretory tissues. *J Immunol* **136**, 3631-3635 (1986).

32   Crago, S. S. *et al.* Distribution of IgA1-, IgA2-, and J chain-containing cells in human tissues. *J Immunol* **132**, 16-18 (1984).

33   He, B. *et al.* Intestinal bacteria trigger T cell-independent immunoglobulin A(2) class switching by inducing epithelial-cell secretion of the cytokine APRIL. *Immunity* **26**, 812-826, doi:10.1016/j.immuni.2007.04.014 (2007).

34   Lin, M., Du, L., Brandtzaeg, P. & Pan-Hammarstrom, Q. IgA subclass switch recombination in human mucosal and systemic immune compartments. *Mucosal Immunol* **7**, 511-520, doi:10.1038/mi.2013.68 (2014).

35   Clevers, H. C. & Bevins, C. L. Paneth cells: maestros of the small intestinal crypts. *Annu Rev Physiol* **75**, 289-311, doi:10.1146/annurev-physiol-030212-183744 (2013).

36   Lasserre, C., Colnot, C., Brechot, C. & Poirier, F. HIP/PAP gene, encoding a C-type lectin overexpressed in primary liver cancer, is expressed in nervous system as well as in intestine and pancreas of the postimplantation mouse embryo. *Am J Pathol* **154**, 1601-1610, doi:10.1016/s0002-9440(10)65413-2 (1999).

37   Ghoos, Y. & Vantrappen, G. The cytochemical localization of lysozyme in Paneth cell granules. *Histochem J* **3**, 175-178, doi:10.1007/bf01002560 (1971).

38   Kiyohara, H. *et al.* Light microscopic immunohistochemical analysis of the distribution of group II phospholipase A2 in human digestive organs. *J Histochem Cytochem* **40**, 1659-1664, doi:10.1177/40.11.1431054 (1992).

39   Ayabe, T. *et al.* Secretion of microbicidal alpha-defensins by intestinal Paneth cells in response to bacteria. *Nat Immunol* **1**, 113-118, doi:10.1038/77783 (2000).

40   Peterson, L. W. & Artis, D. Intestinal epithelial cells: regulators of barrier function and immune homeostasis. *Nat Rev Immunol* **14**, 141-153, doi:10.1038/nri3608 (2014).

41   Ganz, T. Defensins: antimicrobial peptides of innate immunity. *Nat Rev Immunol* **3**, 710-720, doi:10.1038/nri1180 (2003).

42   Linzmeier, R., Ho, C. H., Hoang, B. V. & Ganz, T. A 450-kb contig of defensin genes on human chromosome 8p23. *Gene* **233**, 205-211, doi:10.1016/s0378-1119(99)00136-5 (1999).

43   O'Hara, A. M. & Shanahan, F. The gut flora as a forgotten organ. *EMBO Rep* **7**, 688-693, doi:10.1038/sj.embor.7400731 (2006).

44   Round, J. L. & Mazmanian, S. K. The gut microbiota shapes intestinal immune responses during health and disease. *Nat Rev Immunol* **9**, 313-323, doi:10.1038/nri2515 (2009).

45   Hooper, L. V. & Macpherson, A. J. Immune adaptations that maintain homeostasis with the intestinal microbiota. *Nat Rev Immunol* **10**, 159-169, doi:10.1038/nri2710 (2010).

46   Bouma, G. & Strober, W. The immunological and genetic basis of inflammatory bowel disease. *Nat Rev Immunol* **3**, 521-533, doi:10.1038/nri1132 (2003).

47   Koenig, J. E. *et al.* Succession of microbial consortia in the developing infant gut microbiome. *Proc Natl Acad Sci U S A* **108 Suppl 1**, 4578-4585, doi:10.1073/pnas.1000081107 (2011).

48   Turnbaugh, P. J. *et al.* The human microbiome project. *Nature* **449**, 804-810, doi:10.1038/nature06244 (2007).

49   Moore, W. E. & Holdeman, L. V. Human fecal flora: the normal flora of 20 Japanese-Hawaiians. *Appl Microbiol* **27**, 961-979 (1974).

50   Gill, S. R. *et al.* Metagenomic analysis of the human distal gut microbiome. *Science* **312**, 1355-1359, doi:10.1126/science.1124234 (2006).

51   Ley, R. E. *et al.* Evolution of mammals and their gut microbes. *Science* **320**, 1647-1651, doi:10.1126/science.1155725 (2008).

52   Rinninella, E. *et al.* What is the Healthy Gut Microbiota Composition? A Changing Ecosystem across Age, Environment, Diet, and Diseases. *Microorganisms* **7**, doi:10.3390/microorganisms7010014 (2019).

53   Ley, R. E., Turnbaugh, P. J., Klein, S. & Gordon, J. I. Microbial ecology: human gut microbes associated with obesity. *Nature* **444**, 1022-1023, doi:10.1038/4441022a (2006).

54   LeBlanc, J. G. *et al.* Bacteria as vitamin suppliers to their host: a gut microbiota perspective. *Curr Opin Biotechnol* **24**, 160-168, doi:10.1016/j.copbio.2012.08.005 (2013).

55   Cummings, J. H. & Macfarlane, G. T. Colonic microflora: nutrition and health. *Nutrition* **13**, 476-478, doi:10.1016/s0899-9007(97)00114-7 (1997).

56   Macfarlane, G. T., Cummings, J. H. & Allison, C. Protein degradation by human intestinal bacteria. *J Gen Microbiol* **132**, 1647-1656, doi:10.1099/00221287-132-6-1647 (1986).

57   Toor, D. *et al.* Dysbiosis Disrupts Gut Immune Homeostasis and Promotes Gastric Diseases. *Int J Mol Sci* **20**, 2432, doi:10.3390/ijms20102432 (2019).

58   Turnbaugh, P. J. *et al.* An obesity-associated gut microbiome with increased capacity for energy harvest. *Nature* **444**, 1027-1031, doi:10.1038/nature05414 (2006).

59   Qin, J. *et al.* A metagenome-wide association study of gut microbiota in type 2 diabetes. *Nature* **490**, 55-60, doi:10.1038/nature11450 (2012).

60   Yang, T. *et al.* Gut dysbiosis is linked to hypertension. *Hypertension* **65**, 1331-1340, doi:10.1161/hypertensionaha.115.05315 (2015).

61   Frank, D. N. *et al.* Molecular-phylogenetic characterization of microbial community imbalances in human inflammatory bowel diseases. *Proc Natl Acad Sci U S A* **104**, 13780-13785, doi:10.1073/pnas.0706625104 (2007).

62   Bjorksten, B., Naaber, P., Sepp, E. & Mikelsaar, M. The intestinal microflora in allergic Estonian and Swedish 2-year-old children. *Clin Exp Allergy* **29**, 342-346, doi:10.1046/j.1365-2222.1999.00560.x (1999).

63   Penders, J. *et al.* Gut microbiota composition and development of atopic manifestations in infancy: the KOALA Birth Cohort Study. *Gut* **56**, 661-667, doi:10.1136/gut.2006.100164 (2007).

64   Vaahtovuo, J., Munukka, E., Korkeamaki, M., Luukkainen, R. & Toivanen, P. Fecal microbiota in early rheumatoid arthritis. *J Rheumatol* **35**, 1500-1505 (2008).

65   Nguyen, T. L., Vieira-Silva, S., Liston, A. & Raes, J. How informative is the mouse for human gut microbiota research? *Dis Model Mech* **8**, 1-16, doi:10.1242/dmm.017400 (2015).

66   Youssef, N. *et al.* Comparison of species richness estimates obtained using nearly complete fragments and simulated pyrosequencing-generated fragments in 16S rRNA gene-based environmental surveys. *Appl Environ Microbiol* **75**, 5227-5236, doi:10.1128/aem.00592-09 (2009).

67   Huse, S. M., Welch, D. M., Morrison, H. G. & Sogin, M. L. Ironing out the wrinkles in the rare biosphere through improved OTU clustering. *Environ Microbiol* **12**, 1889-1898, doi:10.1111/j.1462-2920.2010.02193.x (2010).

68   Poretsky, R., Rodriguez-R, L. M., Luo, C., Tsementzi, D. & Konstantinidis, K. T. Strengths and limitations of 16S rRNA gene amplicon sequencing in revealing temporal microbial community dynamics. *PLoS One* **9**, e93827-e93827, doi:10.1371/journal.pone.0093827 (2014).

69   Johnson, J. S. *et al.* Evaluation of 16S rRNA gene sequencing for species and strain-level microbiome analysis. *Nat Commun* **10**, 5029, doi:10.1038/s41467-019-13036-1 (2019).

70   Beutler, B. & Rietschel, E. T. Innate immune sensing and its roots: the story of endotoxin. *Nat Rev Immunol* **3**, 169-176, doi:10.1038/nri1004 (2003).

71   Gay, N. J. & Gangloff, M. Structure and function of Toll receptors and their ligands. *Annu Rev Biochem* **76**, 141-165, doi:10.1146/annurev.biochem.76.060305.151318 (2007).

72   Khakpour, S., Wilhelmsen, K. & Hellman, J. Vascular endothelial cell Toll-like receptor pathways in sepsis. *Innate Immun* **21**, 827-846, doi:10.1177/1753425915606525 (2015).

73   West, A. P., Koblansky, A. A. & Ghosh, S. Recognition and signaling by toll-like receptors. *Annu Rev Cell Dev Biol* **22**, 409-437, doi:10.1146/annurev.cellbio.21.122303.115827 (2006).

74   Bell, J. K. *et al.* Leucine-rich repeats and pathogen recognition in Toll-like receptors. *Trends Immunol* **24**, 528-533, doi:10.1016/s1471-4906(03)00242-4 (2003).

75   Akira, S., Takeda, K. & Kaisho, T. Toll-like receptors: critical proteins linking innate and acquired immunity. *Nat Immunol* **2**, 675-680, doi:10.1038/90609 (2001).

76   Akira, S. & Takeda, K. Toll-like receptor signalling. *Nat Rev Immunol* **4**, 499-511, doi:10.1038/nri1391 (2004).

77   Takeuchi, O. *et al.* Differential roles of TLR2 and TLR4 in recognition of gram-negative and gram-positive bacterial cell wall components. *Immunity* **11**, 443-451, doi:10.1016/s1074-7613(00)80119-3 (1999).

78   Hayashi, F. *et al.* The innate immune response to bacterial flagellin is mediated by Toll-like receptor 5. *Nature* **410**, 1099-1103, doi:10.1038/35074106 (2001).

79   Heil, F. *et al.* Species-specific recognition of single-stranded RNA via toll-like receptor 7 and 8. *Science* **303**, 1526-1529, doi:10.1126/science.1093620 (2004).

80   Lund, J. M. *et al.* Recognition of single-stranded RNA viruses by Toll-like receptor 7. *Proc Natl Acad Sci U S A* **101**, 5598-5603, doi:10.1073/pnas.0400937101 (2004).

81   Meier, A. *et al.* Toll-like receptor (TLR) 2 and TLR4 are essential for Aspergillus-induced activation of murine macrophages. *Cell Microbiol* **5**, 561-570, doi:10.1046/j.1462-5822.2003.00301.x (2003).

82   Campos, M. A. S. *et al.* Activation of Toll-Like Receptor-2 by Glycosylphosphatidylinositol Anchors from a Protozoan Parasite. *The Journal of Immunology* **167**, 416-423, doi:10.4049/jimmunol.167.1.416 (2001).

83   Sindhu, S. *et al.* Increased Expression of the Innate Immune Receptor TLR10 in Obesity and Type-2 Diabetes: Association with ROS-Mediated Oxidative Stress. *Cellular Physiology and Biochemistry* **45**, 572-590, doi:10.1159/000487034 (2018).

84   Jiang, S., Li, X., Hess, N. J., Guan, Y. & Tapping, R. I. TLR10 Is a Negative Regulator of Both MyD88-Dependent and -Independent TLR Signaling. *J Immunol* **196**, 3834-3841, doi:10.4049/jimmunol.1502599 (2016).

85   Koblansky, A. A. *et al.* Recognition of Profilin by Toll-like Receptor 12 Is Critical for Host Resistance to Toxoplasma gondii. *Immunity* **38**, 119-130, doi:https://doi.org/10.1016/j.immuni.2012.09.016 (2013).

86   Hidmark, A., von Saint Paul, A. & Dalpke, A. H. Cutting edge: TLR13 is a receptor for bacterial RNA. *J Immunol* **189**, 2717-2721, doi:10.4049/jimmunol.1200898 (2012).

87   Li, X. D. & Chen, Z. J. Sequence specific detection of bacterial 23S ribosomal RNA by TLR13. *Elife* **1**, e00102, doi:10.7554/eLife.00102 (2012).

88   Oldenburg, M. *et al.* TLR13 recognizes bacterial 23S rRNA devoid of erythromycin resistance-forming modification. *Science* **337**, 1111-1115, doi:10.1126/science.1220363 (2012).

89   O'Neill, L. A., Golenbock, D. & Bowie, A. G. The history of Toll-like receptors - redefining innate immunity. *Nat Rev Immunol* **13**, 453-460, doi:10.1038/nri3446 (2013).

90   Botos, I., Segal, D. M. & Davies, D. R. The structural biology of Toll-like receptors. *Structure* **19**, 447-459, doi:10.1016/j.str.2011.02.004 (2011).

91   Gay, N. J., Gangloff, M. & Weber, A. N. Toll-like receptors as molecular switches. *Nat Rev Immunol* **6**, 693-698, doi:10.1038/nri1916 (2006).

92   Dunne, A., Ejdeback, M., Ludidi, P. L., O'Neill, L. A. & Gay, N. J. Structural complementarity of Toll/interleukin-1 receptor domains in Toll-like receptors and the adaptors Mal and MyD88. *J Biol Chem* **278**, 41443-41451, doi:10.1074/jbc.M301742200 (2003).

93   Burns, K. *et al.* Inhibition of interleukin 1 receptor/Toll-like receptor signaling through the alternatively spliced, short form of MyD88 is due to its failure to recruit IRAK-4. *J Exp Med* **197**, 263-268, doi:10.1084/jem.20021790 (2003).

94   Medzhitov, R. *et al.* MyD88 is an adaptor protein in the hToll/IL-1 receptor family signaling pathways. *Mol Cell* **2**, 253-258, doi:10.1016/s1097-2765(00)80136-7 (1998).

95   Muzio, M., Ni, J., Feng, P. & Dixit, V. M. IRAK (Pelle) family member IRAK-2 and MyD88 as proximal mediators of IL-1 signaling. *Science* **278**, 1612-1615, doi:10.1126/science.278.5343.1612 (1997).

96   Suzuki, N. *et al.* Severe impairment of interleukin-1 and Toll-like receptor signalling in mice lacking IRAK-4. *Nature* **416**, 750-756, doi:10.1038/nature736 (2002).

97   Li, S., Strelow, A., Fontana, E. J. & Wesche, H. IRAK-4: a novel member of the IRAK family with the properties of an IRAK-kinase. *Proc. Natl. Acad. Sci. U. S. A.* **99**, 5567-5572, doi:10.1073/pnas.082100399 (2002).

98   Takaesu, G. *et al.* TAK1 is critical for IkappaB kinase-mediated activation of the NF-kappaB pathway. *J Mol Biol* **326**, 105-115, doi:10.1016/s0022-2836(02)01404-3 (2003).

99   Takaesu, G. *et al.* TAB2, a novel adaptor protein, mediates activation of TAK1 MAPKKK by linking TAK1 to TRAF6 in the IL-1 signal transduction pathway. *Mol Cell* **5**, 649-658, doi:10.1016/s1097-2765(00)80244-0 (2000).

100   Ishitani, T. *et al.* Role of the TAB2-related protein TAB3 in IL-1 and TNF signaling. *Embo j* **22**, 6277-6288, doi:10.1093/emboj/cdg605 (2003).

101   Beg, A. A., Finco, T. S., Nantermet, P. V. & Baldwin, A. S. Tumor necrosis factor and interleukin-1 lead to phosphorylation and loss of I kappa B alpha: a mechanism for NF-kappa B activation. *Molecular and Cellular Biology* **13**, 3301-3310, doi:10.1128/mcb.13.6.3301 (1993).

102   Henkel, T. *et al.* Rapid proteolysis of IκB-α is necessary for activation of transcription factor NF-κB. *Nature* **365**, 182-185, doi:10.1038/365182a0 (1993).

103   Chen, G. & Goeddel, D. V. TNF-R1 signaling: a beautiful pathway. *Science* **296**, 1634-1635, doi:10.1126/science.1071924 (2002).

104   Hayden, M. S. & Ghosh, S. Signaling to NF-kappaB. *Genes Dev* **18**, 2195-2224, doi:10.1101/gad.1228704 (2004).

105   Takeda, K. & Akira, S. Toll-like receptors in innate immunity. *Int Immunol* **17**, 1-14, doi:10.1093/intimm/dxh186 (2005).

106   Verma, I. M., Stevenson, J. K., Schwarz, E. M., Van Antwerp, D. & Miyamoto, S. Rel/NF-kappa B/I kappa B family: intimate tales of association and dissociation. *Genes Dev* **9**, 2723-2735, doi:10.1101/gad.9.22.2723 (1995).

107   Ghosh, S., May, M. J. & Kopp, E. B. NF-kappa B and Rel proteins: evolutionarily conserved mediators of immune responses. *Annu Rev Immunol* **16**, 225-260, doi:10.1146/annurev.immunol.16.1.225 (1998).

108   Pahl, H. L. Activators and target genes of Rel/NF-kappaB transcription factors. *Oncogene* **18**, 6853-6866, doi:10.1038/sj.onc.1203239 (1999).

109   Li, Q. & Verma, I. M. NF-kappaB regulation in the immune system. *Nat Rev Immunol* **2**, 725-734, doi:10.1038/nri910 (2002).

110 Vallabhapurapu, S. & Karin, M. Regulation and function of NF-kappaB transcription factors in the immune system. *Annu Rev Immunol* **27**, 693-733, doi:10.1146/annurev.immunol.021908.132641 (2009).

111 Gewirtz, A. T., Navas, T. A., Lyons, S., Godowski, P. J. & Madara, J. L. Cutting edge: bacterial flagellin activates basolaterally expressed TLR5 to induce epithelial proinflammatory gene expression. *J Immunol* **167**, 1882-1885, doi:10.4049/jimmunol.167.4.1882 (2001).

112 Tsujimoto, H. *et al.* Flagellin enhances NK cell proliferation and activation directly and through dendritic cell-NK cell interactions. *J Leukoc Biol* **78**, 888-897, doi:10.1189/jlb.0105051 (2005).

113 Vicente-Suarez, I., Brayer, J., Villagra, A., Cheng, F. & Sotomayor, E. M. TLR5 ligation by flagellin converts tolerogenic dendritic cells into activating antigen-presenting cells that preferentially induce T-helper 1 responses. *Immunol Lett* **125**, 114-118, doi:10.1016/j.imlet.2009.06.007 (2009).

114 Uematsu, S. & Akira, S. Immune responses of TLR5(+) lamina propria dendritic cells in enterobacterial infection. *J Gastroenterol* **44**, 803-811, doi:10.1007/s00535-009-0094-y (2009).

115 Smith, K. D. *et al.* Toll-like receptor 5 recognizes a conserved site on flagellin required for protofilament formation and bacterial motility. *Nat Immunol* **4**, 1247-1253, doi:10.1038/ni1011 (2003).

116 Lu, J. & Sun, P. D. The structure of the TLR5-flagellin complex: a new mode of pathogen detection, conserved receptor dimerization for signaling. *Sci Signal* **5**, pe11 (2012).

117 Forstnerič, V., Ivičak-Kocjan, K., Plaper, T., Jerala, R. & Benčina, M. The role of the C-terminal D0 domain of flagellin in activation of Toll like receptor 5. *PLoS Pathog* **13**, e1006574, doi:10.1371/journal.ppat.1006574 (2017).

118 Eaves-Pyles, T. D., Wong, H. R., Odoms, K. & Pyles, R. B. Salmonella flagellin-dependent proinflammatory responses are localized to the conserved amino and carboxyl regions of the protein. *J Immunol* **167**, 7009-7016, doi:10.4049/jimmunol.167.12.7009 (2001).

119 Murthy, K. G., Deb, A., Goonesekera, S., Szabó, C. & Salzman, A. L. Identification of conserved domains in Salmonella muenchen flagellin that are essential for its ability to activate TLR5 and to induce an inflammatory response in vitro. *J Biol Chem* **279**, 5667-5675, doi:10.1074/jbc.M307759200 (2004).

120 Yoon, S. I. *et al.* Structural basis of TLR5-flagellin recognition and signaling. *Science* **335**, 859-864, doi:10.1126/science.1215584 (2012).

121 Eckhard, U. *et al.* Discovery of a proteolytic flagellin family in diverse bacterial phyla that assembles enzymatically active flagella. *Nature Communications* **8**, 521, doi:10.1038/s41467-017-00599-0 (2017).

122 Vijay-Kumar, M. & Gewirtz, A. T. Flagellin: key target of mucosal innate immunity. *Mucosal Immunol* **2**, 197-205, doi:10.1038/mi.2009.9 (2009).

123 Aldridge, P. & Hughes, K. T. Regulation of flagellar assembly. *Curr Opin Microbiol* **5**, 160-165, doi:10.1016/s1369-5274(02)00302-8 (2002).

124   Macnab, R. M. How bacteria assemble flagella. *Annu Rev Microbiol* **57**, 77-100, doi:10.1146/annurev.micro.57.030502.090832 (2003).

125   Akira, S., Uematsu, S. & Takeuchi, O. Pathogen recognition and innate immunity. *Cell* **124**, 783-801, doi:10.1016/j.cell.2006.02.015 (2006).

126   Vijay-Kumar, M. *et al.* Flagellin treatment protects against chemicals, bacteria, viruses, and radiation. *J Immunol* **180**, 8280-8285, doi:10.4049/jimmunol.180.12.8280 (2008).

127   Hajam, I. A. *et al.* Expression, purification, and functional characterisation of flagellin, a TLR5-ligand. *Vet Ital* **49**, 181-186 (2013).

128   Zeng, H. *et al.* Flagellin/TLR5 responses in epithelia reveal intertwined activation of inflammatory and apoptotic pathways. *Am J Physiol Gastrointest Liver Physiol* **290**, G96-g108, doi:10.1152/ajpgi.00273.2005 (2006).

129   Ramos, H. C., Rumbo, M. & Sirard, J.-C. Bacterial flagellins: mediators of pathogenicity and host immune responses in mucosa. *Trends in Microbiology* **12**, 509-517, doi:https://doi.org/10.1016/j.tim.2004.09.002 (2004).

130   Zeng, H. *et al.* Flagellin Is the Major Proinflammatory Determinant of Enteropathogenic Salmonella. *The Journal of Immunology* **171**, 3668-3674, doi:10.4049/jimmunol.171.7.3668 (2003).

131   Eaves-Pyles, T. *et al.* Flagellin, a Novel Mediator of Salmonella-Induced Epithelial Activation and Systemic Inflammation: IκBα Degradation, Induction of Nitric Oxide Synthase, Induction of Proinflammatory Mediators, and Cardiovascular Dysfunction. *The Journal of Immunology* **166**, 1248-1260, doi:10.4049/jimmunol.166.2.1248 (2001).

132   Rhee, S. H., Im, E. & Pothoulakis, C. Toll-like receptor 5 engagement modulates tumor development and growth in a mouse xenograft model of human colon cancer. *Gastroenterology* **135**, 518-528, doi:10.1053/j.gastro.2008.04.022 (2008).

133   Mizel, S. B., Honko, A. N., Moors, M. A., Smith, P. S. & West, A. P. Induction of macrophage nitric oxide production by Gram-negative flagellin involves signaling via heteromeric Toll-like receptor 5/Toll-like receptor 4 complexes. *J Immunol* **170**, 6217-6223, doi:10.4049/jimmunol.170.12.6217 (2003).

134   Macpherson, A. J., Slack, E., Geuking, M. B. & McCoy, K. D. The mucosal firewalls against commensal intestinal microbes. *Semin Immunopathol* **31**, 145-149, doi:10.1007/s00281-009-0174-3 (2009).

135   Slack, E. *et al.* Innate and adaptive immunity cooperate flexibly to maintain host-microbiota mutualism. *Science* **325**, 617-620, doi:10.1126/science.1172747 (2009).

136   Lodes, M. J. *et al.* Bacterial flagellin is a dominant antigen in Crohn disease. *J Clin Invest* **113**, 1296-1306, doi:10.1172/jci20295 (2004).

137   Rhee, S. H. *et al.* Pathophysiological role of Toll-like receptor 5 engagement by bacterial flagellin in colonic inflammation. *Proc Natl Acad Sci U S A* **102**, 13610-13615, doi:10.1073/pnas.0502174102 (2005).

138   Cario, E. & Podolsky, D. K. Differential alteration in intestinal epithelial cell expression of toll-like receptor 3 (TLR3) and TLR4 in inflammatory bowel disease. *Infect Immun* **68**, 7010-7017, doi:10.1128/iai.68.12.7010-7017.2000 (2000).

139   Carvalho, F. A. *et al.* Transient inability to manage proteobacteria promotes chronic gut inflammation in TLR5-deficient mice. *Cell Host Microbe* **12**, 139-152, doi:10.1016/j.chom.2012.07.004 (2012).

140   Vijay-Kumar, M. *et al.* Metabolic syndrome and altered gut microbiota in mice lacking Toll-like receptor 5. *Science* **328**, 228-231, doi:10.1126/science.1179721 (2010).

141   Vijay-Kumar, M. *et al.* Deletion of TLR5 results in spontaneous colitis in mice. *J Clin Invest* **117**, 3909-3921, doi:10.1172/jci33084 (2007).

142   Kaper, J. B., Nataro, J. P. & Mobley, H. L. T. Pathogenic Escherichia coli. *Nature Reviews Microbiology* **2**, 123-140, doi:10.1038/nrmicro818 (2004).

143   Lupp, C. *et al.* Host-mediated inflammation disrupts the intestinal microbiota and promotes the overgrowth of Enterobacteriaceae. *Cell Host Microbe* **2**, 204, doi:10.1016/j.chom.2007.08.002 (2007).

144   Nagalingam, N. A., Kao, J. Y. & Young, V. B. Microbial ecology of the murine gut associated with the development of dextran sodium sulfate-induced colitis. *Inflamm Bowel Dis* **17**, 917-926, doi:10.1002/ibd.21462 (2011).

145   Cullender, T. C. *et al.* Innate and adaptive immunity interact to quench microbiome flagellar motility in the gut. *Cell Host Microbe* **14**, 571-581, doi:10.1016/j.chom.2013.10.009 (2013).

146   Bradley, P. H. & Pollard, K. S. Proteobacteria explain significant functional variability in the human gut microbiome. *Microbiome* **5**, 36, doi:10.1186/s40168-017-0244-z (2017).

147   Klimosch, S. N. *et al.* Functional TLR5 genetic variants affect human colorectal cancer survival. *Cancer Res* **73**, 7232-7242, doi:10.1158/0008-5472.Can-13-1746 (2013).

148   Hawn, T. R. *et al.* A common dominant TLR5 stop codon polymorphism abolishes flagellin signaling and is associated with susceptibility to legionnaires' disease. *J Exp Med* **198**, 1563-1572, doi:10.1084/jem.20031220 (2003).

149   Waldner, M. J., Foersch, S. & Neurath, M. F. Interleukin-6--a key regulator of colorectal cancer development. *Int J Biol Sci* **8**, 1248-1253, doi:10.7150/ijbs.4614 (2012).

150   Al-Daghri, N. M. *et al.* A nonsense polymorphism (R392X) in TLR5 protects from obesity but predisposes to diabetes. *J Immunol* **190**, 3716-3720, doi:10.4049/jimmunol.1202936 (2013).

151   Min, Y. *et al.* Sex-specific association between gut microbiome and fat distribution. *Nat Commun* **10**, 2408, doi:10.1038/s41467-019-10440-5 (2019).

152   Beale, A. L., Kaye, D. M. & Marques, F. Z. The role of the gut microbiome in sex differences in arterial pressure. *Biol Sex Differ* **10**, 22, doi:10.1186/s13293-019-0236-8 (2019).

153 Peng, C. *et al.* Sex-specific association between the gut microbiome and high-fat diet-induced metabolic disorders in mice. *Biol Sex Differ* **11**, 5, doi:10.1186/s13293-020-0281-3 (2020).

154 Merx, S., Zimmer, W., Neumaier, M. & Ahmad-Nejad, P. Characterization and functional investigation of single nucleotide polymorphisms (SNPs) in the human TLR5 gene. *Hum Mutat* **27**, 293, doi:10.1002/humu.9409 (2006).

155 Hawn, T. R. *et al.* Toll-like receptor polymorphisms and susceptibility to urinary tract infections in adult women. *PLoS One* **4**, e5990, doi:10.1371/journal.pone.0005990 (2009).

156 Sampath, V. *et al.* A TLR5 (g.1174C > T) variant that encodes a stop codon (R392X) is associated with bronchopulmonary dysplasia. *Pediatr Pulmonol* **47**, 460-468, doi:10.1002/ppul.21568 (2012).

157 Meena, N. K., Ahuja, V., Meena, K. & Paul, J. Association of TLR5 gene polymorphisms in ulcerative colitis patients of north India and their role in cytokine homeostasis. *PLoS One* **10**, e0120697, doi:10.1371/journal.pone.0120697 (2015).

158 Sheridan, J. *et al.* A Non-Synonymous Coding Variant (L616F) in the TLR5 Gene Is Potentially Associated with Crohn's Disease and Influences Responses to Bacterial Flagellin. *PLOS ONE* **8**, e61326, doi:10.1371/journal.pone.0061326 (2013).

159 Rutkowski, M. R. *et al.* Microbially driven TLR5-dependent signaling governs distal malignant progression through tumor-promoting inflammation. *Cancer Cell* **27**, 27-40, doi:10.1016/j.ccell.2014.11.009 (2015).

160 Oviedo-Boyso, J., Bravo-Patiño, A. & Baizabal-Aguirre, V. M. Collaborative action of Toll-like and NOD-like receptors as modulators of the inflammatory response to pathogenic bacteria. *Mediators Inflamm* **2014**, 432785-432785, doi:10.1155/2014/432785 (2014).

161 Bryant, C. E. & Monie, T. P. Mice, men and the relatives: cross-species studies underpin innate immunity. *Open Biol* **2**, 120015, doi:10.1098/rsob.120015 (2012).

162 Franchi, L., Warner, N., Viani, K. & Nuñez, G. Function of Nod-like receptors in microbial recognition and host defense. *Immunol Rev* **227**, 106-128, doi:10.1111/j.1600-065X.2008.00734.x (2009).

163 Martinon, F., Burns, K. & Tschopp, J. The inflammasome: a molecular platform triggering activation of inflammatory caspases and processing of proIL-beta. *Mol Cell* **10**, 417-426, doi:10.1016/s1097-2765(02)00599-3 (2002).

164 Zhong, Y., Kinio, A. & Saleh, M. Functions of NOD-Like Receptors in Human Diseases. *Front Immunol* **4**, 333, doi:10.3389/fimmu.2013.00333 (2013).

165 Ting, J. P. *et al.* The NLR gene family: a standard nomenclature. *Immunity* **28**, 285-287, doi:10.1016/j.immuni.2008.02.005 (2008).

166 Gharagozloo, M. *et al.* NLR-Dependent Regulation of Inflammation in Multiple Sclerosis. *Front Immunol* **8**, 2012, doi:10.3389/fimmu.2017.02012 (2017).

167   Zhu, H. & Cao, X. NLR members in inflammation-associated carcinogenesis. *Cell Mol Immunol* **14**, 403-405, doi:10.1038/cmi.2017.14 (2017).

168   Davis, B. K., Wen, H. & Ting, J. P. Y. The inflammasome NLRs in immunity, inflammation, and associated diseases. *Annual review of immunology* **29**, 707-735, doi:10.1146/annurev-immunol-031210-101405 (2011).

169   Man, S. M. & Kanneganti, T.-D. Converging roles of caspases in inflammasome activation, cell death and innate immunity. *Nature reviews. Immunology* **16**, 7-21, doi:10.1038/nri.2015.7 (2016).

170   McIlwain, D. R., Berger, T. & Mak, T. W. Caspase functions in cell death and disease. *Cold Spring Harb Perspect Biol* **7**, doi:10.1101/cshperspect.a026716 (2015).

171   Keller, M., Rüegg, A., Werner, S. & Beer, H. D. Active caspase-1 is a regulator of unconventional protein secretion. *Cell* **132**, 818-831, doi:10.1016/j.cell.2007.12.040 (2008).

172   Rathinam, V. A. K., Vanaja, S. K. & Fitzgerald, K. A. Regulation of inflammasome signaling. *Nature Immunology* **13**, 333-342, doi:10.1038/ni.2237 (2012).

173   Wang, S. *et al.* Identification and characterization of Ich-3, a member of the interleukin-1beta converting enzyme (ICE)/Ced-3 family and an upstream regulator of ICE. *J Biol Chem* **271**, 20580-20587, doi:10.1074/jbc.271.34.20580 (1996).

174   Wang, S. *et al.* Murine caspase-11, an ICE-interacting protease, is essential for the activation of ICE. *Cell* **92**, 501-509, doi:10.1016/s0092-8674(00)80943-5 (1998).

175   Antonopoulos, C. *et al.* Caspase-8 as an Effector and Regulator of NLRP3 Inflammasome Signaling. *J Biol Chem* **290**, 20167-20184, doi:10.1074/jbc.M115.652321 (2015).

176   Broz, P. & Dixit, V. M. Inflammasomes: mechanism of assembly, regulation and signalling. *Nat Rev Immunol* **16**, 407-420, doi:10.1038/nri.2016.58 (2016).

177   Latz, E., Xiao, T. S. & Stutz, A. Activation and regulation of the inflammasomes. *Nat Rev Immunol* **13**, 397-411, doi:10.1038/nri3452 (2013).

178   Martinon, F., Petrilli, V., Mayor, A., Tardivel, A. & Tschopp, J. Gout-associated uric acid crystals activate the NALP3 inflammasome. *Nature* **440**, 237-241, doi:10.1038/nature04516 (2006).

179   Idzko, M. *et al.* Extracellular ATP triggers and maintains asthmatic airway inflammation by activating dendritic cells. *Nat Med* **13**, 913-919, doi:10.1038/nm1617 (2007).

180   Zanoni, I. *et al.* An endogenous caspase-11 ligand elicits interleukin-1 release from living dendritic cells. *Science* **352**, 1232-1236, doi:10.1126/science.aaf3036 (2016).

181   Matzinger, P. The Danger Model: A Renewed Sense of Self. *Science* **296**, 301-305, doi:10.1126/science.1071059 (2002).

182 Bauernfeind, F. G. *et al.* Cutting edge: NF-kappaB activating pattern recognition and cytokine receptors license NLRP3 inflammasome activation by regulating NLRP3 expression. *J Immunol* **183**, 787-791, doi:10.4049/jimmunol.0901363 (2009).

183 Franchi, L., Eigenbrod, T. & Núñez, G. Cutting edge: TNF-alpha mediates sensitization to ATP and silica via the NLRP3 inflammasome in the absence of microbial stimulation. *J Immunol* **183**, 792-796, doi:10.4049/jimmunol.0900173 (2009).

184 Agostini, L. *et al.* NALP3 forms an IL-1beta-processing inflammasome with increased activity in Muckle-Wells autoinflammatory disorder. *Immunity* **20**, 319-325, doi:10.1016/s1074-7613(04)00046-9 (2004).

185 Gremel, G. *et al.* The human gastrointestinal tract-specific transcriptome and proteome as defined by RNA sequencing and antibody-based profiling. *J Gastroenterol* **50**, 46-57, doi:10.1007/s00535-014-0958-7 (2015).

186 Normand, S. *et al.* Nod-like receptor pyrin domain-containing protein 6 (NLRP6) controls epithelial self-renewal and colorectal carcinogenesis upon injury. *Proc Natl Acad Sci U S A* **108**, 9601-9606, doi:10.1073/pnas.1100981108 (2011).

187 Anand, P. K. & Kanneganti, T. D. NLRP6 in infection and inflammation. *Microbes Infect* **15**, 661-668, doi:10.1016/j.micinf.2013.06.009 (2013).

188 Wang, P. *et al.* Nlrp6 regulates intestinal antiviral innate immunity. *Science* **350**, 826-830, doi:10.1126/science.aab3145 (2015).

189 Grenier, J. M. *et al.* Functional screening of five PYPAF family members identifies PYPAF5 as a novel regulator of NF-kappaB and caspase-1. *FEBS Lett* **530**, 73-78, doi:10.1016/s0014-5793(02)03416-6 (2002).

190 Kempster, S. L. *et al.* Developmental control of the Nlrp6 inflammasome and a substrate, IL-18, in mammalian intestine. *Am J Physiol Gastrointest Liver Physiol* **300**, G253-263, doi:10.1152/ajpgi.00397.2010 (2011).

191 Levy, M. *et al.* Microbiota-Modulated Metabolites Shape the Intestinal Microenvironment by Regulating NLRP6 Inflammasome Signaling. *Cell* **163**, 1428-1443, doi:10.1016/j.cell.2015.10.048 (2015).

192 Elinav, E. *et al.* NLRP6 inflammasome regulates colonic microbial ecology and risk for colitis. *Cell* **145**, 745-757, doi:10.1016/j.cell.2011.04.022 (2011).

193 Mamantopoulos, M. *et al.* Nlrp6- and ASC-Dependent Inflammasomes Do Not Shape the Commensal Gut Microbiota Composition. *Immunity* **47**, 339-348.e334, doi:10.1016/j.immuni.2017.07.011 (2017).

194 Hara, H. *et al.* The NLRP6 Inflammasome Recognizes Lipoteichoic Acid and Regulates Gram-Positive Pathogen Infection. *Cell* **175**, 1651-1664.e1614, doi:10.1016/j.cell.2018.09.047 (2018).

195 Birchenough, G. M., Nystrom, E. E., Johansson, M. E. & Hansson, G. C. A sentinel goblet cell guards the colonic crypt by triggering Nlrp6-dependent Muc2 secretion. *Science* **352**, 1535-1542, doi:10.1126/science.aaf7419 (2016).

196   Saxena, M. & Yeretssian, G. NOD-Like Receptors: Master Regulators of Inflammation and Cancer. *Front Immunol* **5**, 327, doi:10.3389/fimmu.2014.00327 (2014).

197   Huhn, S. *et al.* Coding variants in NOD-like receptors: An association study on risk and survival of colorectal cancer. *PLoS One* **13**, e0199350, doi:10.1371/journal.pone.0199350 (2018).

198   Johansson, M. E. Fast renewal of the distal colonic mucus layers by the surface goblet cells as measured by in vivo labeling of mucin glycoproteins. *PLoS One* **7**, e41009, doi:10.1371/journal.pone.0041009 (2012).

199   Knoop, K. A., McDonald, K. G., McCrate, S., McDole, J. R. & Newberry, R. D. Microbial sensing by goblet cells controls immune surveillance of luminal antigens in the colon. *Mucosal Immunol* **8**, 198-210, doi:10.1038/mi.2014.58 (2015).

200   Wlodarska, M. *et al.* NLRP6 inflammasome orchestrates the colonic host-microbial interface by regulating goblet cell mucus secretion. *Cell* **156**, 1045-1059, doi:10.1016/j.cell.2014.01.026 (2014).

201   Johansson, M. E. *et al.* The inner of the two Muc2 mucin-dependent mucus layers in colon is devoid of bacteria. *Proc Natl Acad Sci U S A* **105**, 15064-15069, doi:10.1073/pnas.0803124105 (2008).

202   Velcich, A. *et al.* Colorectal cancer in mice genetically deficient in the mucin Muc2. *Science* **295**, 1726-1729, doi:10.1126/science.1069094 (2002).

203   Siegmund, B. Interleukin-18 in intestinal inflammation: friend and foe? *Immunity* **32**, 300-302, doi:10.1016/j.immuni.2010.03.010 (2010).

204   Mamantopoulos, M., Ronchi, F., McCoy, K. D. & Wullaert, A. Inflammasomes make the case for littermate-controlled experimental design in studying host-microbiota interactions. *Gut Microbes* **9**, 374-381, doi:10.1080/19490976.2017.1421888 (2018).

205   Wehkamp, J. *et al.* Reduced Paneth cell alpha-defensins in ileal Crohn's disease. *Proc Natl Acad Sci U S A* **102**, 18129-18134, doi:10.1073/pnas.0505256102 (2005).

206   Ungerbäck, J. *et al.* Genetic variation and alterations of genes involved in NFκB/TNFAIP3- and NLRP3-inflammasome signaling affect susceptibility and outcome of colorectal cancer. *Carcinogenesis* **33**, 2126-2134, doi:10.1093/carcin/bgs256 (2012).

207   Weber, A. N. & Försti, A. Toll-like receptor genetic variants and colorectal cancer. *Oncoimmunology* **3**, e27763-e27763, doi:10.4161/onci.27763 (2014).

208   Kibbe, W. A. OligoCalc: an online oligonucleotide properties calculator. *Nucleic Acids Res* **35**, W43-46, doi:10.1093/nar/gkm234 (2007).

209   Barrios-Rodiles, M. *et al.* High-throughput mapping of a dynamic signaling network in mammalian cells. *Science* **307**, 1621-1625, doi:10.1126/science.1105776 (2005).

210   Huang, H. D., Lee, T. Y., Tzeng, S. W. & Horng, J. T. KinasePhos: a web tool for identifying protein kinase-specific phosphorylation sites. *Nucleic Acids Res* **33**, W226-229, doi:10.1093/nar/gki471 (2005).

211   Wesche, H., Henzel, W. J., Shillinglaw, W., Li, S. & Cao, Z. MyD88: an adapter that recruits IRAK to the IL-1 receptor complex. *Immunity* **7**, 837-847, doi:10.1016/s1074-7613(00)80402-1 (1997).

212   Oroz, J., Barrera-Vilarmau, S., Alfonso, C., Rivas, G. & de Alba, E. ASC Pyrin Domain Self-associates and Binds NLRP3 Protein Using Equivalent Binding Interfaces. *The Journal of biological chemistry* **291**, 19487-19501, doi:10.1074/jbc.M116.741082 (2016).

213   Shen, C. *et al.* Molecular mechanism for NLRP6 inflammasome assembly and activation. *Proc Natl Acad Sci U S A* **116**, 2052-2057, doi:10.1073/pnas.1817221116 (2019).

214   Stanislawowski, M. *et al.* Decreased Toll-like receptor-5 (TLR-5) expression in the mucosa of ulcerative colitis patients. *J Physiol Pharmacol* **60 Suppl 4**, 71-75 (2009).

215   Vijay-Kumar, M., Carvalho, F. A., Aitken, J. D., Fifadara, N. H. & Gewirtz, A. T. TLR5 or NLRC4 is necessary and sufficient for promotion of humoral immunity by flagellin. *Eur J Immunol* **40**, 3528-3534, doi:10.1002/eji.201040421 (2010).

216   Park, B. S. & Lee, J.-O. Recognition of lipopolysaccharide pattern by TLR4 complexes. *Experimental & Molecular Medicine* **45**, e66-e66, doi:10.1038/emm.2013.97 (2013).

217   Futoma-Koloch, B. Immune Response against Bacterial Lipopolysaccharide. *Journal of Molecular Immunology* **2**, 105 (2016).

218   Ostaff, M. J., Stange, E. F. & Wehkamp, J. Antimicrobial peptides and gut microbiota in homeostasis and pathology. *EMBO Mol Med* **5**, 1465-1483, doi:10.1002/emmm.201201773 (2013).

219   Frye, M., Bargon, J., Lembcke, B., Wagner, T. O. & Gropp, R. Differential expression of human alpha- and beta-defensins mRNA in gastrointestinal epithelia. *Eur J Clin Invest* **30**, 695-701, doi:10.1046/j.1365-2362.2000.00696.x (2000).

220   Wehkamp, J. *et al.* NF-kappaB- and AP-1-mediated induction of human beta defensin-2 in intestinal epithelial cells by Escherichia coli Nissle 1917: a novel effect of a probiotic bacterium. *Infection and immunity* **72**, 5750-5758, doi:10.1128/IAI.72.10.5750-5758.2004 (2004).

221   Vora, P. *et al.* Beta-defensin-2 expression is regulated by TLR signaling in intestinal epithelial cells. *J Immunol* **173**, 5398-5405, doi:10.4049/jimmunol.173.9.5398 (2004).

222   Cobo, E. R. & Chadee, K. Antimicrobial Human β-Defensins in the Colon and Their Role in Infectious and Non-Infectious Diseases. *Pathogens* **2**, 177-192, doi:10.3390/pathogens2010177 (2013).

223   Wehkamp, J., Koslowski, M., Wang, G. & Stange, E. F. Barrier dysfunction due to distinct defensin deficiencies in small intestinal and colonic Crohn's disease. *Mucosal Immunology* **1**, S67-S74, doi:10.1038/mi.2008.48 (2008).

224   Summerton, C. B., Longlands, M. G., Wiener, K. & Shreeve, D. R. Faecal calprotectin: a marker of inflammation throughout the intestinal tract. *Eur J Gastroenterol Hepatol* **14**, 841-845, doi:10.1097/00042737-200208000-00005 (2002).

225   Johne, B. *et al.* Functional and clinical aspects of the myelomonocyte protein calprotectin. *Mol Pathol* **50**, 113-123, doi:10.1136/mp.50.3.113 (1997).

226   Pathirana, W. G. W., Chubb, S. P., Gillett, M. J. & Vasikaran, S. D. Faecal Calprotectin. *Clin Biochem Rev* **39**, 77-90 (2018).

227   Hu, Z. *et al.* Crystal structure of NLRC4 reveals its autoinhibition mechanism. *Science* **341**, 172-175, doi:10.1126/science.1236381 (2013).

228   Maekawa, S., Ohto, U., Shibata, T., Miyake, K. & Shimizu, T. Crystal structure of NOD2 and its implications in human disease. *Nat Commun* **7**, 11813, doi:10.1038/ncomms11813 (2016).

229   Tapia-Abellan, A. *et al.* MCC950 closes the active conformation of NLRP3 to an inactive state. *Nat Chem Biol* **15**, 560-564, doi:10.1038/s41589-019-0278-6 (2019).

230   Song, N. *et al.* NLRP3 Phosphorylation Is an Essential Priming Event for Inflammasome Activation. *Mol Cell* **68**, 185-197.e186, doi:10.1016/j.molcel.2017.08.017 (2017).

231   Hara, H. *et al.* Phosphorylation of the adaptor ASC acts as a molecular switch that controls the formation of speck-like aggregates and inflammasome activity. *Nat Immunol* **14**, 1247-1255, doi:10.1038/ni.2749 (2013).

232   Qu, Y. *et al.* Phosphorylation of NLRC4 is critical for inflammasome activation. *Nature* **490**, 539-542, doi:10.1038/nature11429 (2012).

233   Song, N. & Li, T. Regulation of NLRP3 Inflammasome by Phosphorylation. *Frontiers in Immunology* **9**, doi:10.3389/fimmu.2018.02305 (2018).

234   Xia, Y., Shen, S. & Verma, I. M. NF-κB, an active player in human cancers. *Cancer Immunol Res* **2**, 823-830, doi:10.1158/2326-6066.CIR-14-0112 (2014).

235   Boeuf, P. *et al.* CyProQuant-PCR: a real time RT-PCR technique for profiling human cytokines, based on external RNA standards, readily automatable for clinical use. *BMC Immunol* **6**, 5, doi:10.1186/1471-2172-6-5 (2005).

236   Kolho, K. L., Sipponen, T., Valtonen, E. & Savilahti, E. Fecal calprotectin, MMP-9, and human beta-defensin-2 levels in pediatric inflammatory bowel disease. *Int J Colorectal Dis* **29**, 43-50, doi:10.1007/s00384-013-1775-9 (2014).

237   Ooi, C. Y. *et al.* Fecal Human beta-Defensin 2 in Children with Cystic Fibrosis: Is There a Diminished Intestinal Innate Immune Response? *Dig Dis Sci* **60**, 2946-2952, doi:10.1007/s10620-015-3842-2 (2015).

238   Chang, J. Y. & Cheon, J. H. Fecal Immunochemical Test and Fecal Calprotectin Measurement Are Noninvasive Monitoring Tools for Predicting Endoscopic Activity in Patients with Ulcerative Colitis. *Gut Liver* **12**, 117-118, doi:10.5009/gnl17445 (2018).

239   Seregin, S. S. *et al.* NLRP6 Protects Il10(-/-) Mice from Colitis by Limiting
       Colonization of Akkermansia muciniphila. *Cell Rep* **19**, 733-745,
       doi:10.1016/j.celrep.2017.03.080 (2017).

Contribution declaration

for data presented in the results and appendix of this thesis

Contribution of others:

1. Figure 3.10: Whole blood was drawn by Dr. med. Markus Löffler. Whole blood stimulation was conducted by me. RNA isolation and RT-qPCR were performed by Sabine Dickhöfer. Data from experiments of other donors conducted earlier by Dr. Sascha Klimosch were included.

2. Figure 3.12: HEK Flp-In™ TRex™ 293T cells stably expressing TLR5 WT were generated by Dr. Sascha Klimosch. Cells were stimulated, RNA isolated and RT conducted by me for TLR5 assay. QPCR was performed by Sabine Dickhöfer.

3. Figure 3.13 and Figure 3.14: HEK-Dual™ hTLR5 assay determining NF-κB and AP-1 activation was performed by Sabine Dickhöfer.

4. Figure 3.15: HEK-Dual™ hTLR4 assay determining NF-κB activation was done by Sabine Dickhöfer.

5. Figure 5.8: Experiment was conducted by Yesim Tuzcu.

General:

Recruitment and sampling of individuals was organized and conducted by me. Genotyping of the cohort was mainly conducted by Sabine Dickhöfer.

Stool sampling was organized by me. The processing of samples upon receipt was done by me and Yesim Tuzcu.

Preliminary experiments to determine dry weight and establish conditions for the TLR5 assay were conducted by me and Yesim Tuzcu.

Own contribution: All other experimental work that is not indicated otherwise above, including experimental planning, experiment performance, data acquisition, analysis of data and preparation of figures as presented in the results and appendix of this thesis.
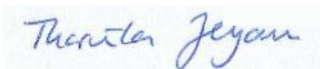
Statutory declaration

Hereby I affirm that I wrote this Doctoral thesis with the topic

"Employing disease-associated genetic variants to study the influence of *TLR5* and *NLRP6* on gut immunity in humans"

independently and that I used no other aids than those cited.

In each individual case, I have clearly identified the source of the passages that are taken paraphrased from other works and the linked manuscript. Moreover, I acknowledge the work done by collaborators.

I affirm that I performed the scientific studies according to the principles of good scientific practice.

_____

Tharmila Jeyam